

Dissertation

Engineering *Escherichia coli* to glycosylate
polyphenols

with the aim of achieving the degree of Doctor rerum naturalium (Dr. rer. nat.)
at the Faculty of Mathematics, Informatics and Natural Sciences
Department of Biology
Universität Hamburg

Submitted by
Constantin Ruprecht
Hamburg 2019

Genehmigt vom Fachbereich Biologie der Universität Hamburg

auf Antrag von Prof. Dr. Wolfgang R. Streit

Weiterer Gutachter der Dissertation: Prof. Dr. Nina Schützenmeister

Tag der Disputation: 31.01.2020

Eidesstattliche Erklärung

Hiermit erkläre ich an Eides statt, dass ich die vorliegende Dissertationsschrift selbst verfasst und keine anderen als die angegebenen Quellen und Hilfsmittel benutzt habe.

Declaration on oath

I hereby declare, on oath, that I have written the present dissertation by my own and have not used any other than the acknowledged resources and aids.

Hamburg, 13.12.2019

Constantin Ruprecht

As a native speaker, I hereby declare that I have checked the thesis "Engineering Escherichia coli to glycosylate polyphenols" by Constantin Ruprecht for grammatically correct English.

Sincerely

Alvin Wong

A handwritten signature in blue ink, consisting of a stylized first name followed by a surname, written in a cursive style.

Contents

Abstract	VI
Zusammenfassung	VIII
1. Introduction	1
1.1. Flavonoids	3
1.1.1. Antioxidant activities of flavonoids	6
1.1.2. Bioavailability of flavonoids	7
1.2. Glycosylation of small molecules	10
1.2.1. Glycosyltransferases	11
1.2.2. Glycosylation of flavonoids by GtfC	13
1.3. Metabolic engineering	15
1.3.1. Metabolic engineering in a cyclic manner	16
1.3.2. <i>Escherichia coli</i> as metabolic engineering chassis	18
1.4. Aim of this thesis	20
I. Growth-coupled rhamnosylation of flavonoids in <i>Escherichia coli</i>	21
2. Introduction	23
2.1. Metabolic engineering strategies	24
2.1.1. Growth-decoupled glycosylation of flavonoids in <i>E. coli</i>	25
2.1.2. Growth-coupled glycosylation of flavonoids in <i>E. coli</i>	26
2.1.3. Growth-coupled glycosylation utilizing the maltodextrin system	27
3. Results & Discussion	29
3.1. Generation of expression systems for <i>E. coli</i> K-12	29
3.1.1. Generation of <i>E. coli</i> K-12 deletion mutants	30
3.2. Hesperetin rhamnosylation in 48 well plates	30
3.3. Hesperetin rhamnosylation in batch fermentations	34
3.4. Glycosylation in solid fed-batch fermentations	36
II. Development of a modular glycosylation platform	39
4. Introduction	41
4.1. Design of a modular glycosylation platform for flavonoids	43
4.2. Auto-induction using the maltodextrin system	45
5. Results & Discussion	47
5.1. Genetic design of <i>E. coli</i> for modular glycosylation	47
5.2. Generation of Glycoswitch and GT-module	50
5.2.1. GT-module generation	50
5.2.2. Glyco-switch generation	51

5.3.	Naringenin rhamnosylation using Glyco-switch and GT-module	52
5.3.1.	Proof of principle experiment by <i>rml</i> operon complementation	53
5.3.2.	Deletion of <i>glgC</i> and <i>ushA</i>	56
5.3.3.	Comparison of medium and high copy-number Glyco-switch plasmids	58
5.4.	Glycodiversification of flavonoids	60
5.4.1.	Rhamnosylation	61
5.4.2.	Glucosylation	63
5.4.3.	Glucuronidation	64
III.	Development of a rhamnosyltransferase activity screen	67
6.	Introduction	69
6.1.	Glycosyltransferase activity screening	69
7.	Results & Discussion	71
7.1.	Blue/white screening for rhamnosyltransferase activity	71
7.2.	Application of blue/white screening	72
7.3.	Application potential for blue/white screening method	73
IV.	Conclusion & Outlook	75
8.	Conclusion & Outlook	77
8.1.	Future developments of the glycodiversification platform	79
V.	Materials & Methods	83
9.	Bacterial strains & Cultivation	85
9.1.	Strains used within the study	85
9.2.	Cultivation media	88
9.3.	Glycosylation in whole cell biotransformations	90
10.	Molecular Biology	93
10.1.	Primers and Plasmids	93
10.2.	Molecular biology methods	100
10.3.	Molecular cloning methods	102
10.4.	Construction of production plasmids	103
11.	Analytical Methods	107
11.1.	High Performance Liquid Chromatography (HPLC)	107
11.2.	Thin Layer Chromatography	107
12.	Acknowledgments	109
	Glossary	111
	Bibliography	113
VI.	Appendix	123

List of Figures

1.1.	Examples of natural processes involving glycosyltransferases	2
1.2.	The core structure of the major flavonoid classes	4
1.3.	Overview of flavonoid biosynthesis in plants	5
1.4.	Antioxidant activity of quercetin	6
1.5.	Polyphenolic absorption, metabolism, distribution, and excretion	8
1.6.	The formation of a glycosidic bond using enzymatic catalysis	10
1.7.	3D structure of GT-A, GT-B and GT-C fold adopted by glycosyltransferases	12
1.8.	Reaction mechanism of inverting and retaining glycosyltransferases	13
1.9.	Rhamnosylation of flavonoids by glycosyltransferase C	14
1.10.	Major bioprocess stages relevant to metabolic engineering	15
1.11.	General metabolic engineering cycle of a non natural producer	16
2.1.	Glycosylation in whole-cell biotransformations	23
2.2.	Production of <i>d</i> TDP-rhamnose from glucose-1-phosphate via the <i>rml</i> operon.	24
2.3.	Growth-decoupled glycosylation strategy for flavonoids in <i>E. coli</i>	25
2.4.	Growth-coupled glycosylation strategy of flavonoids in <i>E. coli</i>	26
2.5.	Metabolic engineering approach using dextrans of starch as carbon source . .	27
3.1.	Production plasmids used for glycosylation in <i>E. coli</i> K-12	29
3.2.	Production of hesperetin rhamnosides in <i>E. coli</i> deletion strains.	31
3.3.	Hesperetin rhamnosylation of <i>E. coli</i> batch fermentations	34
3.4.	Comparison of batch and fed-batch fermentations of <i>E. coli</i> UHH_CR5-A .	36
4.1.	<i>In vitro</i> bioactivities of naringenin glycosides.	41
4.2.	Concept for a modular glycosylation platform	43
4.3.	Possible Glyco-switch pathways with corresponding GT-modules.	44
4.4.	Regulation of MalT activity	45
4.5.	Auto-induction of Glyco-switch and GT-module	46
5.1.	Genetic modification of <i>E. coli</i> UHH_CR14	47
5.2.	Creation of GT-module plasmid pK44-MalT::GtfD(opt)	50
5.3.	Creation of Glyco-switch plasmid pCDF-malZp:: <i>rmlAB</i> :: <i>rmlCD</i>	51
5.4.	Production of Naringenin-5-O-rhamnoside by autoinduced GtfD	53
5.5.	Complementation of the <i>rml</i> operon on the Glyco-switch plasmid	55
5.6.	Effect of <i>glgC</i> and <i>ushA</i> gene deletions	56
5.7.	Comparison of high-copy- and medium-copy number Glyco-switch.	58
5.8.	Glyco-switch and GT-modules generated for glycodiversification experiments	60
5.9.	Glyco-switch and GT-module combination to produce rhamnosides.	61
5.10.	Glyco-switch and GT-module combination to produce glucosides.	63
5.11.	Glyco-switch and GT-module combination to produce glucuronides.	64
7.1.	Molecular basis of blue/white screening.	72
7.2.	Proposed workflow for a mutagenesis approach using blue/white screening. .	74
8.1.	Examples of <i>d</i> TDP sugars derived from G1P as central precursors	80
9.1.	Design and deletion of malZ in <i>E. coli</i> K-12(MG1655)	87
12.1.	HPLC analysis of hesperetin rhamnosylation	126
12.2.	Screening of an RBS library for autoinduced glycosylation by GtfD	127
12.3.	Phylogenetic tree of the glycosyltrasnferases used in blue/whote screening. .	128

List of Tables

3.1. Production strains created in Part I	31
3.2. Flavonoid rhamnosylations in <i>E. coli</i>	37
5.1. Bacterial strains created leading up to <i>E. coli</i> UHH_CR14	48
5.2. <i>E. coli</i> production strains created and used within Part II	52
5.3. Glycodiversification of flavonoids in <i>E. coli</i>	62
7.1. Blue/white screening of rhamnosyltransferases in <i>E. coli</i> UHH_CR14	73
9.1. Bacterial strains used and created in this study	86
9.2. Antibiotics stock solution and working concentrations used within this study	88
9.3. M9 composition for 1 L medium, containing glucose as carbon source	89
10.1. Plasmids used within this study	94
10.2. Primers used to generate and verify deletion or insertion mutants	95
10.3. Primers used within this study to generate and verify production plasmids	97
10.4. Glycosyltransferases used within this study	99

Abstract

A group of exciting molecules for the pharmaceutical and healthcare industry are flavonoids, exerting a wide variety of biological functions. These functions are limited by their toxicity, low water solubility, and bioavailability, which can be relieved through glycosylation. Glycosylation reactions are found throughout nature, performed by glycosyltransferases (EC 2.4.-.-). The natural functions of glycosylations range from protein glycosylation, creation of storage glycosides to detoxification mechanisms of small molecules. Previous work by Rabausch et al. [1] identified a bacterial, metagenome derived glycosyltransferase, GtfC, able to rhamnosylate various polyphenolic substances in whole-cell biotransformations using *Escherichia coli* as the host organism. This work significantly contributes to the field of glycobioengineering by firstly increasing glycosylation capabilities of *E. coli* K-12, secondly by the development of a modular glycosylation platform and finally by the establishment of a rhamnosyltransferase activity screen.

A new metabolic engineering strategy was created, to increase the rhamnosylation capacity of *E. coli* K-12, by coupling its growth on maltodextrins to the rhamnosylation of polyphenols using the model flavonoid hesperetin. The maltodextrin metabolism ensures the constant production of the central precursor of *d*TDP-rhamnose (*d*TDP-rha) synthesis, glucose-1-phosphate (G1P). The highest production titers were achieved by the deletion of the phosphoglucomutase (*pgm*) and UTP-glucose-1-phosphate uridylyltransferase (*galU*) genes, in cooperation with the overexpression of the *d*TDP-rha synthesis pathway, the *rml* operon (*rmlBDAC*). The expression of a glucan 1,4- α -maltohexaosidase for increased maltodextrin degradation led to the highest production titers using heterologously expressed GtfC in *E. coli* UHH_CR5-A. Using *E. coli* UHH_CR5-A, a final product titer of 2.4 g/L of hesperetin-3'-*O*-rhamnoside, 4.3 g/L of quercetin-3-*O*-rhamnoside and 1.9 g/L of kaempferol-3-*O*-rhamnoside were produced, the so-far highest published production titers of flavonoid rhamnosides.

Not only *d*TDP-rhamnose but nearly all *d*TDP-sugars and various UDP-, CDP-sugars are derived from G1P. A plasmid-based expression platform was created, to enable the modular glycosylation of different flavonoids with different NDP-sugars. The expression system combines a glycosyltransferase on one plasmid (GT-module) with a NDP-sugar synthesis

pathway (Glyco-switch), leading to the formation of the desired NDP-sugar from G1P, on a secondary plasmid. The expression of target genes was controlled by the maltodextrin glucosidase promoter region, regulated by the transcriptional activator of the maltodextrin system, MalT. The incorporation of MalT onto the GT-module led to a strong increase in rhamnosylation of naringenin by glycosyltransferase D (GtfD) from *Dyadobacter fermentans* and the *rml* operon expressed on pCDF-malZp::*rmlAB*::*rmlCD*. Changing the backbone of the Glyco-switch plasmid from the medium copy pCDF backbone to a high copy pRSF backbone reduced the production of naringenin rhamnosides. The created base-strain *E. coli* UHH_CR14 was able to produce a total of 14.2 g/L of naringenin rhamnosides by combining *d*TDP-rha synthesis Glyco-switch (pCDF-malZp::*rmlAB*::*rmlCD*) with GtfD expressed on the GT-module (pK44-MalT::GtfD). The glycodiversification potential was shown by the creation of Glyco-switches leading to the formation of UDP-glucose (pCDF-malZp::*galU*), UDP-rhamnose (pCDF-malZp::*galU*::*MUM4*) and UDP-glucuronic acid (pCDF-malZp::*galU*::*ugd*). These Glyco-switches were combined with GTs known from the literature to transfer the activated sugars onto flavonoid aglycones. In this manner, 4.9 g/L naringenin-7-*O*-glucoside were produced using UDP-glucose and GtfW from *Bacillus weihenstephanensis*, and 1.41 g/L quercetin-3-*O*-rhamnoside using UDP-rhamnose and *RhaGT* from *Arabidopsis thaliana*.

Not all GTs show high substrate or product specificity, while others are highly specific for a particular substrate. In order to engineer GTs for increased production rates and certain aglycone or product specificities, a novel glycosyltransferase screening method was developed based on the hydrolysis of chromogenic 5-Brom-4-chloro-indoxyl- β -D-galactose (X-gal) by the *E. coli* β -galactosidase (LacZ) upon IPTG induction. The released 5-Brom-4-chloro-indoxyl (X) can dimerize in the presence of oxygen to form a blue colored *E. coli* colony on agar plates. However, GTs able to rhamnosylate 5-Brom-4-chloro-indoxyl create a colorless rhamnoside, leading to the formation of white colonies. In future work, this assay can be used for engineering of GTs or for the identification of novel NDP-sugar pathways from metagenomes, whose X-glycosides can not be hydrolyzed by *E. coli*.

This work established a toolbox enabling the fast and easy development of a wide variety of glycosides, producible in g/L scale. The developed modular glycosylation platform sets the current state of the art glycosylation platform of flavonoids in *E. coli*.

Zusammenfassung

Die Glykosylierung von Molekülen ist eine weit verbreitete Modifizierung, die von Glykosyltransferasen katalysiert wird. Glykosylierungsmodifikation sind allgegenwärtig und reichen von der Glykosylierung von Proteinen bis zur Speicherung von Energie in langkettigen Zuckerketten über die Reduzierung der Giftwirkung von Molekülen. Flavonoide, eine Stoffklasse mit interessanten Bioaktivitäten, werden oft durch deren geringe Löslichkeit, Stabilität oder Bioverfügbarkeit in ihrer Verwendung eingeschränkt. Diese Einschränkungen können durch eine Glykosylierung aufgehoben werden.

Diese Arbeit befasst sich mit dem Metabolic Engineering eines *Escherichia coli* Stammes zur Rhamnosylierung von Flavonoiden. Ausgehend von der Entwicklung einer vorhergehenden Arbeit, die eine metagenomische Glykosyltransferase entdeckte, die verschiedenste Polyphenole rhamnosylieren konnte, wurde ein *E. coli* Stamm entwickelt, der in der Lage ist Flavonoide im g/L Maßstab zu glykosylieren. Um die Glykosylierungskapazität von *E. coli* zu steigern, wurde sich auf die Bereitstellung von Glukose-1-Phosphat (G1P), dem zentralen Metaboliten in der Herstellung von vielen Nukleotiddiphosphat-(NDP) Zuckern, konzentriert. *E. coli* produziert G1P in seinem natürlichen Maltodextrinstoffwechsel. Die höchsten Produktionskonzentrationen wurden durch die genomische Deletion der Phosphoglucomutase (*pgm*) und Glukose-1-phosphat-Uridyltransferase (*galU*) und der simultanen Überexpression des dTDP-Rhamnose-Stoffwechselweges erzielt. Die Inkooperation einer Stärke abbauenden G6-Amylase ermöglichte zusätzlich den Abbau langer Maltodextrinketten wodurch die Produktion stark gesteigert werden konnte. Durch diesen Ansatz konnten 2.4 g/L Hesperetin-3'-O-rhamnoside, 4.3 g/L of Quercetin-3-O-rhamnoside und 1.9 g/L Kaempferol-3-O-rhamnoside hergestellt werden.

G1P ist das zentrale Vorläufermolekül für verschiedene NDP-Zucker. Um diese mit den dazugehörigen Glykosyltransferasen kombinieren zu können wurde ein modulares, plasmidbasiertes System entwickelt. Der NDP-Zucker-Stoffwechselweg wird auf dem *Glyco-switch* und die Glykosyltransferase auf dem *GT-module* exprimiert. Die Expression auf den Plasmiden mit kompatiblen Replikationsursprüngen erfolgt durch Promotoren des Maltodextrinsystems und macht dadurch die Zugabe eines Induktors überflüssig. Zusätzlich wurde auf dem *GT-module* der Transkriptionsinitiator des Maltodextrinsystems,

MalT, exprimiert. Die Funktionalität des Systems wurde für *d*TDP-Rhamnose (pCDF-malZp::*rmlAB::rmlCD*), UDP-Glukose (pCDF-malZp::*galU*) und UDP-Rhamnose (pCDF-malZp::*galU::MUM4*) gezeigt. Auf diese Weise konnten zum ersten mal eine Produktion von Rhamnosiden, i.e 14.2 g/L Naringenin-Rhamnoside, jenseits von 10 g/L gezeigt werden.

Zusätzlich wurde ein Aktivitätsscreen für Rhamnosyltransferasen entwickelt. Der neu entwickelte Assay basiert auf dem chromogenen Substrat 5-Brom-4-chloro-indoxyl- β -D-Galaktose (X-Gal). Das Galaktosid wird von *E. coli* gespalten und 5-Brom-4-chloro-indoxyl (X) wird freigesetzt. In der Anwesenheit von Sauerstoff dimerisiert X und bildet das blau gefärbte Dimer. Einige Glykosyltransferasen können X rhamnosylieren, wodurch die Dimerisierung und die daraus entstehende Färbung ausbleibt. Durch diesen Prozess können auf einer Agar Platte aktive von nicht aktiven Mutanten eines solchen Enzymes unterschieden werden.

Die Forschungsergebnisse zeigen die bisher höchsten Rhamnosylierungskonzentrationen von Flavonoiden in *E. coli*. Die Glykodiversifizierungsplattform bietet enormes Potential für die Produktion und schnelle Entwicklung neuartiger Glykoside mit interessanten, bisher nicht bekannten Funktionen.

1. Introduction

Glycosylation is a highly abundant modification in nature found within all domains of life, performed predominantly by glycosyltransferases (GTs). GTs catalyze the transfer of sugar moieties from activated donor molecules, often activated nucleotide diphosphate sugars (NDP-sugars) to specific acceptor substrates (aglycones) to yield the corresponding glycoside. Glycosyltransferases are classified in the Carbohydrate-Active enZYMes (CAZymes) database, according to their sequence similarities regarding their donor, acceptor, or product specificity [2]. Currently 108 GT families account for a total amount of 599236 classified GTs, listed in the CAZY database (<http://www.cazy.org/GlycosylTransferases.html> - 05.11.2019) [3]. GTs can make up between 1 and 2 % of the gene products of an organism, ranging from a few to no detected glycosyltransferases in some obligate symbiotic bacteria, to hundreds in some plant species, as e.g., *Arabidopsis* containing ~ 450 GTs [4]. The natural processes involving glycosyltransferases are of great diversity and widespread, involving primary functions like generation of storage glycans, structural functions, recognition and detoxification mechanisms, or the production of secondary metabolites (figure 1.1).

The storage of excess carbon source in the form of glycan chains, as, e.g. glycogen, is a well-conserved feature throughout living organisms. The linear α -1,4-dextrin chain is synthesized by a single glycosyltransferase, whereas the diversity of different glycogen or starch storage forms is derived from secondary branching or modifying enzymes. In contrast to the unregulated bacterial and plant glycogen/starch synthase (GS) utilizing ADP- α -D-glucose, mammalian and yeast GS are tightly regulated and utilize UDP- α -D-glucose [5].

Glycans do not only function in storage but also have structural functions like forming the extracellular matrix or the exoskeleton consisting of chitin or cellulose. The natural diversity of these glycans has been theoretically calculated to be 10^{12} [6], whereas the actual

1. Introduction

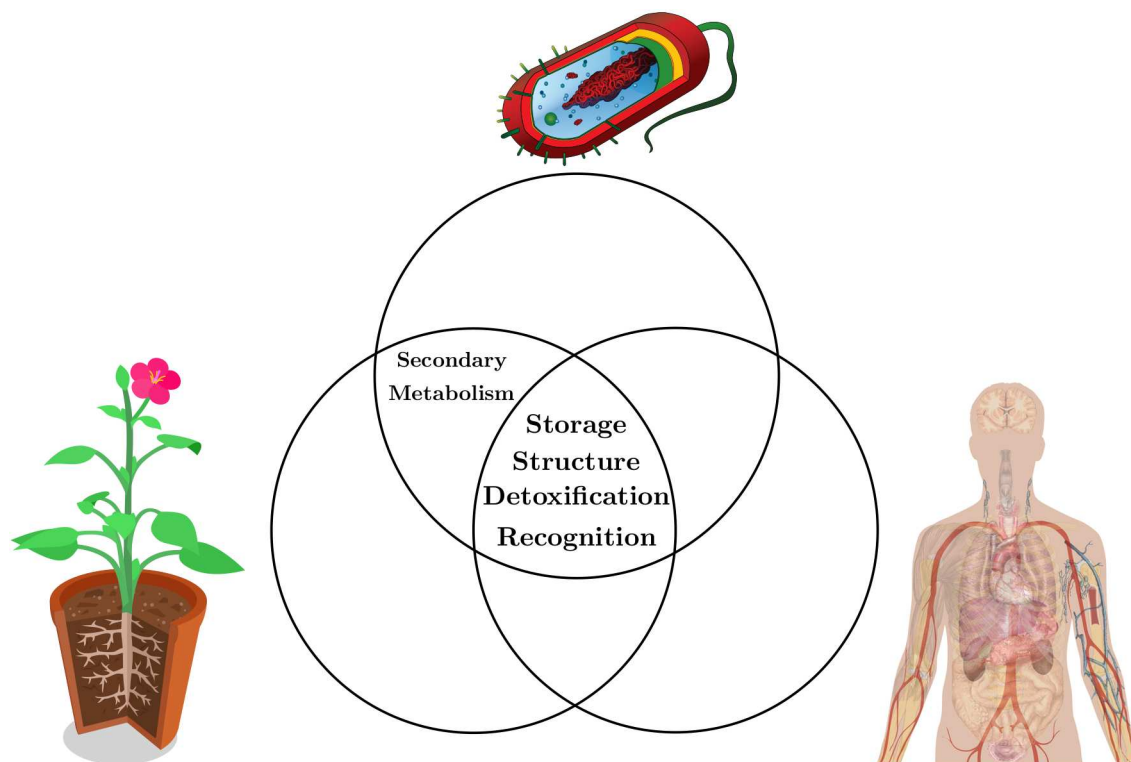


Figure 1.1.: Examples of natural processes involving glycosyltransferases.

Pictograms in this figure are derived and may be adapted from creative commons licens (CC0).

The plant diagram is adapted from “Plant diagram with Gujarati Lable” created by Sushant savla and is licensed under CC BY-SA 3.0.

diversity is believed to be magnitudes lower [7]. Also, gram-negative bacteria contain unique polysaccharide chains on their outer membrane, the lipopolysaccharides (LPS), synthesized by the sequential addition of sugar moieties by GTs [8].

The cellular identity of a cell in an organism results in different cell surface glycosylation patterns, thereby enabling recognition of self-nonself, a cell’s developmental state, and the tissue type. The O-antigens found on pathogenic bacterial surfaces differ widely from mammalian cell surface glycans. These can be recognized by innate host defense systems (lectins) and can trigger an immune response [9]. The long thought to be definite fact that prokaryotic organisms do not perform protein glycosylation has been overthrown in the last decades. Bacterial protein glycosylation can play a role in pathogenesis, glycosylating extracellular proteins to increase their stability and evade a immune response by coating antigenic protein structures with glycans [10, 11].

Another general natural function of glycosyltransferases is a detoxification process. The human liver uses a detoxification mechanism by glucuronidation. It is estimated that

human UDP dependent glucuronyl transferases account for 35 % of the drugs metabolized by phase II enzymes [12]. Also, plants utilize GTs for detoxification purposes, shown by the plant-fungal interaction between *Fusarium* and *Arabidopsis*, in which an *Arabidopsis* GT glycosylates the mycotoxin deoxynivalenol, thereby conferring increased tolerance to the invading pathogen [13, 14].

In addition to primary metabolites, plants and microorganisms can produce a wide array of secondary metabolites, enabling them to gain a selective advantage [15]. The macrolide antibiotic-producing *Streptomyces oleandomycin* detoxifies its secondary metabolite oleandomycin intracellularly, leading to an export of the glucoside. The glycosidic moiety is hydrolyzed extracellularly by a β -glycosidase creating the functional antibiotic, which can act on competing microorganisms [16]. Glycosyltransferases play a vital role in the modification of plant secondary metabolites [17], as, e.g., anthocyanins, natural plant pigments responsible for the blue, red, and purple color of fruits, vegetables, and flowers [18]. The glycosylation of these secondary metabolites greatly influences their solubility, stability and bioavailability, leading to a molecule with altered properties compared to its aglycone. Many of these glycosides are biologically active compounds in which the glycosidic moiety can be crucial for the activity or improve the pharmacokinetic properties of the molecules [19, 20]. The enhanced properties of these small molecules make them interesting candidates for applications in various industries.

1.1. Flavonoids

Flavonoids are bioactive molecules produced as secondary metabolites within many plants. In the 1930s, a plant component termed citrin or vitamin P, from citrus fruits, was believed to have vitamin-like effects [21]. Citrin was identified to contain a mixture of hesperetin-7-O-rutinoside and eriodictyol glucoside [22], whose essentiality was for a long time a scientific controversy. Nowadays, flavonoids are often referred to as bioflavonoids due to their often beneficial health traits, which, however, do not share the essentiality of vitamins.

The core flavonoids structure is a C6-C3-C6 system, the A-, C-, and B-ring, respectively. The substitution of the C-ring structure gives rise to the different classes of flavonoids (figure 1.2). The major flavonoid classes are flavanones, flavones, flavonols, flavanols,

1. Introduction

flavanonols, and anthocyanidins. The structurally diverse class of flavonoids, constituting for more than 9000 flavonoids [23], function in plants defense against UV-B radiation and pathogen infection, nodulation, and pollen fertility [24]

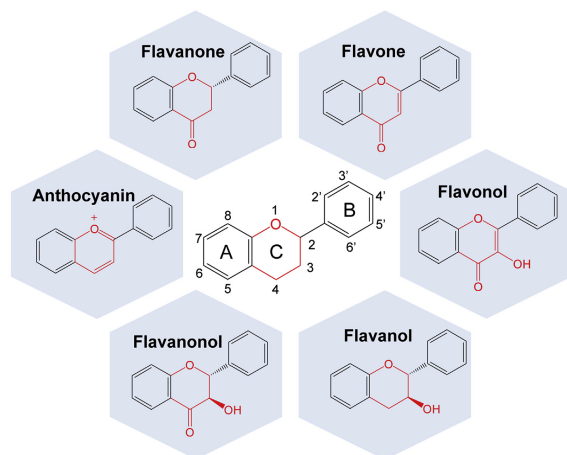


Figure 1.2.: The core structure of the major flavonoid classes. Flavonoids are composed of a C6-C3-C6 ring system, denoted A-, C-, and B-ring. The core structure is substituted with various modifications catalyzed by isomerases, reductases, hydroxylases, glycosyltransferases, acyltransferases, and prenyltransferases, leading to the high structural diversity of flavonoids.

This figure is derived from Zha et al. [25].

The flavonoid biosynthesis is derived from the phenylpropanoid pathway, in which phenylalanine is deaminated and hydroxylated leading to the formation of *p*-coumaric acid, which is then activated by Coenzyme A (CoA). The first flavonoid specific catalyation is the formation of a chalcone scaffold by the chalcone synthase (CHS) from which all flavonoids are derived (figure 1.3). CHS condenses and cyclazises three acetates from malonyl-CoA onto *p*-coumaroyl-CoA. After the formation of the chalcone, a variety of enzymatic modifications are possible, including isomerases, reductases, hydroxylases, glycosyltransferases, acyltransferases, and prenyltransferases. These variations lead to a large variety of flavonoid substances known.[26]

Due to their high structural diversity, flavonoids also show various biological functions. In addition to their functions in plants, flavonoids have been widely utilized in plant extracts for their beneficial properties. In human health, dietary flavonoids are most commonly reported to have activities and applications targeted against cardiovascular diseases, cardiometabolic disorders, type 2 diabetes [28], cancer, and neurodegeneration [29]. A global working mechanisms of flavonoids has not yet been identified and is believed to be a com-

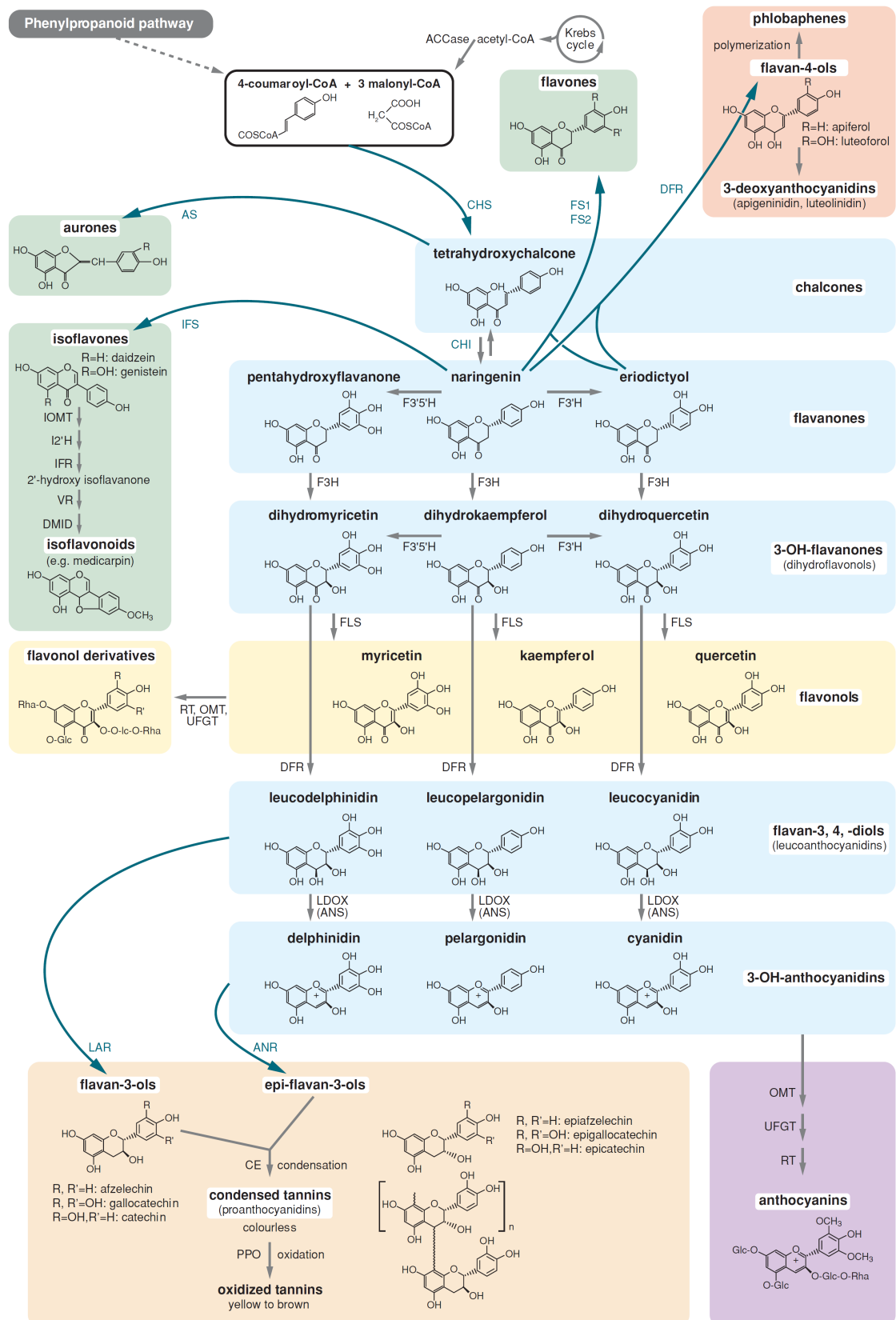


Figure 1.3: Overview of flavonoid biosynthesis in plants. Precursors of flavonoid biosynthesis are derived from the phenylpropanoid pathway. The synthesis is initiated by chalcone formation from *p*-coumaroyl-CoA, followed by various enzymatic modifications, leading to an immense structural diversity of flavonoids.

This figure is derived from Lepiniec et al. [27]

1. Introduction

combination of different effects. However, the working mechanisms that are present in the disorders which flavonoids are beneficial for can be reduced to mainly anti-inflammatory effects of flavonoids and redox regulation [29].

1.1.1. Antioxidant activities of flavonoids

Flavonoids are often termed and advertised as antioxidants. One of the primary phytochemicals with antioxidant capacities in apple juice is quercetin [30]. Quercetin can reduce reactive oxygen species (ROS), e.g., H_2O_2 leading to the formation of oxidized quercetin quinones (figure 1.4).

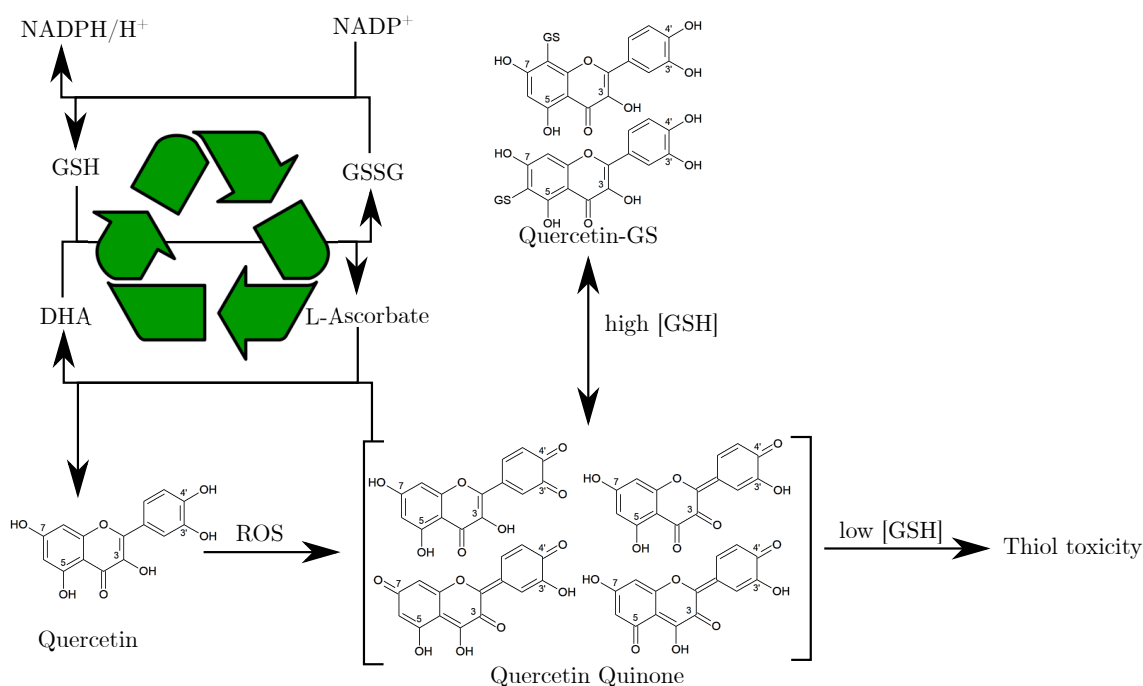


Figure 1.4.: Antioxidant activity of quercetin. Upon reduction of quercetin by a reactive oxygen species (ROS), quercetin quinones (QQ) are formed. QQs can be regenerated by the antioxidant network by L-ascorbate or glutathione (GSH). QQs can cause thiol toxicity if not regenerated. DHA, dihydroxyascorbate; GSSG, glutathione disulfide

Chemical structures were drawn using ChemSketch. Pictograms in this figure are derived and may be adapted from creative commons licens (CC0).

These quinones are themselves reactive species, that if not reduced, can cause severe protein and DNA damage, also referred to as thiol toxicity as they covalently bind to thiol residues present in cysteine amino acids of proteins. However, the antioxidant network can regenerate the reduced flavonoid as shown for quercetin, which can be regenerated by L-ascorbic acid or can react with a higher specificity with glutathione (GSH), forming

quercetin-6-GS or quercetin-8-GS [31]. In contrast to earlier believes, that Quercetin-GS complexes are removed from the antioxidant network via excretion, it was shown that the complexes are formed reversibly. Therefore, high GSH concentrations are needed to prevent thiol toxicity [32]. Flavonoids vary in their antioxidative capabilities and in their degree of thiol toxicity depending on their structure [33–35]. The glycosides of quercetin still possess antioxidative properties (shown in linoleate oil) in the order of Quercetin > Quercetrin (3-*O*-rhamnoside) > Isoquercetrin (3-*O*-glucoside) > Rutin (3-*O*-Rutinoside) [36].

1.1.2. Bioavailability of flavonoids

The bioavailability of polyphenols is limited due to their low water solubility. The glycosylation of such small lipophilic molecules generally increases their water solubility [37–39] and stability [40–43]. It is often generalized that the glycosylation of flavonoids or polyphenolic substances increases their bioavailability [19, 44]; however, the bioavailability is dependent on the route of administration, i.e., oral, intravenous, or topical. Furthermore, the desired target of a flavonoid and the type of sugar attached to a flavonoid is critical for its bioavailability. Most studies regarding increased bioavailability refer to oral, dietary, uptake of flavonoids, and their glycosides. The type and position of the glycosidic residue can strongly influence the resulting bioavailability of the glycosides, as shown for hesperetin 7-*O*-glucoside, which exhibits an increased bioavailability in contrast to hesperidin (Hesperetin-7-*O*-rutinoside) [45].

The vast majority of flavonoids occur as glycosides, often in the β -glycosidic form [46]. Bioavailability of flavonoids after oral administration is, in general, higher for the β -glucosides compared to their aglycones, even though they are too hydrophobic for absorption by passive diffusion [46]. The glycosidic moiety determines the point of absorption, β -glucosides are deglycosylated by hydrolases located at the border membrane of the small intestine (figure 1.5). The released aglycones are subsequently absorbed. The hydrolases only efficiently hydrolyze glucosides, whereas other glycosides are digested with the help of the microbiome in the colon [47].

1. Introduction

MOUTH

- Release from food matrix
- Deconjugation
- Polyphenol-protein interaction

STOMACH

- Release from food particles
- Hydrolysis/deconjugation
- Absorption

SMALL INTESTINE

- Deglycosylation
- Methylation
- Glucuronidation
- Degradation to small phenolics
- Absorption

COLON (bacteria)

- Deconjugation/conjugation
- Hydrolysis/dehydroxylation
- Demethylation/decarboxylation
- Flavonoids ring fission (production of hydroxylated aromatic compounds and phenolic acids)
- Absorption

LIVER

- Methylation
- Glucuronidation
- Sulfation
- Oxidation
- Hydrogenation/dehydrogenation

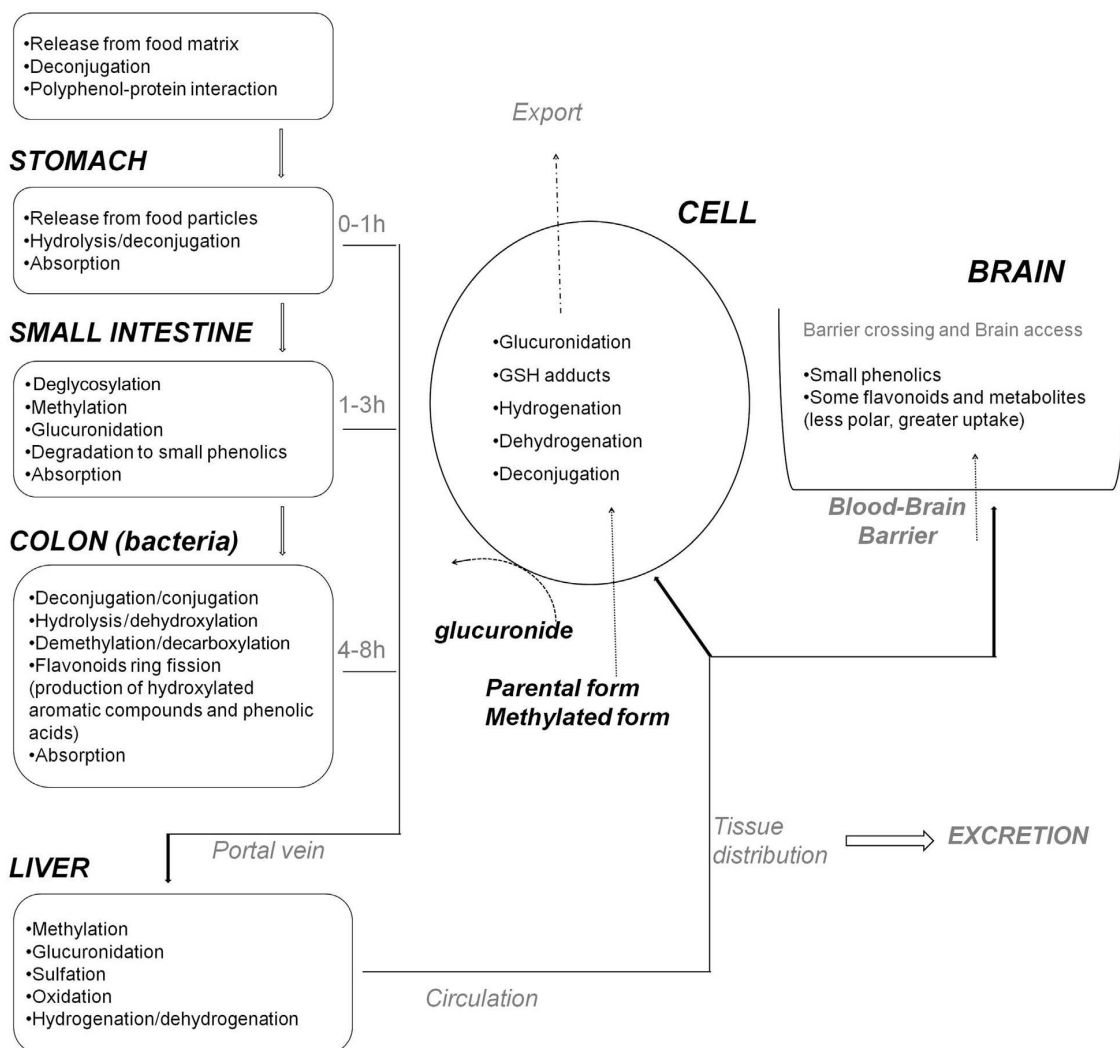


Figure 1.5.: Polyphenolic absorption, metabolism, distribution, and excretion. After dietary intake, polyphenols from their food particles in the stomach. Depending on the presence and type of glycosidic residue, they are deglycosylated and absorbed in the small intestine (glucosides) or pass on to the colon where they are digested by the microbiome, releasing aromatic compounds. Absorbed compounds travel via the portal vein to the liver, where they are derivatized and enter circulation, followed by tissue distribution and excretion.

This figure is derived from Corona et al. [48]

In the colon, not only deglycosylation takes place, but also the flavonoids are metabolized to release new compounds with potential beneficial health effects [48]. The deglycosylation of flavonoids is usually performed by *Bacteroidetes* species, whereas *Clostridium* and *Eubacterium* species perform the ring-cleavage of the aglycone structure. *E. coli* is unable to deglycosylate flavonoids or perform the ring-cleavage [49]. Upon successful absorption, polyphenols are transported through the portal vein to the liver, where further modifica-

tion occurs, often glucuronidation, after which they are distributed in tissues or excreted [46]. The excretion of intact flavonoid structures (flavonoids and their conjugates detected in urine) is below 10 % for flavonols, catechins, flavanones, and anthocyanins, suggesting extensive metabolism of flavonoids after dietary intake [46].

Most research focuses on the oral administration of polyphenols and their glycosides and the response to health traits in humans or model animals. Less attention has been paid to topical applications. Dermal delivery usually is used for local cutaneous targeting, so-called skin deposition, to minimize systemic absorption. The outer most layer of the skin, the *stratum corneum* (SC), poses the main barrier for flavonoids and their glycosides. The passage through the SC is higher for aglycones compared to their glycosides [50]. In general, a lipophilic nature for crossing the SC is required, but in order to cross the epidermis and dermis, a more hydrophilic nature is beneficial, leading to skin deposition of hydrophobic flavonoids able to cross the SC. More hydrophilic flavonoids like naringenin can be absorbed via the skin [50].

Because the glycosidic moiety of biologically active glycosides can not only influence the activity of the molecule itself but also the point of absorption, it can be used as a tool for the design of biologically active ingredients in the healthcare and pharmaceutical industry.

1. Introduction

1.2. Glycosylation of small molecules

Glycosylation of small molecules can be performed chemically using protection group chemistry and classically via Königs-Knorr addition [51, 52], or enzymatically either *in vitro* or *in vivo* [53]. Glycochemistry typically struggles with regioselectivity and configurations of the glycosidic bonds. To solve the regioselectivity issues, laborious protection group chemistry is applied. The long synthetic routes used are usually ineffective and use toxic catalysts while producing high waste quantities [54]. In contrast, enzymatic glycosylation has the advantage of high regio- and stereoselectivity. *In vitro* glycosylation can be performed using cheap co-substrates by glycoside hydrolases, transglycosidases, and glycosylphosphorylases or by glycosyltransferases (GTs) using expensive nucleotide diphosphate (NDP) sugars (Figure 1.6) [55].

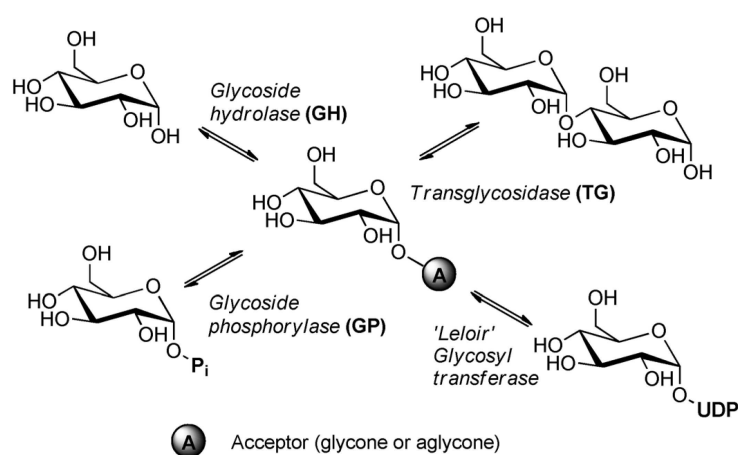


Figure 1.6.: The formation of a glycosidic bond using enzymatic catalysis. Leloir glycosyltransferases naturally perform glycosylation reactions utilizing expensive NDP-sugars. The hydrolytic Glycoside hydrolases and glycoside phosphorylases, as well as transglycosidases, can be used to perform *in vitro* glycosylation, although usually enzyme and reaction engineering is required.

This figure is derived from Desmet et al. [55]

Glycoside hydrolases (GHs) are *in vivo* purely hydrolytic enzymes that split saccharide chains while transferring the cleaved glycosidic moiety to water as an acceptor molecule [55]. GHs can use other molecules as acceptor containing a hydroxyl function, enabling the new formation of a glycosidic bond [56]. However, glycosylation using GHs usually leads to the formation of a mixture of glycosides due to low regioselectivity and show rather low yields. Transglycosidases (TGs) are retaining glycosidases, transferring one saccharide

chain into another. TGs additionally show low activity towards non-carbohydrate acceptor chains and can be engineered for flavonoids transglycosylation using sucrose as sugar donor [57]. The use of cheap substrates like sucrose is a major advantage of the transglycosylation technology.

Glycoside phosphorylases (GPs) naturally function in the degradation of glycosidic bonds by using inorganic phosphate. The resulting glycosylphosphate is a high energy molecule, which allows it to be used in synthesis reaction *in vitro*. However, the yields are quite low, and the substrate spectrum is rather limited. Of the few known GPs most utilize glucose-1-phosphate [58]. Furthermore, GHs, TGs, and GPs often require high aglycone concentrations, which can be very expensive [59].

Glycosyltransferases are very efficient catalysts, able to glycosylate with nearly 100 % efficiency, but are not often employed *in vitro* due to their very expensive NDP-sugar co-substrates [53]. However, there is a large variety of NDP-sugars available, with potential beneficial activities. These more complex sugars are more challenging to transfer using GHs, TGs, or GPs, although they have been shown to be produced by TGs using novel sucrose analogs [60]. For more detailed information on *in vitro* glycosylation, please refer to the review from Desmet et al. [55]. In contrast to *in vitro* glycosylation methods, GTs can also be used in an *in vivo* system in which the heterologous host regenerates the expensive NDP-sugars.

1.2.1. Glycosyltransferases

NDP-sugar dependent glycosyltransferases, often termed Leloir glycosyltransferases, were firstly discovered by Luis F. Leloir (Nobel Prize 1970), able to catalyze the formation of glycosidic linkages using activated sugar donors to nucleophilic acceptor molecules. GTs predominantly form O-glycosides, nevertheless also N-, S-, or C-glycosides are observed [4]. In contrast to Leloir glycosyltransferases utilizing NDP-sugars, non-leloir glycosyltransferases may utilize lipid phosphates or unsubstituted phosphates. In general, GTs can adopt one of three folds, namely GT-A or GT-B or GT-C (figure 1.7)

So far all GT-C fold GTs are non-Leloir, membrane bound GTs, using lipid phosphate sugar donors [61]. In contrast to GT-B, the GT-A fold is divalent metal ion-dependent, in

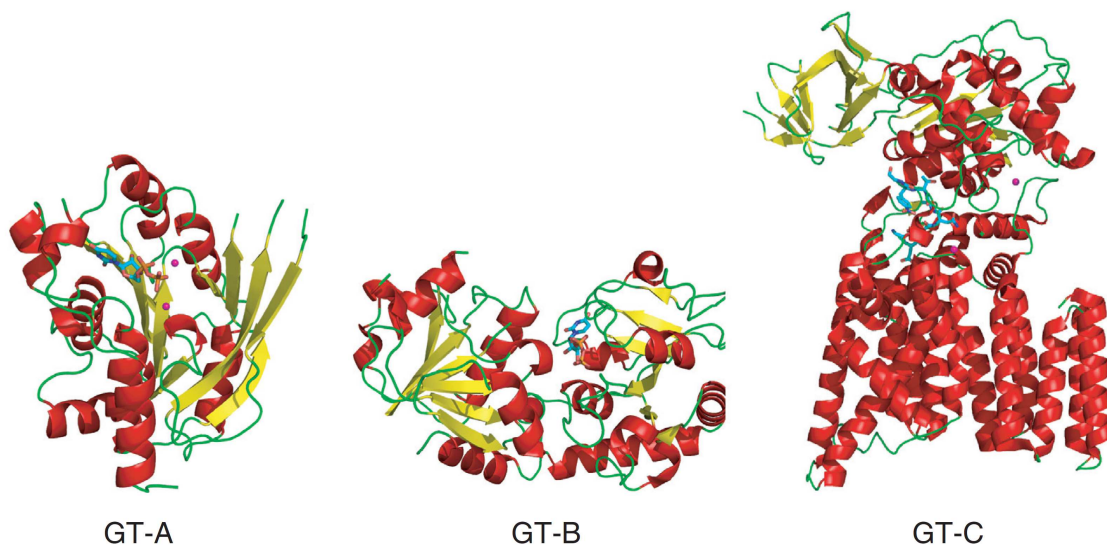


Figure 1.7.: 3D structure of GT-A, GT-B, and GT-C fold adopted by glycosyltransferases. In contrast to GT-B, GTs of the GT-A fold are metal ion-dependent, whereas GT-C fold GTs are so-far all non-Leloir GTs using lipid phosphate sugar donors. This figure is derived from Gloster [61]

which the metal ion aids in the departure of the leaving group by stabilizing the charged phosphate groups of the NDP-sugar donor [61]. GT-B GTs possess two $\beta/\alpha/\beta$ Rossmann-like domains, which are not as tightly associated to each other and the active site lies in the cleft between the two domains [4, 61]. The N-terminal domain binds the acceptor molecule and the C-terminal domain binds the NDP-sugar [62]. GT-B enzymes are independent of metal, and the leaving group departure is facilitated by active site residues [61].

The reaction mechanism of GTs can be either retaining or inverting regarding the stereochemistry of the anomeric atom of the sugar donor, and both inverting and retaining GTs are found in GT-A and GT-B fold glycosyltransferases [2]. The reaction mechanisms between inverting and retaining GTs are different (figure 1.8). Inverting GTs work via an S_N2 -like reaction mechanism, in which a nucleophilic attack by the acceptor at the anomeric carbon is performed. The active-site contains a base catalyst that deprotonates the nucleophile of the acceptor. The deprotonation leads to the direct S_N2 -like displacement of the phosphate leaving group [4]. For retaining GTs, the reaction mechanism is not as conserved as for inverting GTs and may not be attributed to a single mechanism [61]. A common mechanism observed is an S_Ni internal return mechanism, in which the leaving group interacts with the attacking nucleophile [61, 63]. Detailed reviews with further information on glycosyltransferases were published by Lairson et al. [4] and Gloster [61].

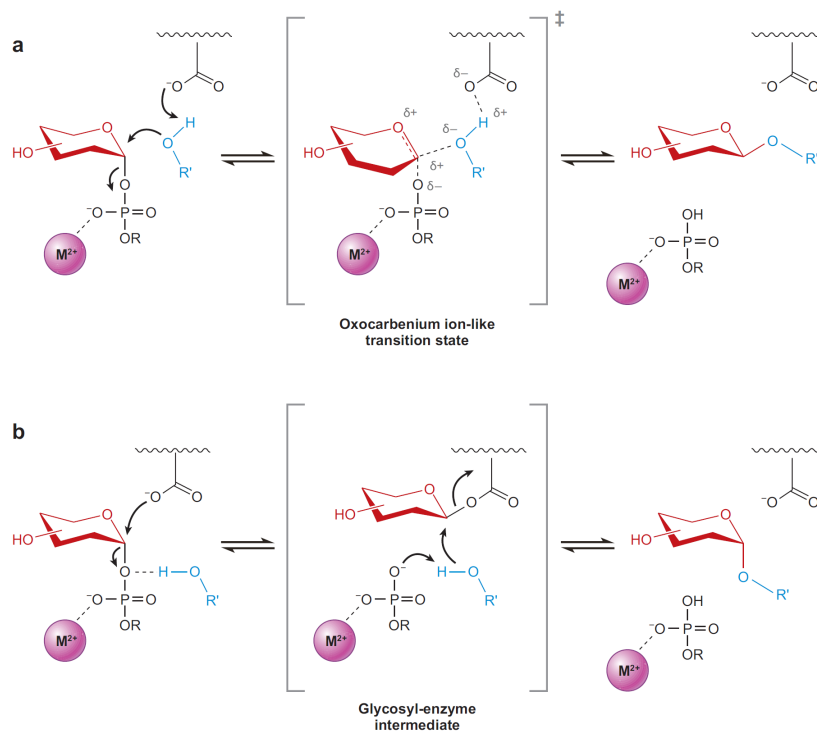


Figure 1.8.: Reaction mechanism of inverting and retaining glycosyltransferases. Inverting GTs (a) facilitate a nucleophilic attack by the acceptor via an S_N2 -like reaction mechanism, whereas retaining GTs commonly use an S_Ni internal return mechanism in which the leaving group interacts with the attacking nucleophile. This figure is derived from Lairson et al. [4]

Most natural product glycosyltransferases belong to the GT family 1 [62]. GT1 glycosyltransferases follow the GT-B fold with an inverting reaction mechanism and catalyze the transfer of sugar moieties from activated NDP-sugars to lipophilic acceptor molecules, including terpenes, steroids, macrolides and polyphenols [4]. In previous research, Rabausch et al. discovered a promiscuous GT, GtfC, in a metagenomic screening approach of the river Elbe sediments (Hamburg, Germany) [1]. GtfC is able to glycosylate flavonoids in whole-cell biotransformations using *E. coli* as the host organism, showing potential as a platform enzyme to produce novel flavonoid rhamnosides.

1.2.2. Glycosylation of flavonoids by GtfC

The most abundant flavonoid glycosides found in nature are the 3-*O*-glycosides of flavonols, e.g., isoquercitrin, as well as the 7-*O*-glycosides of flavones, isoflavones, and flavanones. After initial discovery of GtfC by Rabausch et al. [1] the reaction products of glycosyltransferase C using different polyphenolic substrates including flavones (chrysin, diosmetin),

1. Introduction

isoflavones (genistein, biochanin), flavonols (quercetin, kaempferol) and flavanones (hesperetin, naringenin) were determined by NMR, produced in whole-cell biotransformation approaches using *E. coli*, recombinantly expressing the glycosyltransferase [64]. GtfC is able to produce various flavonoid *O*-rhamnosides (Figure 1.9)¹.

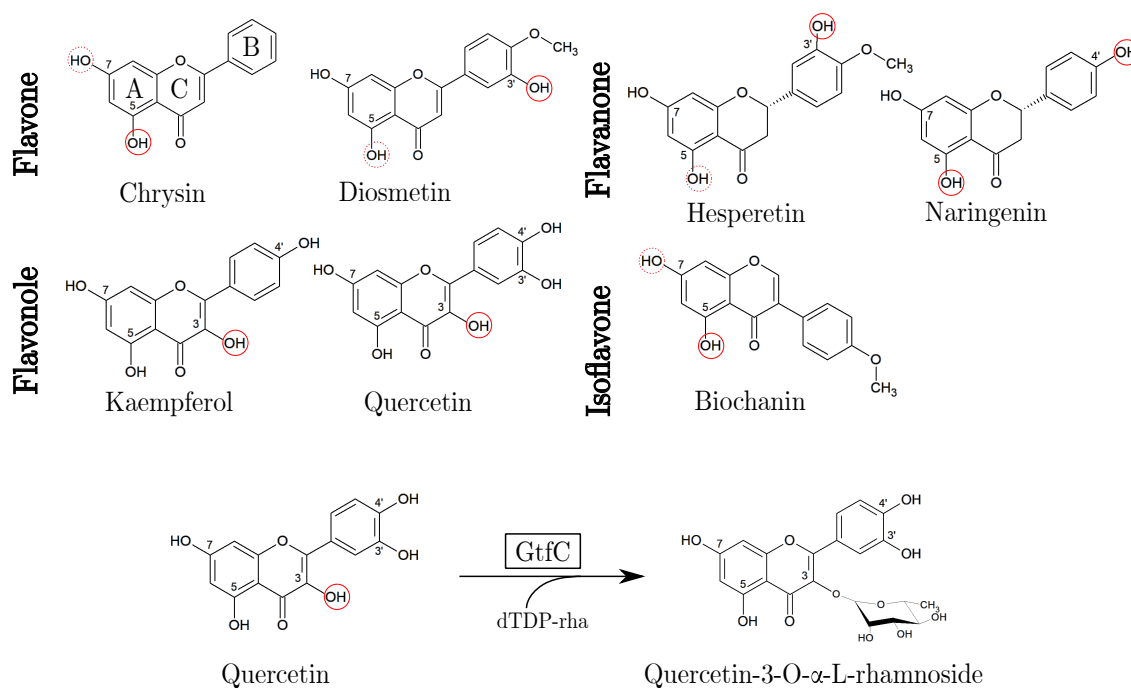


Figure 1.9.: Rhamnosylation of flavonoids by glycosyltransferase C. NMR confirmed hydroxyl functions addressable by GtfC are highlighted with red circles (major product) and dotted circles (side products). Flavonoid rhamnosides were produced in whole-cell biotransformations.

This figure is adapted from Ruprecht et al. [64]

The reaction products of chrysin, diosmetin, biochanin A, and hesperetin, produced in biotransformations with GtfC, were so far unknown rhamnosides [64]. Interestingly, GtfC can address the low reactive C5 hydroxyl function at the A-ring of flavones, isoflavones, and flavanones. The reduced reactivity at C5-OH group is resulting from intramolecular H-bonds with the C-4 carbonyl group [65]. GtfC formed 5-OH rhamnosides as main products for chrysin and biochanin A, where the only other OH group left is the C7-OH at the A-ring (figure 1.9). However, the C5-OH is a minor product formed by GtfC in biotransformations of hesperetin or diosmetin, where the C3'-OH at the C-Ring is available. When the C3-OH at the A-ring of flavanols is available, GtfC produces mainly the 3-O rhamnosides and no 5-OH rhamnosides [64].

¹The production and purification was performed by T. V. Heyer and NMR elucidation by Erhard T. K. Haupt

1.3. Metabolic engineering

Metabolic engineering is a multidisciplinary field aiming for the development of microbial strains for the efficient production of chemicals or biomaterials. For the biotechnological industry to be competitive with the petrochemical industry, very high production titers are needed [66]. In contrast to bulk chemicals, more complex natural products as, e.g. terpenoids, phenylpropanoids, polyketides, or alkaloids, represent interesting candidates for biotechnological production, as their chemical synthesis is inefficient and their natural extraction is limited [67]. Metabolic engineering was first recognized as a scientific discipline in 1991 [68] and has since then evolved into a systems metabolic engineering approach. Modern metabolic engineering tries to integrate systems biology approaches (metabolomics, proteomics, transcriptomics), synthetic biology (pathway assembly, fine-tuning of gene expression and genome engineering), pathway modeling and evolutionary engineering (laboratory evolution) [69]. For modern systems metabolic engineering, it is of great importance to consider the complete bioprocess (figure 1.10), which is generally composed of three major stages, i.e. strain development, fermentation, and separation/purification process [69].

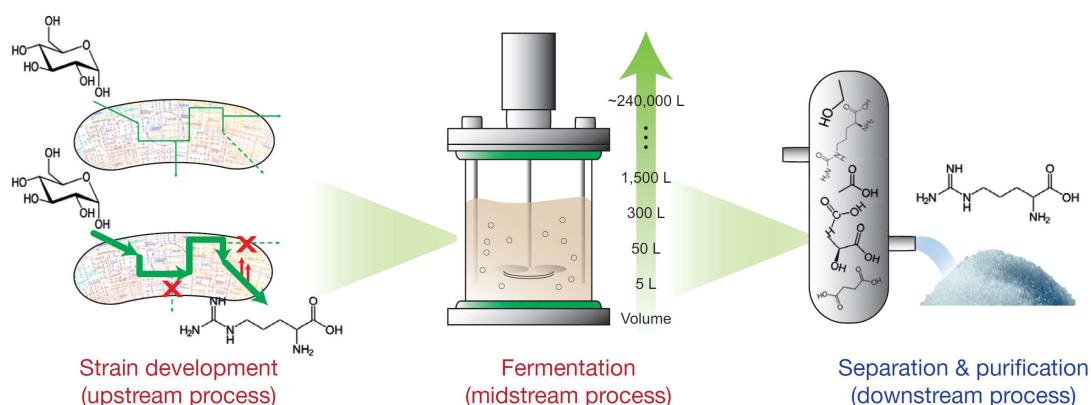


Figure 1.10.: Major bioprocess stages relevant to metabolic engineering. Modern metabolic engineering considers not only strain development but practices a holistic approach considering all major bioprocess stages, i.e., strain development, fermentation, and purification of the product.

This figure is derived from Lee and Kim [69]

1. Introduction

1.3.1. Metabolic engineering in a cyclic manner

Generally, metabolic engineering should be performed in a cyclic manner. A metabolic engineering cycle consists of an *in silico* design-, organism engineering-, screening- and a process development-phase, followed by a scaled-down experiment, which is used to assess the performance and identify new targets for a new engineering cycle (figure 1.11).

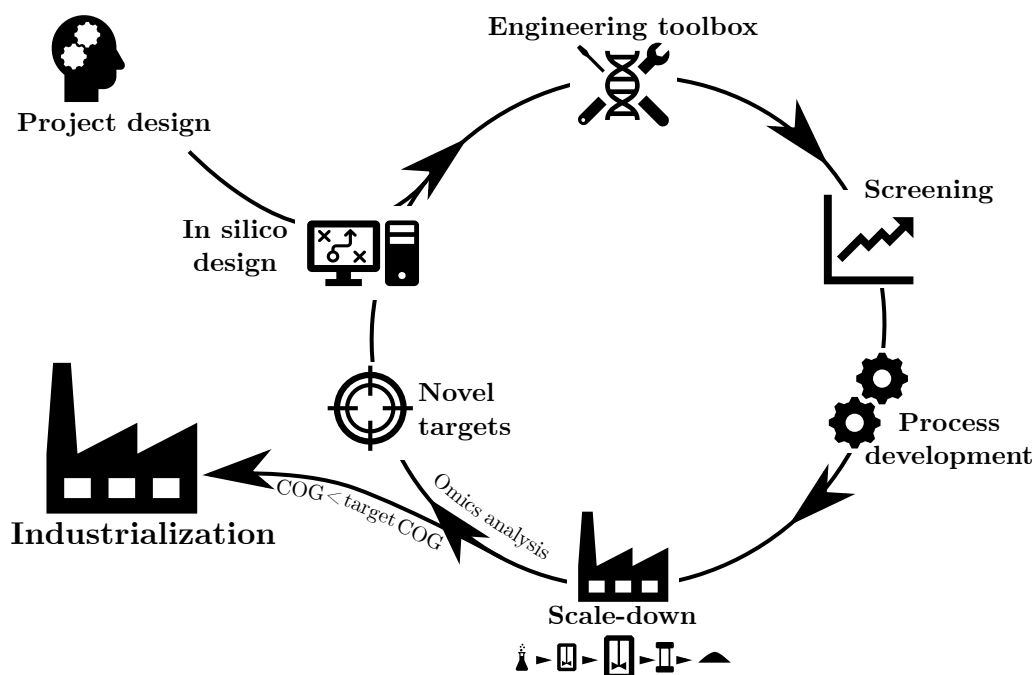


Figure 1.11.: General metabolic engineering cycle composed of design-, engineering-, screening-, process development-phase and a scaled-down experiment for a non-natural producer. After a first engineering cycle, an omics (i.e., metabolomics, proteomics, transcriptomics) experiment should be performed on a scaled-down experiment to identify new targets for a subsequent engineering cycle. As soon as the cost of goods (COG) is reached, industrialization can be performed.

The Project design phase of a metabolic engineering project should ideally define critical project objectives that include technical, economic, legal, and regulatory requirements of a product and strain. The economic analysis should include a target cost of goods (COG), comprising all manufacturing costs needed per kilogram of product, including, e.g., material-, energy, and utilities -, labor- and maintenance and depreciation costs [70]. The industrial and regulatory design of a bioprocess is a very challenging task for an academic environment and usually requires collaboration with an industrial partner. As metabolically engineered strains are usually genetically modified strains, they and their products are regulated by GMO regulations which have to be taken into account for the

desired use case and the country in which the product is supposed to be released, which influences the base-strain of choice for a metabolic engineering project.

After the definition of key parameters, the project design phase starts with the selection of a heterologous host strain for engineering. To choose a suitable host for metabolic engineering, various considerations can be taken into account, including knowledge about preceding engineering strategies for the desired product, availability of key metabolites or cofactors for production in the host strain, ability of the host strain to degrade the available feedstock, tolerance of the host strain towards the desired product, and last but not least the availability of engineering tools. Many metabolic engineering projects are based on *Saccharomyces cerevisiae*, and *E. coli* strains as their metabolism, physiology, and genome sequences are known, and a wide variety of engineering tools are available. The initial *in silico* design phase chooses a pathway or a combination of pathways leading from the feedstock (carbon source, often glucose or sucrose) to the desired product. Pathways can be modeled *in silico* using, e.g., flux-based reconstruction analysis. Different natural sources of genes within a pathway are used to construct pathways. The design phase furthermore pays attention to metabolic flux enhancement, which can be done by various methods, e.g., enzyme engineering, pathway balancing, overexpression of genes, variation in gene sources, cofactor engineering, or gene deletions. [67]

The design phase is tightly connected to the available engineering toolbox for an organism. Gene deletions can be efficiently performed in *E. coli* via a Lambda Red system derived from the lambda red bacteriophage, or recently developed CRISPR/CAS9 methods. The balancing of pathways can be performed by combining promoter-, ribosome binding site (RBS)-, and terminator-libraries with different strengths; these pathways can either be assembled using *in vitro* or *in vivo* methods. Pathways can be engineered onto plasmids or into genomes. Enzyme engineering might be required for a specific activity or a reduced side-product formation, or to create feedback-insensitive mutants. Transport into and out of the cells is dependent on knowledge about different transport systems.

Usually, a screening method for the production of the compound needs to be developed to enable its quantification. Screening capability is a very crucial part and is often considered to be the bottleneck in metabolic engineering projects. Creating large promoter RBS libraries require a high amount of screening effort. Nowadays, the increased screening

1. Introduction

demands are met by a high degree of automation using microwell plate assays or even fluorescent activated cell sorting of single performant cells expressing a bioluminescent sensor.

In systems metabolic engineering, the production process should be developed in concert with the production strain, including the optimization of carbon sources, media development, feed-strategies, and abiotic parameters as, e.g., pH value and dissolved oxygen rate. Process development should ideally directly include the DSP process and should be seen as a holistic approach, in which a scaled-down version of an industrial bioprocess is created. The scaled-down bioprocess should imitate the industrial process as closely as possible, including a seed trajectory, a production plant bioreactor, followed by cell harvest and product purification.

To assess the productivity of an engineering cycle, the scaled-down experiment should be performed in which omics data (metabolomics, proteomics, transcriptomics) is gathered, and the economics of the scaled-down process is calculated. The Omics data gathered is then used to identify new targets and bottlenecks of production after initial engineering and pathway constructions. The resulting data is then reintroduced into *in silico* design and metabolic flux enhancement for the second cycle of engineering. As soon as the cost of goods in the scale-down experiment is lower than the target defined in the project design phase, the process can be scaled-up, and industrialization can be performed. In order to create a strain, capable of industrial production, development times of 10 years are not unusual. To reduce long development times, high-throughput techniques in combination with a systems biological approach are employed [69].

1.3.2. *Escherichia coli* as metabolic engineering chassis

Due to the intensive knowledge of its metabolism, physiology, and growth conditions, in combination with the availability of a wide array of engineering tools, *E. coli* has become the primary host for metabolic engineering projects. *E. coli* is a commensal inhabitant of the human colon firstly discovered in 1885 by Theodor Escherich while investigating the commensal flora of newborn infants [71]. *E. coli* is a gram-negative, rod-shaped bacterium, facultative anaerobic, mesophilic bacterium with a size of 0.5 to 1 μm , belonging to the

family of Enterobacteriaceae in the class of γ -proteobacteria [72]. After the isolation of *E. coli* K-12 in 1922 [73], the bacterium became a model organism and is to date one of the most studied microorganisms. The main reason for the intensive use of *E. coli* for metabolic engineering is the high degree of knowledge and tools freely available and easily accessible for *E. coli* through databases like EcoCyc [74]. For a more detailed examination of *E. coli* K-12 strains utilized in metabolic engineering, please consult the recently published review of Pontrelli et al. [75].

1.4. Aim of this thesis

In preceding work by Rabausch et al. [1], the metagenomic rhamnosyltransferase GtfC was identified, and its potential for the production of flavonoid rhamnosides was shown. Interesting properties for applications in the healthcare and pharmaceutical industry were identified for naringenin and hesperetin rhamnosides. The central goal of this work was to metabolically engineer *E. coli* to achieve the production flavonoids rhamnosides, especially of hesperetin and naringenin, in a g/L scale. Therefore, hesperetin and naringenin were utilized as model substrates throughout this work. To achieve a more holistic approach, Tanja V. Heyer was tasked in her Ph.D. thesis with the process engineering, including up- and downstream-process of the production process.

In Part I the metabolic engineering of *E. coli* is described coupling the growth of *E. coli* on dextrans of starch to the rhamnosylation of model substrate hesperetin by GtfC. Furthermore, the applicability of the engineered strain is shown for the production of kaempferol-3-*O*-rhamnoside (afzelin) and quercetin-3-*O*-rhamnoside (quercitrin). The metabolic engineering work of Part I was published in *Metabolic Engineering* in 2019; the full paper is given in the appendix.

At a certain point, our working group had acquired over 20 glycosyltransferases, which showed different NDP-sugar specificities. To be able to combine these glycosyltransferases with different NDP-sugars in a glycorandomization approach for flavonoids, a modular approach was needed. In Part II, a modular plasmid system able to tackle this task, is described, enabling the use of *d*TDP-glucose, *d*TDP-rhamnose, UDP-glucose, UDP-rhamnose, and UDP-glucuronic acid as NDP sugar donors and combining them with the corresponding glycosyltransferases for flavonoid glycosylation.

As the glycosyltransferase platform technology progressed, a need was discovered for engineering GTs with a specific activity in order to reduce unwanted side products, increase production titers, or shift NDP-sugar dependency of GTs. Part III deals with the development of a new activity screen for glycosyltransferases that shows potential for increased throughput in GT engineering using a spin-off of the classic Blue/white screening method, used regularly in molecular biology.

Part I.

Growth-coupled rhamnosylation of
flavonoids in *Escherichia coli*

2. Introduction

The degradation of flavonoid glycosides in the human colon is a community effort, in which *Bacteroidetes* species cleave the initial glycosidic bond. In this process, the aglycone is released, which is further metabolized through ring cleavage by *Clostridium* or *Eubacterium* species. *E. coli* K-12 is unable to perform the hydrolysis of the glycosidic bond or the ring cleavage of the aglycone structure [49]. Furthermore, *E. coli* does not possess a flavonoid glycosyltransferase or other flavonoid modifying enzymes, making it a good host for heterologous expression of foreign GTs. In addition to its wide use in metabolic engineering and the great variety of tools available [75], this inability to degrade the substrate and product of interest make *E. coli* K-12 a suitable host strain for a whole-cell biotransformation approach. The whole-cell biotransformation approach uses the advantage of a living host cell, that constantly regenerates the expensive nucleotide sugar donors (figure 2.1) [76–81].

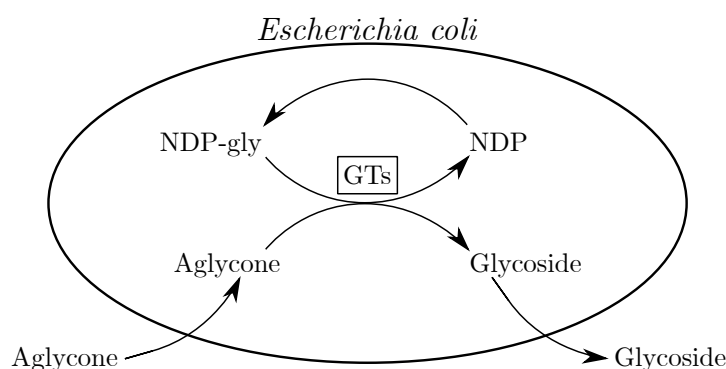


Figure 2.1.: Glycosylation in whole-cell biotransformations. The aglycone is added to a growing *E. coli* culture heterologously expressing a glycosyltransferase. *E. coli* naturally regenerates NDP-sugars, and the produced glycosides are primarily found in the culture supernatant.

In whole-cell biotransformation, the aglycone is added to a growing *E. coli* culture, heterologously expressing a glycosyltransferase. The aglycone is taken up by *E. coli* and

2. Introduction

is glycosylated using a cytoplasmic GT and an NDP-sugar as co-substrate. The glycoside is primarily found in the supernatant of *E. coli* cultures, simplifying its purification.

The transport of flavonoid aglycones and glycosides is performed in *E. coli* by a yet unknown mechanism. Generally, there are different paths to cross a cell membrane, i.e., active transport or passive transport, that can be performed with the help of transporters, termed facilitated diffusion, or simple diffusion across membranes [82]. The transport of flavonoids across membranes is a scientific topic of much controversial debate [82, 83]; up to date, no specific import protein has been identified in *E. coli* facilitating the diffusion or actively transporting flavonoids and their glycosides. Nearly all glycosides are found in the extracellular media of whole-cell biotransformations, suggesting an export mechanism. The Ph.D. thesis of Tanja Plambeck indicated the involvement of the outer membrane channel TolC, showing increased production of flavonoid rhamnosides upon overexpression.

2.1. Metabolic engineering strategies

Engineering strategies to increase the glycosylation capabilities of *E. coli* are usually based on the supply of the co-substrate, the NDP-sugar. GtfC was hypothesized to utilize *d*TDP-rhamnose (*d*TDP-rha) which is synthesized in *E. coli* from glucose-1-phosphate (G1P) and *d*TTP by the *rml* operon (RmlABCD), a four-step enzymatic pathway (figure 2.2) [84, 85].

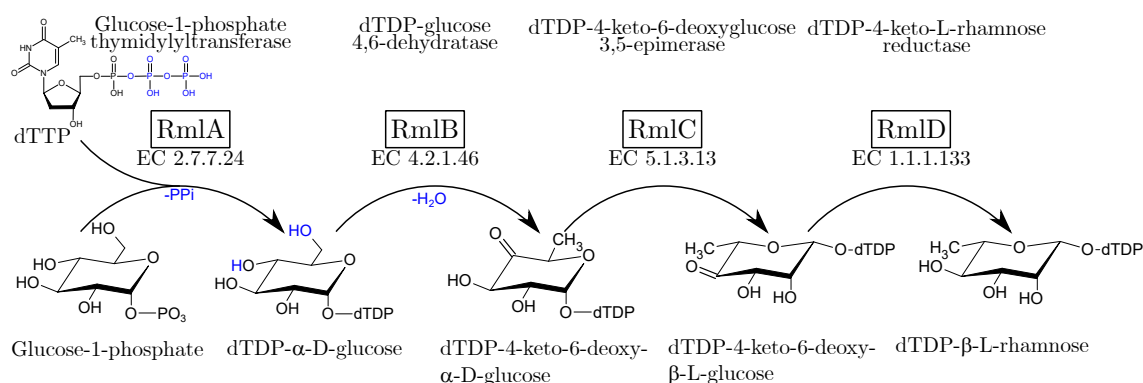


Figure 2.2.: Production of *d*TDP-rhamnose from glucose-1-phosphate via the *rml* operon. Every mol of GtfC co-substrate *d*TDP-rhamnose produced is essentially derived from a mol of glucose-1-phosphate, making it the central precursor for glycosylation reactions.

The regeneration of G1P is crucial for a successful *in vivo* glycosylation process, as for every mol of glycoside produced, essentially, a mol of G1P is required. Consequently, the

generation of G1P to increase *in vivo* glycosylation titers has received a growing interest, resulting in two opposite approaches, i.e., growth-coupled and growth-decoupled glycosylation.

2.1.1. Growth-decoupled glycosylation of flavonoids in *E. coli*

In growth-decoupled glycosylation the genes encoding the glucose-6-phosphate isomerase (*pgi*) and NADP⁺-dependent glucose-6-phosphate dehydrogenase (*zwf*) are usually removed, thereby blocking the energy metabolism through glycolysis and the pentose-phosphate pathway (figure 2.3). In this approach, glucose is channeled to G1P through overexpression of the phosphoglucomutase gene, and a lower level carbon source is fed for energy generation [81, 86–89]. *In vivo* production titers have been rather low using growth uncoupled engineering approaches, below 1 g/L for rhamnosylation using either UDP-rhamnose or *d*TDP-rhamnose as NDP-sugar donor (table 3.2).

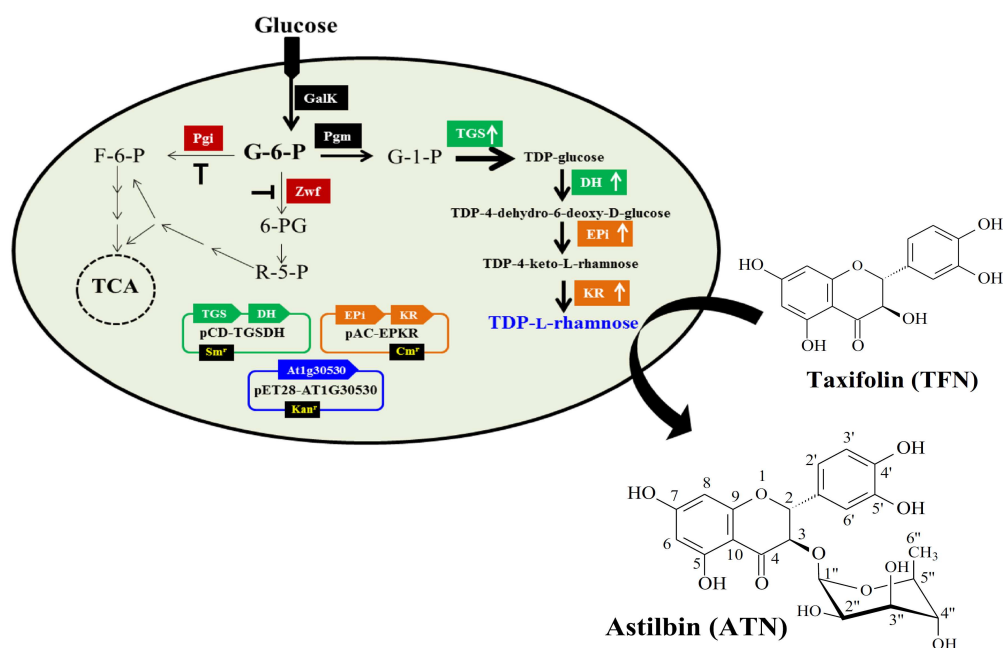


Figure 2.3.: Growth-decoupled glycosylation strategy for flavonoids in *E. coli*. Glucose is fed for the generation of glucose-1-phosphate (G1P) by the overexpressed phosphoglucomutase (Pgm). Deletion of glucose-6-phosphate isomerase (*pgi*) and glucose-6-phosphate dehydrogenase (*zwf*) genes uncouple glucose consumption from biomass formation and a lower level carbon source, e.g., glycerol is fed for biomass generation.

This figure is derived from Thuan et al. [88]

2. Introduction

2.1.2. Growth-coupled glycosylation of flavonoids in *E. coli*

De Bruyn et al. developed a growth-coupled glycosylation system based on coupling sucrose metabolism of *E. coli* to the glycosylation of polyphenols using plant glycosyltransferases (figure 2.4). An integrated sucrose phosphorylase creates a split metabolism consistently producing G1P for glycosylation and fructose, which is used for energy generation. The genes that can link the glycosylation metabolism to the formation of biomass, i.e., *pgm*, *agp*, *ushA*, and *galETKM*, were removed. The development of a growth-coupled approach led to rhamnoside production titers beyond 1 g/L [77].

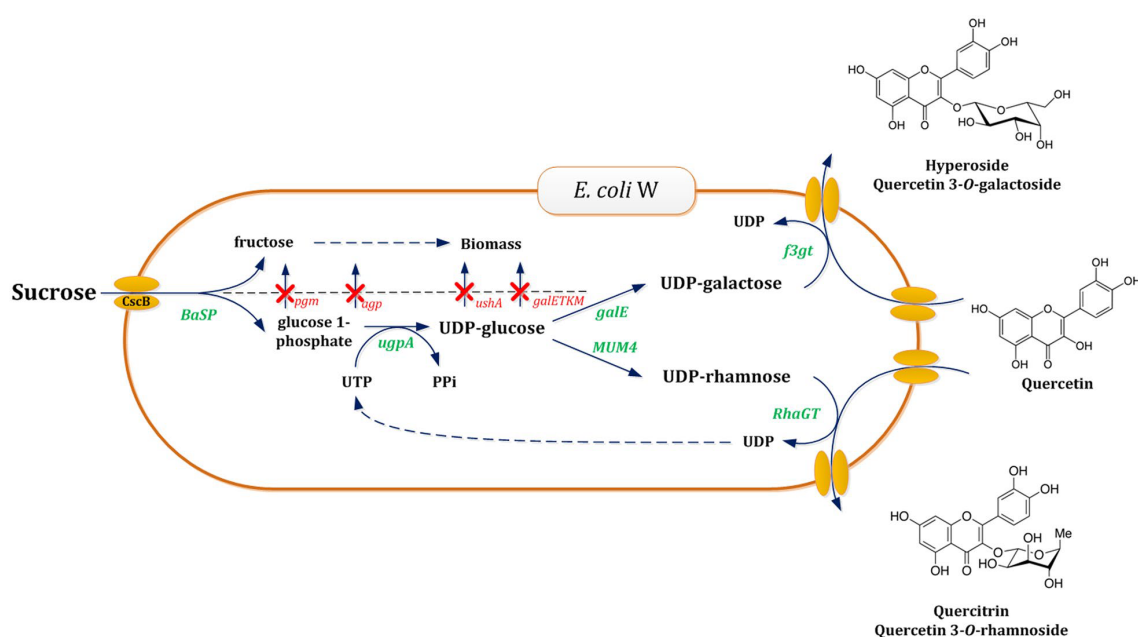


Figure 2.4.: Growth-coupled glycosylation strategy of flavonoids using sucrose as carbon source. Sucrose is fed as carbon source, which is split by a sucrose phosphorylase (*BaSP*) into glucose-1-phosphate (G1P) and fructose. G1P is then used for NDP-sugar production, whereas fructose is utilized for biomass formation. Genes with interconnecting fluxes between biomass and NDP-sugar formation were removed.

This figure is derived from De Bruyn et al. [78]

2.1.3. Growth-coupled glycosylation utilizing the maltodextrin system

In order to increase the rhamnosylation capabilities of *E. coli*, a novel growth-coupled glycosylation approach, making use of the maltodextrin system of *E. coli*, coupling its growth on dextrans of starch to the rhamnosylation of flavonoids by GtfC, was developed (figure 2.5).

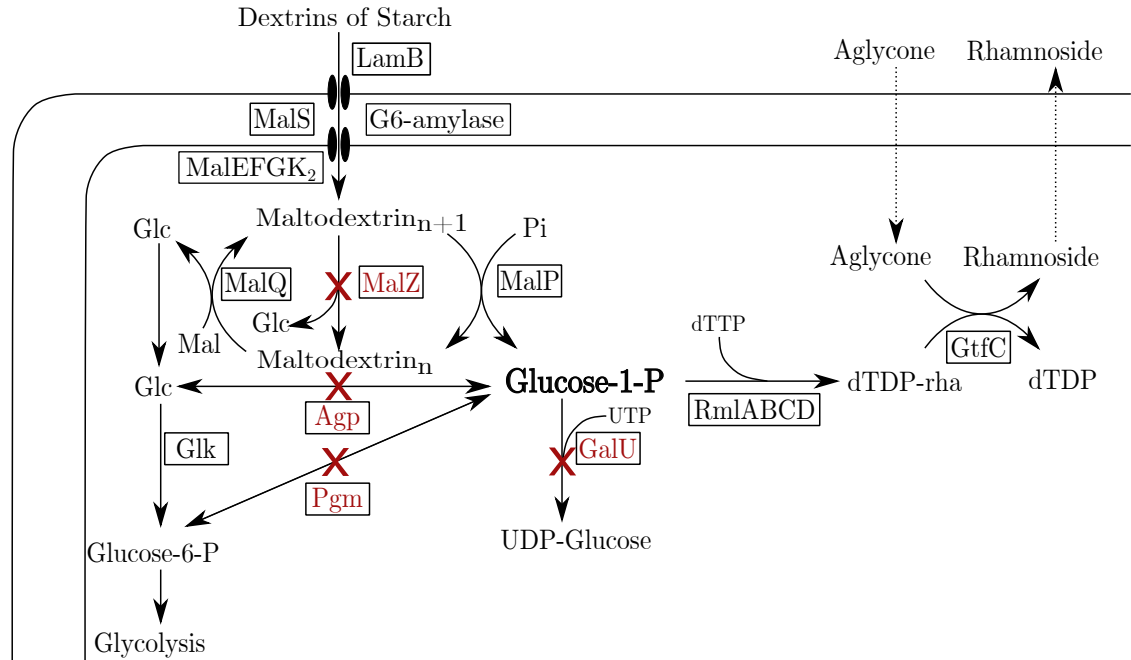


Figure 2.5.: Metabolic engineering approach using dextrans of starch as carbon source. Long-chain dextrans are degraded by G6-amylase to maltohexaose and shorter chain dextrans, which can be taken up and metabolized by *E. coli*. Glucose 1-phosphate (G1P) is produced via the maltodextrin phosphorylase (MalP) as a precursor for *d*TDP-rhamnose (*d*TDP-rha) synthesis, whereas glucose is generated by the amylomaltase (MalQ) and the maltodextringlucosidase (MalZ) to enter glycolysis. G1P can reenter glycolysis through the action of the glucose-1-phosphatase (Agp) or the phosphoglucomutase (Pgm) and can furthermore be converted to UDP-glucose via the action of UTP-glucose-1-phosphate uridyltransferase (GalU). Heterologously expressed rhamnosyltransferase C (GtfC) converts flavonoid aglycones into their corresponding rhamnosides. Red crosses indicate potential genes for removal to increase the rhamnosylation capabilities of *E. coli*.

This figure is derived from Ruprecht et al. [64]

The maltodextrin system of *E. coli* naturally produces glucose-1-phosphate via the action of the maltodextrin phosphorylase (MalP). The maltodextrin system is comprised of the maltose outer membrane channel (LamB), a periplasmic amylase MalS, a maltodextrin ABC transport system MalEFGK₂, and the degradative enzymes MalP, MalQ, and MalZ [90]. The *mal* genes are controlled by the transcriptional activator MalT, which induces

2. Introduction

the transcription of the *mal* genes in the presence of maltotriose. Maltose or long-chain maltodextrins can enter the periplasmic space via the outer membrane pore LamB and bind to the maltose-binding protein. However, only maltodextrin chains of a length up to maltoheptaose are transported and metabolized by *E. coli* [91, 92]. Even though *E. coli* possesses a periplasmic α -amylase, it cannot utilize starch as a carbon source naturally but can be engineered to do so by the expression of an additional periplasmic amylase [93].

Maltose is a rather expensive carbon source and, therefore, not suitable for industrial purposes. To be able to use the cheaper dextrins of starch or starch as a carbon source, an additional periplasmic amylase, the G6-amylase (EC 3.2.1.98) derived from *Bacillus* Sp. 707, was codon-optimized for *E. coli* K-12 and expressed periplasmically, to ensure sufficient starch degradation. The G6-amylase is highly active on starch, preferably cleaving maltohexaose units from amylose chains [94]. The advantage of using the G6-amylase is that these maltohexaose sugars can be transported by the maltose ABC transport system and can be used directly by MalP to create the crucial co-substrate glucose-1-phosphate. The secretion of G6-amylase was performed by the addition of a secretion signal from the periplasmic siderophore binding protein FhuD, which has been shown to be advantageous for periplasmic amylase expression in *E. coli* [95].

The G6-amylase degrades long-chain dextrins to shorter chain dextrins, which are taken up by *E. coli* through its ABC transporter. The shorter chain maltodextrins are further metabolized by MalZ, releasing glucose and by MalQ using Maltose for chain elongation, thereby releasing glucose. In contrast, MalP reduces the chain length by the release of G1P. G1P is then used by *E. coli* to produce *d*TDP-rhamnose, via the *rml* operon, which is used by the heterologously expressed glycosyltransferase to produce flavonoid rhamnosides.

To increase the rhamnosylation capabilities of *E. coli*, genes diverting flux from G1P, *pgm*, *agg*, *malZ*, and *galU* were removed, and the *d*TDP-rha synthesis genes were overexpressed. Furthermore, the effect of increased dextrin degradation via the periplasmic expression of the G6-amylase is shown. The metabolic engineering efforts enabled the production of flavonoid rhamnosides in g/L scale using a metagenomically derived glycosyltransferase.

3. Results & Discussion

3.1. Generation of expression systems for *E. coli* K-12

In previous work, expression systems based on the T7-promotor were used. However, *E. coli* K-12 does not possess a T7 polymerase, necessary for the expression of T7-promotors. For the generation of the expression plasmids see section §10.4. In order to use multiple plasmids in *E. coli*, their origins of replication need to be compatible; too closely related origins will compete for the replication machinery leading to unstable plasmid maintenance. Therefore, three production plasmids with compatible origins of replication were created, firstly glycosyltransferase C is expressed on pTrcHisA, secondly, the *rml* operon on the pCDF-Duet backbone, and finally, the G6-amylase is expressed on a pCC1Fos backbone (figure 3.1).

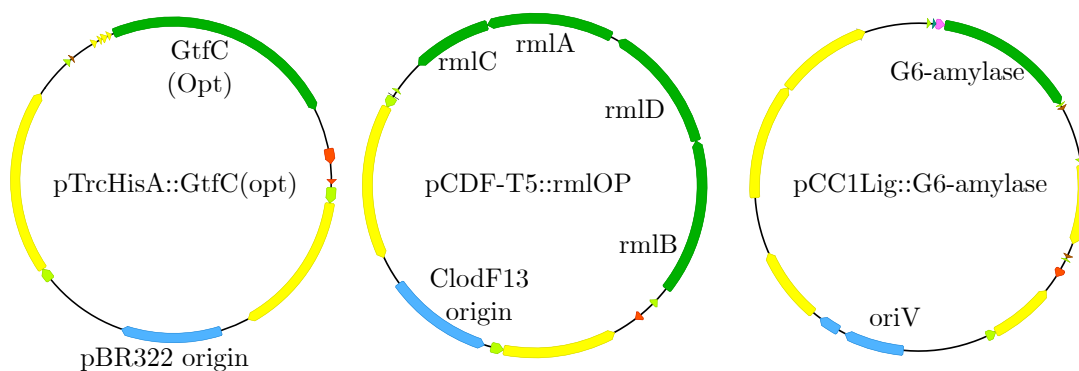


Figure 3.1.: Production plasmids used for glycosylation in *E. coli* K-12. The origins of the three production plasmids are compatible and can be used simultaneously. GtfC is expressed under the control of a *trc* promoter, inducible by IPTG. The *rml* operon (*rmlBDAC*) is expressed under the control of a T5-promotor sequence, also induced by IPTG, whereas the G6-amylase is constitutively expressed using a medium strength constitutive promoter (BBa_J23108).

The G6-amylase activity was verified by using M9-starch (1 %) agar plates containing only starch as carbon source. *E. coli* K-12 transformed with pCC1Lig::G6-amylase was

3. Results & Discussion

able to grow and form clear zones on M9-starch plates, whereas the wild-type strain did not show growth (data not shown). The pCC1 vector origin is a very low copy vector (1-2 copies per cell), making it a good candidate for expression of a gene that should, subsequently, be incorporated into the genome. The created pCC1Lig vector uses a constitutive promoter derived from the Anderson collection (BBa_J23108) for amylase expression. GtfC is expressed on pTrcHisA, a medium copy vector with 15 to 20 copies per cell under the control of a *trc* promoter. The *trc* promoter is a moderately high expression promoter inducible by IPTG. The *rml* operon (*rmlBDAC*) is expressed on a pCDF-Duett backbone under the control of a T5-promotor (IPTG inducible), derived from PQE30. The ClodF13 origin is a medium copy vector with 20 to 40 copies per cell.

3.1.1. Generation of *E. coli* K-12 deletion mutants

In order to potentially increase the rhamnosylation capabilities of *E. coli* K-12, deletion strains of genes, diverting flux from G1P, i.e., *agp*, *pgm*, *malZ*, and *galU*, were created. The confirmation of the gene deletions was performed using distinct verification PCRs, verifying the correct location of resistance cassette insertion, the removal of the target gene, and the FRT mediated removal of the resistance cassette (Example of *malZ* deletion and verification is shown in figure 9.1 on page 87). The deletion strains were used to create production strains, which are shown in table 3.1.

3.2. Hesperetin rhamnosylation in 48 well plates

The metabolic engineering strategy, focused on a constant supply of the co-substrate *d*TDP-rhamnose, to increase the glycosylation capability of *E. coli*. To compare the engineered *E. coli* strains, biotransformations were performed in flower plates in minimal media containing dextrans of starch as sole carbon source and hesperetin as substrate (figure 3.2A). The glycoside formation of the model substrate hesperetin was monitored by HPLC analyses (figure 3.2B; Appendix figure 12.1 on page 126 for additional HPLC chromatograms). To ensure sufficient maltodextrin degradation, all strains used in this study expressed a plasmid-encoded maltohexaosidase (G6-amylase) gene with a codon-optimized secretory signal peptide from *fhuD* [95] if not stated otherwise.

3.2. Hesperetin rhamnosylation in 48 well plates

Table 3.1.: Production strains created in Part I

<i>E. coli</i> strain	Genotype
K-12-WT-A	pCC1Lig::G6-amylase, pTrcHisA::GtfC(opt)
K-12-WT-B	pCC1Lig::G6-amylase, pTrcHisA::GtfC(opt), pCDF-T5::rmlOP
K-12-WT-C	pTrcHisA::GtfC(opt)
UHH_CR1-A	$\Delta malZ$, pCC1Lig::G6-amylase, pTrcHisA::GtfC(opt), pCDF-T5::rmlOP
UHH_CR2-A	Δagp , pCC1Lig::G6-amylase, pTrcHisA::GtfC(opt), pCDF-T5::rmlOP
UHH_CR3-A	Δpgm , pCC1Lig::G6-amylase, pTrcHisA::GtfC(opt), pCDF-T5::rmlOP
UHH_CR4-A	$\Delta galU$, pCC1Lig::G6-amylase, pTrcHisA::GtfC(opt), pCDF-T5::rmlOP
UHH_CR5-A	Δpgm , $\Delta galU$, pCC1Lig::G6-amylase, pTrcHisA::GtfC(opt), pCDF-T5::rmlOP
UHH_CR5-B	Δpgm , $\Delta galU$, pTrcHisA::GtfC(opt), pCDF-T5::rmlOP
UHH_CR6-A	Δagp , Δpgm , pCC1Lig::G6-amylase, pTrcHisA::GtfC(opt), pCDF-T5::rmlOP
UHH_CR7-A	Δagp , $\Delta malZ$, pCC1Lig::G6-amylase, pTrcHisA::GtfC(opt), pCDF-T5::rmlOP
UHH_CR8-A	Δpgm , $\Delta malZ$, pCC1Lig::G6-amylase, pTrcHisA::GtfC(opt), pCDF-T5::rmlOP

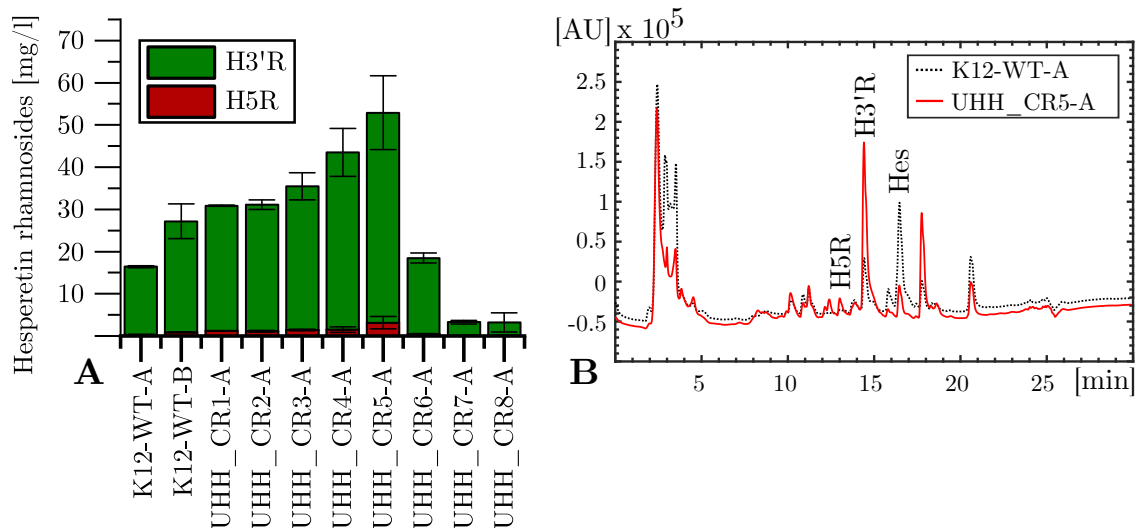


Figure 3.2.: Production of hesperetin rhamnosides in *E. coli* deletion strains. **A:** Biotransformations performed in M9 media (48 well flower plates) containing 1 % dextrans as carbon source. Production strains heterologously expressed Glycosyltransferase C (pTrcHisA::GtfC) and the G6-amylase (pCC1Lig::G6-amylase), all strains except K-12-WT-A overexpressed the native *E. coli* *rml*-operon (*rmlBDAC*), regulated by a T5 promoter (pCDF-T5::rmlOP). Genotypes of the production strains is given in table 3.1. Experiments were performed in triplicates, error-bars indicate confidence intervals based on Students t-distribution ($\alpha=0.05$, $n=3$) **B:** HPLC chromatogram of biotransformation supernatant. H5R, Hesperetin-5-*O*-rhamnoside; H3'R, Hesperetin-3-*O*-rhamnoside; Hes, Hesperetin.

3. Results & Discussion

The level of *d*TDP-sugars can be a rate-limiting factor of glycosylation reactions as concentrations of *d*TDP-rha are about 30-fold lower compared to UDP-glucose in *E. coli* BL21(DE3) [79]. *E. coli* synthesizes *d*TDP-Rhamnose from glucose 1-phosphate via the 4-step enzymatic pathway RmlABCD (figure 2.2). In order to increase *d*TDP-rha levels the native *rml* operon (*rmlBDAC*) of *E. coli* K-12 was overexpressed in a T5-promotor controlled pCDFDuet-1 backbone (pCDF-T5::*rmlOP*). Biotransformations of *E. coli* WT-A, expressing vector encoded GtfC as well as G6-amylase, produced, on average, 16.1 ± 0.2 mg/L of H3'R and 0.3 ± 0.1 mg/L of H5R (figure 3.2). The additional overexpression of the vector encoded *d*TDP-rhamnose synthesis pathway led to a significant increase in hesperetin rhamnoside production to 26.3 ± 4.1 mg/L of H3'R and 0.9 ± 0.1 mg/L of H5R in *E. coli* WT-B after 48 h.

To constantly regenerate *d*TDP-rha, G1P needs to be available throughout the biotransformation which is generated via the action of maltodextrin phosphorylase (MalP) (figure 2.5) [96, 97]. Furthermore, *E. coli* metabolizes maltodextrins liberating glucose by maltodextrin glucosidase (MalZ) and 4-alpha-glucanotransferase (MalQ). G1P can reenter glycolysis through glucose-1-phosphatase (Agp) or phosphoglucomutase-1 (Pgm). The effects of single-gene deletions of *malZ*, *agp*, and *pgm* to maximize the rhamnosylation capabilities of *E. coli* K-12 grown on maltodextrin was investigated. Single gene deletions of the maltodextrin glucosidase gene *malZ*, as well as the deletion of glucose-1-phosphatase gene *agp*, did not lead to significant improvements in productivity. Neither the MalZ deficient *E. coli* strain UHH_CR1-A, nor the Agp deficient *E. coli* UHH_CR2-A showed any significant improvement in hesperetin rhamnosylation with yields of 29.7 ± 0.2 mg/L of H3'R and 1.1 ± 0.2 mg/L of H5R and 30.0 ± 1.1 mg/L of H3'R and 1.2 ± 0.1 mg/L of H5R, respectively (figure 3.2).

In contrast, *E. coli* UHH_CR3-A with perturbed phosphoglucomutase gene *pgm* exhibited increased production of 34.1 ± 3.2 mg/L of H3'R and 1.4 ± 0.2 mg/L of H5R. Pgm deficient *E. coli* strains grown on maltose are known to exhibit Blu phenotype due to the reversed action of MalP at high G1P levels accumulating long-chain maltodextrins that can be stained blue by iodine [98–100].

G1P is the precursor of multiple NDP-sugars. The UTP--glucose-1-phosphate uridylyltransferase (GalU) produces UDP-glc from G1P, at concentrations 30-fold higher com-

pared to *d*TDP-rha in *E. coli* BL21(DE3) [79]. The single deletion of the UTP--glucose-1-phosphate uridylyltransferase gene *galU* in *E. coli* UHH_CR4-A had the strongest effect on the production of hesperetin rhamnosides with an average conversion of 42.0 ± 5.6 mg/L of H3'R and 1.5 ± 0.6 mg/L of H5R. GalU deficient strains produce a deep-rough phenotype, exhibiting a truncated core LPS leading to an increased sensitivity to hydrophobic agents due to a lower diffusion barrier [101–104]. The central role of UDP-Glc in LPS synthesis indicates that a GalU deficient strain might also exhibit increased uptake of the hydrophobic hesperetin, boosting the conversion through higher substrate concentrations in the cytoplasm. Interestingly, RmlA, catalyzing the first enzymatic step in the *d*TDP-rha biosynthesis, is also competitively inhibited by UDP-glc [105]. Thus, the deletion of *galU* might have a ternary effect: the increased production may be attributed to reduced competitive inhibition of the overexpressed RmlA, increased uptake of the substrate hesperetin, and a higher *d*TDP-rha concentration due to eliminated formation of UDP-glc from G1P.

RmlA is not only subject of competitive inhibition by UDP-glc but also feedback inhibited by its product *d*TDP-glucose [106]. Competitive feedback inhibition can generally be relieved through high substrate concentrations, in this case, G1P and *d*TTP. Increased G1P levels and reduced UDP-glc levels should be present in the Pgm and GalU double mutant *E. coli* UHH_CR5-A. *E. coli* UHH_CR5-A led to the highest amount of 49.7 ± 8.7 mg/L of H3'R and 3.2 ± 1.4 mg/L of H5R (figure 3.2). All other double deletion combinations of the examined genes *agg*, *malZ*, *pgm*, and *galU* had no synergistic effect on hesperetin rhamnosylation or even were contra-productive compared to the single deletions. In comparison to *E. coli* WT-A the productivity was increased threefold in engineered *E. coli* UHH_CR5-A.

3.3. Hesperetin rhamnosylation in batch fermentations

As the aim of the study was to create performant production strains for preparative glycoside production, the best performing *E. coli* UHH_CR5-A strain was evaluated in high cell density bioreactor conditions. The experiments were performed in a parallel bioreactor system, using Terrific broth (TB) media to achieve high product formation. As a benchmark, a 24 hours batch fermentation of *E. coli* WT-C only expressing GtfC was performed in TB-media containing an additional 5 % of starch dextrins. *E. coli* WT-C was able to produce 296 ± 51 mg/L of H3'R and 54 ± 10 mg/L of H5R (figure 3.3A). The *E. coli* *pgm* and *galU* double mutant UHH_CR5-B overexpressing the native *E. coli* *rml*-operon showed an increased production of 548 ± 25 mg/L of H3'R and 72 ± 3 mg/L of H5R with a supplement of 5% (w/v) starch dextrins after 24 h.

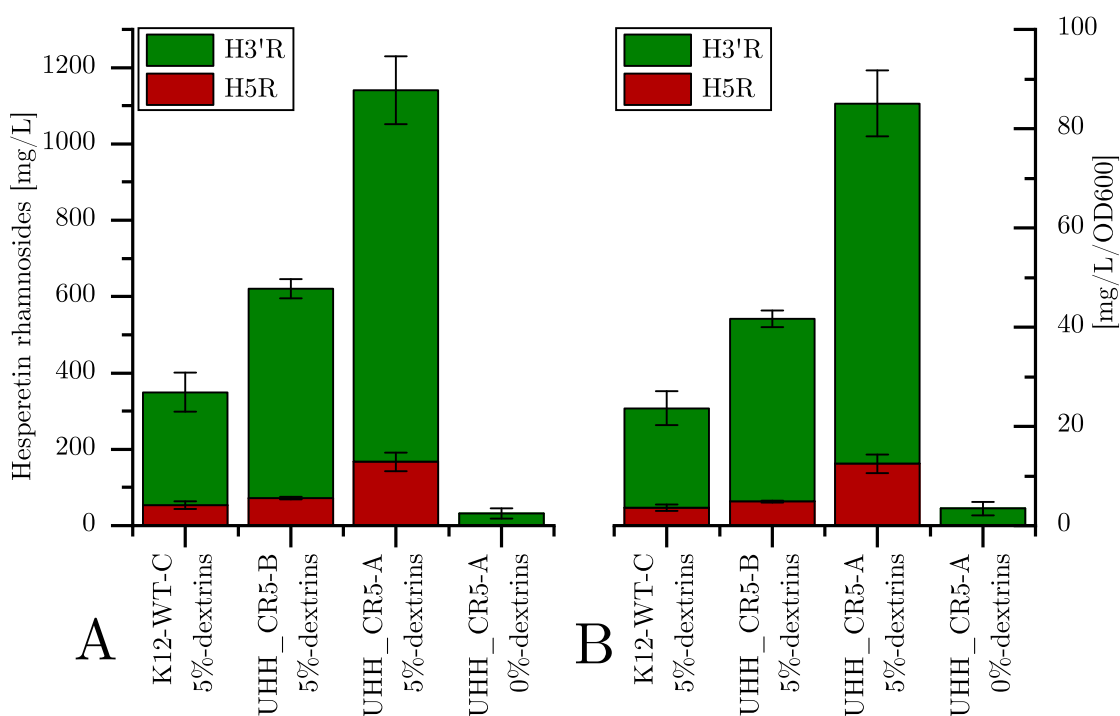


Figure 3.3.: Hesperetin rhamnosylation in *E. coli* batch fermentations. **A:** Hesperetin rhamnosylation in 24 h batch fermentations in mg/L **B:** Hesperetin rhamnosylation normalized for optical density. Genotypes of Production strains (table 3.1): K-12-WT-C (WT, pTrcHisA::GtfC(opt)), UHH_CR5-B (Δ pgm, Δ galU, pTrcHisA::GtfC(opt), pCDF-T5::rmlOP), UHH_CR5-A (Δ pgm, Δ galU, pCC1Lig::G6-amylase, pTrcHisA::GtfC(opt), pCDF-T5::rmlOP). Fermentations were performed in quadruplicates, error-bars indicate confidence intervals based on Student's t-distribution ($\alpha=0.05$, $n=4$).

3.3. Hesperetin rhamnosylation in batch fermentations

E. coli is only able to import and utilize maltodextrin chains up to maltoheptaose, whereas longer chains are not metabolized [91]. To ensure sufficient dextrin degradation a maltohexaosidase (EC 3.2.1.98, G6-amylase) gene from alkalophilic *Bacillus* sp.707 was constitutively expressed and secreted into the periplasm using a codon-optimized secretion signal of FhuD, showing advanced amylase activities [95]. The G6-amylase degrades the longer chain dextrans, reducing the size to accessible chain length, predominantly forming maltohexaose units [94, 107]. *E. coli* UHH_CR5-A, expressing the extracellular G6-amylase for increased dextrin hydrolysis, produced a total amount of 1,140 mg/L composed of 973 ± 89 mg/L of H3'R and 167 ± 25 mg/L of H5R, respectively (see figure 4A). Thus, the presence of G6-amylase seemed to nearly double the productivity of UHH_CR5-A. These product concentrations are comparable to the state of the art glycosylation platform producing 1.12 g/L of quercetin-3-O-rhamnoside in 30 hrs [78].

As a control for dextrin dependency, a biotransformation was performed without supplementation of starch dextrans in TB media. Without dextrans, the production of hesperetin rhamnosides by *E. coli* UHH_CR5-A expressing G6-amylase and overexpressing the *rml*-operon diminished to 32 ± 13 mg of H3'R, whereas H5R production could not be detected after 24 hs (Figure 4A). This clearly indicates the coupling of glycosylation to dextrin metabolism in *E. coli* UHH_CR5-A. In *E. coli* UHH_CR5-A the *pgm* gene was removed. Pgm is responsible for the interconversion of G6P and G1P (figure 2.5), which is required for the synthesis of *d*TDP-rha. Without dextrin supplementation *E. coli* UHH_CR5-A can hardly produce G1P, as the primary source of G1P would be produced via the anabolism of G1P, which is strongly depressed in Pgm deficient *E. coli* strains [98, 108].

To exclude any cell density dependencies, the biotransformations yields were normalized against the determined optical densities at 600 nm (figure 3.3B). The different production titers observed could not be attributed to differences in cell densities as the same relation of yields was observed after normalization. UHH_CR5-B overexpressing the *rml*-operon was nearly two times more performant than *E. coli* WT-C, and the additional integration of the G6-amylase in *E. coli* UHH_CR5-A almost doubled the productivity compared to UHH_CR5-B (figure 3.3B).

3.4. Glycosylation in solid fed-batch fermentations

Dextrin supplementation in presence of G6-amylase proved to be crucial in 24 hours batch fermentations. To determine the influence of a repeated feed of dextrans, an additional 50 g/L of dextrans was added after 24 h of biotransformation. These solid fed-batch fermentations were compared to 48 batch fermentations without additional dextrin feed. The space-time yield (STY) for the main product H3'R was determined in both setups, using linear regression between the measured titer datapoints. As the batch and solid-fed-batch processes were identical up to 24 h, no significant differences were expected in production during this period. Consistently, batch and fed-batch fermentations yielded similar concentrations of 973 ± 89 mg/L and 920 ± 55 mg/L of H3'R and 167 ± 25 mg/L and 137 ± 4 mg/L of H5R, respectively (figure 3.4).

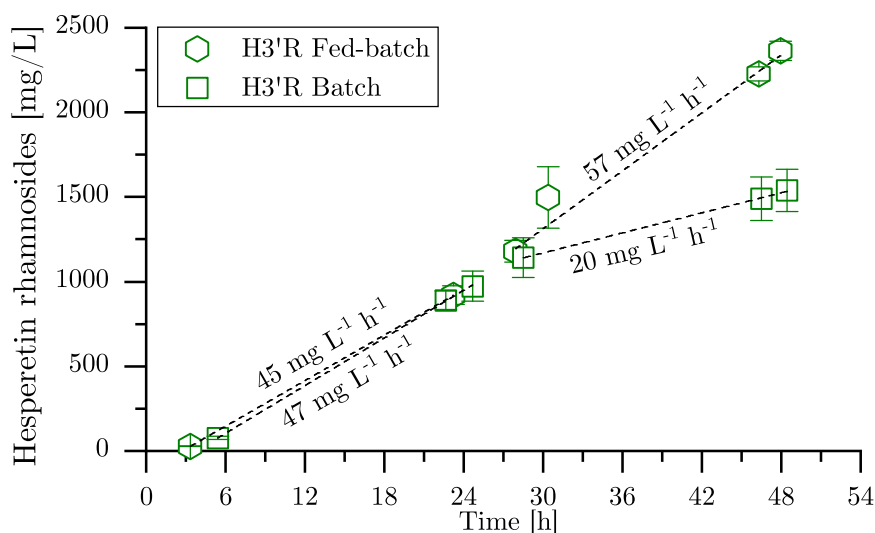


Figure 3.4.: Comparison of batch and solid-fed-batch fermentations of *E. coli* UHH_CR5-A. Biotransformations of *E. coli* UHH_CR5-A expressing Glycosyltransferase C (pTrcHisA::GtfC(opt)), the dTDP-rhamnose synthesis operon (pCDF-T5::rmlOP) and G6-amylase (pCC1Lig::G6-amylase). In fed-batch mode, a feed of 50 g/L solid dextrans was supplemented after 24 h, whereas in batch mode, the reaction was continued to 48 h without any supplementation. Space-time yields were calculated between data points using linear regression (dashed lines) in the intervals between the start and 24 h of incubation as well as after dextrin feed and 48 h of fermentation. As a side product, 367 ± 12 mg/L and 273 ± 20 mg/L H5R were produced after 48 h in fed-batch and batch mode, respectively. Fermentations were performed in quadruplicates, error bars indicate confidence intervals based on Students t-distribution ($\alpha=0.05$, $n=4$).

The calculated STY of the batch process was 47 mg/L/h, and the STY of the solid fed-batch was 45 mg/L/h between the start of biotransformation and 24 h of reaction.

3.4. Glycosylation in solid fed-batch fermentations

During the second 24 h of fermentation, the STY of H3'R in the batch process decreased by more than 2- fold to an average of 20 mg/L/h. *E. coli* UHH_CR5-A in batch mode produced 1489 ± 128 mg/L of H3'R and 273 ± 20 mg/L H5R after 48 h. In solid fed-batch mode, the production rate remained constant at 57 mg/L/h, leading to a final production titer of 2362 ± 57 mg/L of H3'R and 367 ± 12 mg/L of H5R after 48 h.

To show that the engineered production strain *E. coli* UHH_CR5-A can produce high-level rhamnosides of other flavonoids than hesperetin, biotransformations using quercetin and kaempferol as aglycones were performed. Within 48 hrs of biotransformation, *E. coli* UHH_CR5A was able to produce 4.32 g/L of quercetin-3-O-rhamnoside and 1.92 g/L of kaempferol-3-O-rhamnoside (table 3.2). In recent rhamnosylation approaches, the titers of flavonoid rhamnosides produced usually were clearly below concentrations of 1 g/L. Only De Bruyn and colleagues were able to produce 1.18 g/L of quercitrin after 30 h biotransformations in an engineered *E. coli* W strain. This strain was metabolically engineered to enable the coupling of production and growth on sucrose [78]. The coupling of glycosylation to growth on maltodextrin in this study enabled a total production of 4.3 g/L of quercetin-3-O-rhamnoside, 2.4 g/L of hesperetin-3-O-rhamnoside, and 1.9 g/L of kaempferol-3-O-rhamnoside, which is to the best of my knowledge the highest published production of flavonoid rhamnosides.

Table 3.2.: Flavonoid rhamnosylations in *E. coli* exceeding 100 mg/L titers

Conversion Product	Titer [g/L]	Carbon Source	Time [h]	Reference
Quercetin-3-O-rha	4.32 ± 0.14	Dextrins of starch	48	This Study
Hesperetin-3'-O-rha	2.36 ± 0.05	Dextrins of starch	48	This Study
Kaempferol-3-O-rha	1.92 ± 0.53	Dextrins of starch	48	This Study
Quercetin-3-O-rha	1.18	Sucrose	30	De Bruyn et al. [78]
Kaempferol-3-O-rha	0.416	Sucrose	48	De Bruyn et al. [78]
Fisetin-3-O-rha	0.403	Sucrose	48	De Bruyn et al. [78]
Fisetin-3-O-rha	0.34	Glucose	48	Parajuli et al. [109]
Kaempferol-3-O-rha	0.2	Glucose	48	Kim et al. [110]
Morin-3-O-rha	0.12	Sucrose	48	De Bruyn et al. [78]

Part II.

Development of a modular glycosylation platform

4. Introduction

In Part I the glycosylation of *E. coli* K-12 was increased through a growth-coupled approach, combining the natural maltodextrin metabolism of *E. coli* with the overexpression of the *rml* operon leading to *d*TDP-rhamnose synthesis and a heterologous overexpression of glycosyltransferase C. GtfC is known to be quite promiscuous towards different flavonoid substrates, enabling the production of various new actives for the pharmaceutical and healthcare industry [1, 64]. Several of the newly created flavonoid rhamnosides were screened in *in vitro* assays, performed by Bioalternatives (France), to determine new potentially exciting candidates for commercialization. *In vitro* testing was performed using normal human epidermal keratinocytes (NHEK), normal human dermal fibroblasts (NHDF) and normal human epidermal melanocytes (NHEM). A striking example of different bioactivities depending on the glycosidic moiety of a flavonoid was observed for naringenin (figure 4.1).

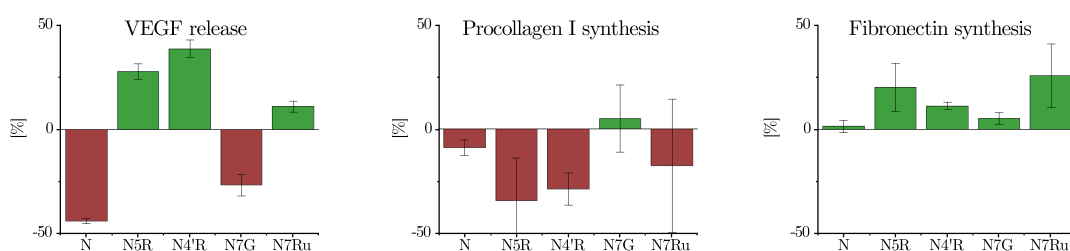


Figure 4.1.: *In vitro* bioactivities of naringenin glycosides. Naringenin-5-O-rhamnoside (N5R) and naringenin-4'-O-rhamnoside (N4'R) *in vitro* assays compared to commercially available naringenin-7-O-glucoside (N7G) and naringenin-7-O-rutinoside (N7Ru) in relation to untreated samples. Fibronectin, Procollagen I, and VEGF assays were performed by Bioalternatives (France) at 100 μ M concentrations.

The newly produced naringenin-4'-O-rhamnoside (N4'R) and naringenin-5-O-rhamnoside (N5R) were evaluated in comparison to commercially available prunin (naringenin-7-O-

4. Introduction

glucoside, N7G), naringin (naringenin-7-O-rutinoside, N7Ru) and their aglycone naringenin for vascular endothelial growth factor (VEGF) release, procollagen I synthesis and fibronectin synthesis. These assays are used to assess the effects of the compounds for extracellular matrix component synthesis. Interestingly the observed bioactivities varied depending on the glycosidic moiety and could even show opposite effects as observed for VEGF release.

The vascular endothelial growth factor (VEGF) plays an essential role in angiogenesis. Increased VEGF levels are observed locally in wound-healing processes or fracture repair [111], but also play an important role in the formation of cancer tissue [112]. Increased VEGF expression has been shown to accelerate hair growth after depilation, with increased hair follicle size and shaft, whereas a VEGF downregulation led to hair growth retardation in mice [113]. The naringenin rhamnosides showed a stimulatory effect, whereas the aglycone naringenin and N7G showed an inhibitory effect. With an opposite effect between aglycone and glycoside, caution is advised to assess possible deglycosylation mechanisms. A hair growth supplement might turn into a depilatory agent in the presence of α -rhamnosides, which occur widely throughout nature with high activities in yeast and fungi [114].

The *in vitro* activities demonstrate that the glycosidic moiety can be used to tune bioactivities of polyphenols, creating a need for a modular approach to glycosylation, in which glycosyltransferases can be combined easily with NDP-sugar pathways to create glycosides with a desired biological function. However, the prediction of a biological function of the resulting glycoside is so far not possible *in silico*, and extensive testing for the glycosides is required. This “combinatorial biosynthesis approach” is performed *in vivo* by having a gene toolbox for glycosyltransferases and a gene toolbox for nucleotide sugar synthesis genes, which can be combined by using plasmids with compatible origins of replications (figure 4.2). Using promiscuous glycosyltransferases, a wide array of glycosides can be produced for various aglycone structures [115].

4.1. Design of a modular glycosylation platform for flavonoids

In Part I the growth of *E. coli* on dextrans of starch was coupled to the constant supply of G1P to increase the rhamnosylation of flavonoid substances. However, G1P is not only the precursor for *d*TDP-rhamnose but is the precursor of a great variety of NDP sugars, utilized by different glycosyltransferases. In order to combine different glycosyltransferases with corresponding NDP-sugar synthesis genes, a modular plasmid-based approach was designed (figure 4.2).

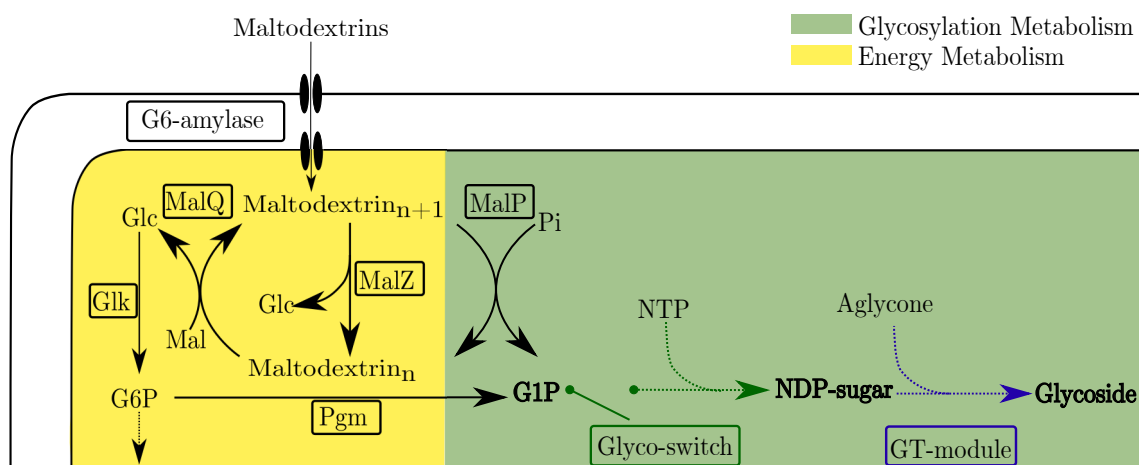


Figure 4.2.: Concept for modular glycodiversification platform using a plasmid-based Glyco-switch and a GT-module. Glucose-1-phosphate (G1P) is the precursor of many different NDP-sugars, which can be utilized by glycosyltransferases, and combined with various aglycone structures. The creation of compatible plasmid modules enables a combinatorial biosynthesis approach.

Using more than one plasmid in *E. coli* requires compatible origins of replication. The origin of replications are assigned to incompatibility groups, in which two plasmids of the same group are not usable within the same host cell. Furthermore, the origin of replication dictates the copy number of the plasmid within a cell. A vector system developed for *E. coli* protein expression using compatible origins of replications and resistance markers is the Duet vector system (Novagen, Germany). For the GT-module, a pTrcHisA (Invitrogen) vector was used as expression-plasmid using β -lactamase (*bla*) for ampicillin resistance and a pBR322 replicon (~ 40 copies). The pCDFDuet-1 was chosen as a base vector for the Glyco-switch, carrying a compatible ClodF13 origin of replication (20-40 copies) with the *aadA* gene conferring streptomycin/spectinomycin resistance.[116]

In the envisioned modular glycosylation approach, an engineered *E. coli* strain is grown

4. Introduction

on maltodextrins to continuously produces G1P; a plasmid-based “Glyco-switch” directs the flux towards the desired NDP-sugar, which is transferred onto an aglycone by the plasmid-expressed glycosyltransferase on the GT-module, producing the desired glycoside. A great diversity of small molecule glycosides can be created using such a combinatorial approach (figure 4.3).

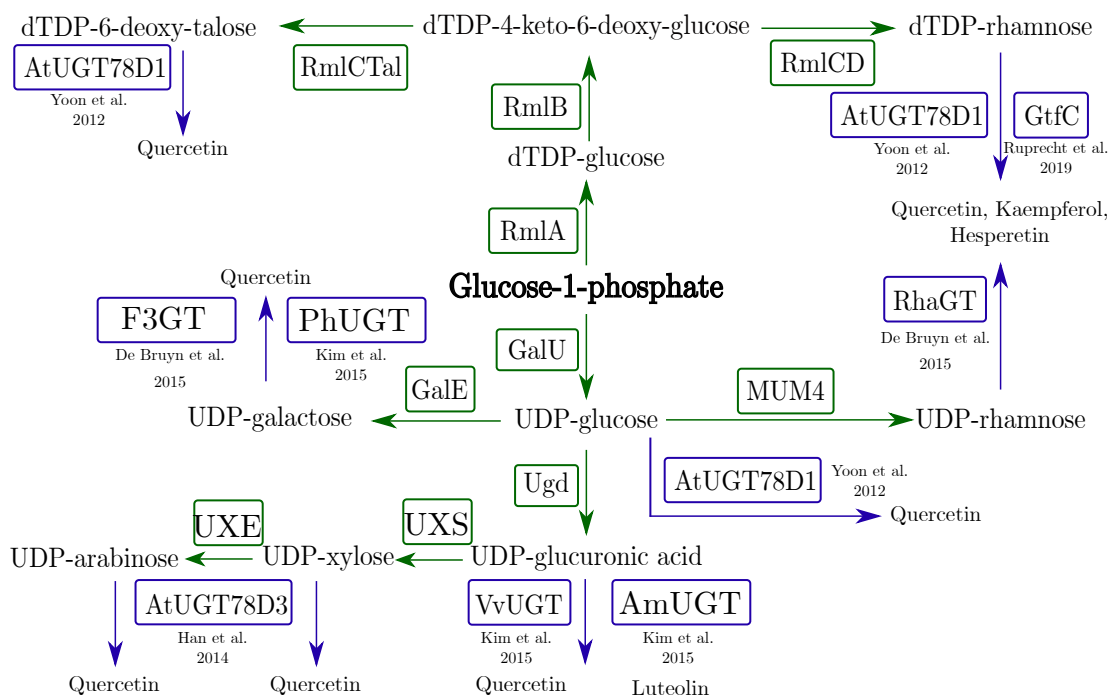


Figure 4.3.: Possible Glyco-switch pathways with corresponding GT-modules. GTs (Blue box) are able to transfer the NDP-sugar, synthesized by the Glyco-switch (Green box), onto flavonoids. Some promiscuous GTs, e.g. AtUGT78D1, are able to transfer more than one type of NDP-sugars.

The Glyco-switch plasmid should ideally have more than one promotor region to express multiple gene pathways, which may become necessary for larger pathways. The pCDF-T5::*rmlOP* plasmid used in Part I, expressed the natural *rml* operon (*rmlBDAC*) under the control of a single T5 promotor. The Glyco-switch for the production of *dTDP*-rhamnose should ideally be build up in 4 steps, cloning firstly *rmlA*, followed by *rmlB*, *rmlC* and *rmlD*. Through this approach, already four potential Glyco-switches can be created. Furthermore, the combination of *rmlAB* is a crucial intermediate step, as *dTDP*-4-keto-6-deoxy-glucose is a branching point for multiple *dTDP* sugars (figure 4.3 and figure 8.1).

4.2. Auto-induction using the maltodextrin system

E. coli growing on glucose as carbon source usually down-regulates the expression of alternative carbon source degradation systems by transcriptional regulation also called catabolite repression. Upon depletion of glucose, the concentration of cAMP rises, leading to an increase in transcription of alternative degradation pathways. Two molecules regulate the expression of MalT, the transcriptional regulator of the maltodextrin system. Firstly it is stimulated by catabolite repression via Crp-cAMP interaction, and secondly, it is regulated by Mlc, a global regulator repressing *malT* transcription depending on the transport status of the glucose specific phosphotransferase system (PTS). [117].

This regulatory combination leads to a low *malT* transcription in glucose-rich media and increased transcription of *malT* and the maltodextrin transport system LamB MalEFGK₂ in glucose depleted media [118]. The transcriptional activator MalT requires maltotriose and ATP for dimerization and subsequent activation of the transcription of the associated promoters. If no active transport of maltose and maltodextrins is present, MalT is inactivated by binding to the transporter MalK, or MalY or Aes (Figure 4.4). Upon active transport of maltodextrins, MalT is released from MalK and the concentration of maltotriose and ATP increases leading to a multimerization of MalT and the full induction of all associated *mal* genes [119, 120].

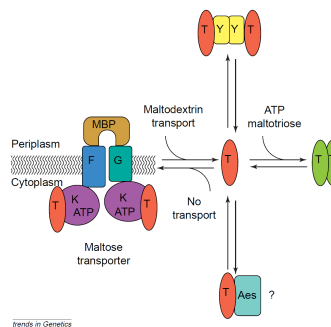


Figure 4.4.: Regulation of MalT activity. In the presence of maltotriose and ATP, MalT dimerizes and activates the transcription of *mal* associated genes. The Mal proteins are given in one-letter abbreviations; inactive monomeric MalT is given in red, and active dimeric MalT is given in green. This figure is derived from Boos [119]

4. Introduction

In industrial applications using IPTG is frowned upon as it is quite expensive in a larger, cubic meter scale. Using the maltodextrin regulation system of *E. coli* to design auto-induced production plasmids, inducing glycosyltransferase and NDP-sugar synthesis genes upon growth on maltodextrins, seemed more than intriguing (figure 4.5). The auto-induced approach leads to a reduction in production costs as no IPTG needs to be supplemented. Furthermore, all production genes will be transcribed as long as maltodextrin is fed as a carbon source, which should lead to a robust production strategy.

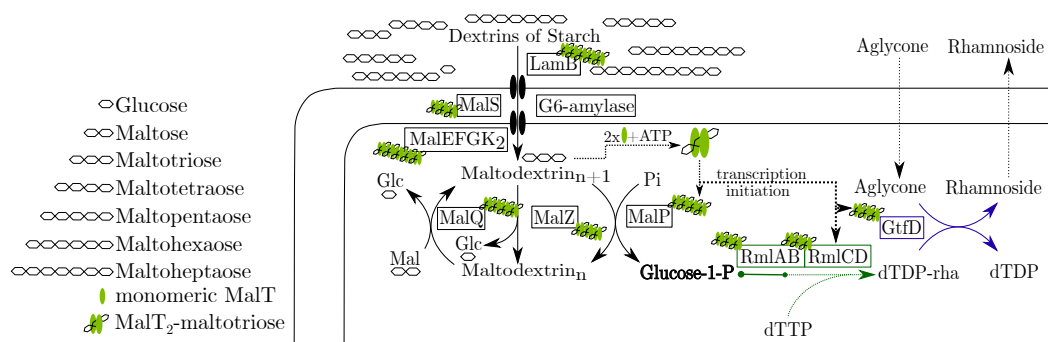


Figure 4.5.: Auto-induction of Glyco-switch and GT-module for the glycosylation of flavonoids using the maltodextrin glucosidase (*malZ*) promoter region. *E. coli* degrading dextrins of starch produces maltotriose. The monomeric transcriptional activator MalT dimerizes in the presence of maltotriose and ATP. The MalT₂-maltotriose complex activates the transcription of all *mal* associated genes, including the synthetic plasmid-based, Glyco-switch, and GT-module. The utilization of maltodextrins thereby ensures the constant production of glucose-1-phosphate and all necessary production genes. The amount of MalT₂-maltotriose complexes represent the amount of annotated MalT binding sites in the promoter region of the respective genes.

The regulon of the maltodextrin system is controlled by the action of MalT, but can be subject to additional regulations as, e.g. cAMP-Crp regulation in the transport system. The only promoter region regulated purely by the action of MalT is the maltodextrin glucosidase promoter region possessing three MalT binding sites. This promoter region was chosen for the creation of maltodextrin dependent expression plasmids. Using the *malZ* promoter region (*malZp*), the expression glycosyltransferase and of the NDP-sugar pathway can be auto-induced, simply by growing on maltodextrins as substrates which are necessary for the growth coupled approach.

5. Results & Discussion

5.1. Genetic design of *E. coli* for modular glycosylation

To create an *E. coli* strain for modular glycosylation, a rational design strategy was performed. The base-strain should ideally be able to produce high glycoside titers, without producing unwanted side-products. Therefore, *E. coli* UHH_CR14 was generated, in which the phosphoglucose isomerase (*pgi*), UTP-glucose-1-phosphate uridylyltransferase (*galU*), the *rml* operon, the glucose-1-phosphate adenylyltransferase (*glgC*), and the UDP-sugar hydrolase (*ushA*) were deleted; furthermore the G6-amyase was integrated for the DNA recombination and repair protein (*recA*). The genetic modifications of *E. coli* UHH_CR14 are shown in figure 5.1; the genotypes of strains created leading up to *E. coli* UHH_CR14 are given in table 5.1.

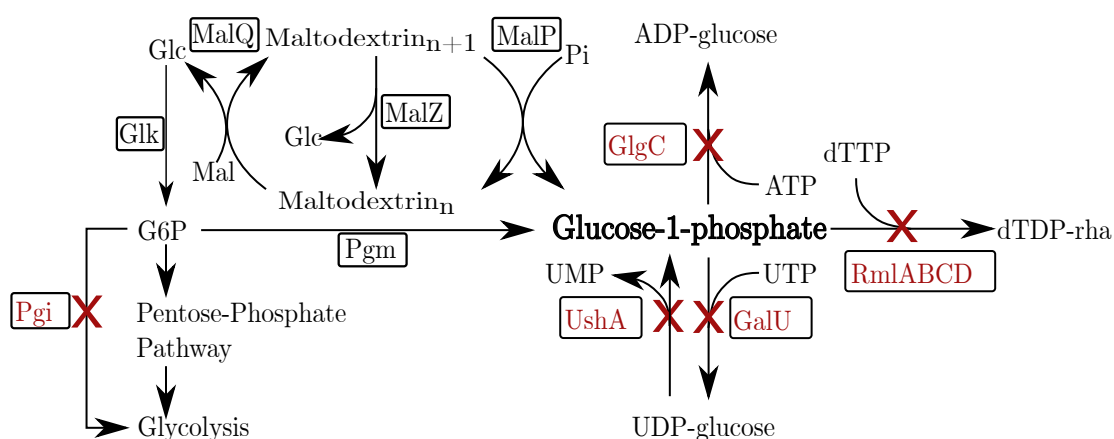


Figure 5.1.: Genetic modification of *E. coli* UHH_CR14, additionally the G6-amyase is integrated for *recA*. To create a base-strain for modular glycosylation genes diverting flux from glucose-1-phosphate were removed. The *pgi* gene was deleted to create a maltose blu phenotype through high G1P concentrations. Furthermore, NDP-sugar synthesis pathways were removed to reduce unwanted side-product formation for promiscuous glycosyltransferases.

5. Results & Discussion

Table 5.1.: Bacterial strains created leading up to *E. coli* UHH_CR14

Strain	Genotype	Source
<i>E. coli</i> UHH_CR9	F^- , λ^- , <i>rph-1</i> , <i>Fnr</i> ⁺ , Δ <i>pgi</i>	This Study
<i>E. coli</i> UHH_CR10	F^- , λ^- , <i>rph-1</i> , <i>Fnr</i> ⁺ , Δ <i>pgi</i> , Δ <i>galU</i>	This Study
<i>E. coli</i> UHH_CR11	F^- , λ^- , <i>rph-1</i> , <i>Fnr</i> ⁺ , Δ <i>pgi</i> , Δ <i>galU</i> , <i>recA::G6-amylase</i>	This Study
<i>E. coli</i> UHH_CR12	F^- , λ^- , <i>rph-1</i> , <i>Fnr</i> ⁺ , Δ <i>pgi</i> , Δ <i>galU</i> , <i>recA::G6-amylase</i> , Δ <i>rmlBDACX</i>	This Study
<i>E. coli</i> UHH_CR13	F^- , λ^- , <i>rph-1</i> , <i>Fnr</i> ⁺ , Δ <i>pgi</i> , Δ <i>galU</i> , <i>recA::G6-amylase</i> , Δ <i>rmlBDACX</i> , Δ <i>glgC</i>	This Study
<i>E. coli</i> UHH_CR14	F^- , λ^- , <i>rph-1</i> , <i>Fnr</i> ⁺ , Δ <i>pgi</i> , Δ <i>galU</i> , <i>recA::G6-amylase</i> , Δ <i>rmlBDACX</i> , Δ <i>glgC</i> , Δ <i>ushA</i>	This Study

Firstly, *E. coli* UHH_CR9 was created by the deletion of the phosphoglucose isomerase (*pgi*) gene in *E. coli* K-12(MG1655). The deletion of *pgi* creates a maltose blu phenotype and ensures high G1P concentrations for NDP-sugar biosynthesis. Pgi catalyzes the second step in glycolysis from glucose-6-phosphate to fructose-6-phosphate. A *pgi* deletion mutant leads to major metabolic changes, rerouting flux through the pentose-phosphate pathway [121]. The metabolic “detour” through the pentose-phosphate pathway creates a maltose blu phenotype [100] and leads to a strong increase in NADPH production [121]. Furthermore, the increased pentose-phosphate pathway-flux leads to an increased nucleotide level [122], as it supplies essential precursors, i.e., D-ribose 5-phosphate for pyrimidine and purine nucleotide biosynthesis [123].

The deletion of *galU* showed the highest production increase in Part I. Therefore, in a second step, the *galU* gene was deleted, creating *E. coli* UHH_CR10. A GalU deficient strain exhibits a deep rough phenotype with increased uptake of hydrophobic substances [101–104] and additionally reduces the flux from G1P to undesired UDP-glc which furthermore competitively inhibits RmlA [105].

Thirdly, the DNA recombination/repair protein RecA was chosen as the integration site for the G6-amylase (*E. coli* UHH_CR11). The G6-amylase proved to be beneficial for glycosylation reactions using maltodextrins or starch as carbon source. RecA plays an essential role in DNA repair and homologous recombination in *E. coli* [124]. Strains deficient in *recA* are known to exhibit higher plasmid stability due to a reduction in plasmid

recombination [125].

In *E. coli* UHH_CR12 the *d*TDP-rhamnose synthesis operon was removed. The removal of the *rml* operon is a necessary step for future applications as the reaction step of RmlB is a branching point for different bacterial *d*TDP-sugars; An *rml* operon deficient *E. coli* strain can be used to create synthetic pathways for *d*TDP sugars without having a constant sink into *d*TDP-rhamnose. It does not always seem necessary to remove competing pathways, especially when overexpressing the desired NDP-sugar pathway and coupling it with a specific GT. However, a non-specific GT will produce side products as shown by Yoon et al. [76], producing quercetin-3-*O*-deoxytalose using *d*TDP-6-deoxytalose with a promiscuous plant GT AtUGT78D1 from *Arabidopsis thaliana* (AtUGT78D1 in figure 4.3). Initially, the GT expressing *E. coli* strain produced mainly quercetin-3-*O*-glucosides and rhamnosides with minute taloside amounts. A deletion of *galU* and *rmlD* significantly reduced by-products and increased the taloside formation, showing the necessity of removing competing pathways with promiscuous GTs and rare NDP-sugars.

Subsequently, the glucose-1-phosphate adenylyltransferase (GlgC) was removed to create (*E. coli* UHH_CR13). GlgC reduces flux from G1P, catalyzing the generation of ADP-glucose. The formation of ADP-glucose catalyzed by GlgC is the first step of glycogen synthesis used in *E. coli* as a storage molecule under growth-limiting conditions, when an excess of carbon source is available. As the storage of G1P into glycogen is unwanted, *glgC* was removed. GlgC deficient strains exhibit a glycogen deficient phenotype, in which the glycogen content decreases to un-measurable amounts [108].

Finally, in *E. coli* UHH_CR14 the *ushA* gene, encoding the UDP-sugar hydrolase was removed, which is able to hydrolyze UDP-sugars, releasing the UMP and the corresponding sugar phosphates, but does not seem to be specific for GDP-, CDP-, ADP- or *d*TDP-sugars [126]. UshA is located to the periplasm, and its activity is inhibited in the cytoplasm as its cytoplasmic 5-nucleotidase activity would be lethal [127]. However, as UshA mutants are often used to increase glycosylation reactions [77, 86, 128, 129].

Using *E. coli* UHH_CR14, a glycosyltransferase (GT-module) can be efficiently coupled to its corresponding NDP-sugar synthesis pathway, which needs to be complemented on a synthetic plasmid (Glyco-switch).

5.2. Generation of Glycoswitch and GT-module

5.2.1. GT-module generation

The GT-module is the plasmid carrying the glycosyltransferase gene. A proof of principle experiment was designed to show the feasibility of auto-induced glycosylation. Therefore, the promoter region of the maltodextrin glucosidase was combined with a ribosome binding site library to balance the transcription and translation of GtfD, a glycosyltransferase derived from *Dyadobacter fermentans*. GtfD is able to rhamnosylate 4-methylumbelliferone (4-MU). A 4-MU screen was performed in 48 well plates to assess malZp-RBS clones of GtfD (Figure 12.2 in the supplementary)¹. The screen led to the identification of clone 44 (denoted pK44::GtfD(opt)), which showed similar production rates to IPTG induced GtfD(Opt) in pTrcHisA [130]. In contrast to pTrcHisA the newly generated pK44 plasmid lacks the transcriptional repressor of the *lac* operon *lacI*. In an opposed approach to repressing transcription (e.g. by *lacI* in T7 promoters), the transcriptional activator MalT was incorporated generating the pK44-MalT::GtfD(opt) plasmid (figure 5.2). The incorporation of MalT should lead to an increase the transcription of all *mal* regulated genes. The generation of pK44 and pK44-MalT were verified using restriction digestion and sanger sequencing (data not shown).

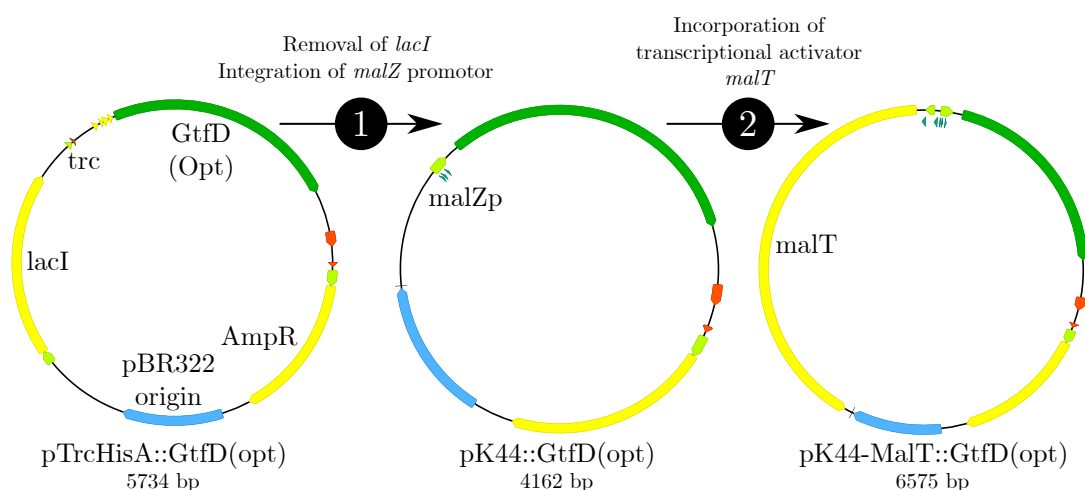


Figure 5.2.: Creation of GT-module plasmid pK44-MalT::GtfD(opt). To create pK44-MaT::GtfD(opt) the *trc* promoter was exchanged with the maltodextrin glucosidase promoter (malZp); in this cloning step the *lac* repressor, *lacI*, was removed. Subsequently, the transcriptional activator MalT was incorporated, generating pK44-MalT::GtfD(opt).

¹The experiments were performed by Max Konersmann in his Bachelor Thesis

5.2.2. Glyco-switch generation

The Glyco-switch plasmid should contain a pathway for the desired NDP-sugar, starting from glucose-1-phosphate. A synthetic DNA fragment was ordered from Eurofins Genomics (Germany), containing maltodextrin glucosidase (*malZ*) promoter regions, to create a compatible, auto-inducible, plasmid. The synthetic fragment was cloned into pCDFDuet-1 (figure 5.3). The cloning step led to the removal of *lacI* from pCDFDuet-1 and exchanged the T7 promoter regions by *malZ* promoter regions while keeping an identical multiple cloning site and terminator sequences, leading to the creation of pCDF-malZp. Subsequently, NDP-sugar synthesis pathways can be integrated into pCDF-malZp, as shown for the *rml* operon. The *rml* operon was cloned from *E. coli* MG1655 genome onto pCDF-malZp in four steps, creating pCDF-malZp::*rmlAB*::*rmlCD* enabling the production of *d*TDP-rhamnose from glucose-1-phosphate. In a similar manner to pCDF-malZp, the high copy-number vector pRSF-malZp was created from pRSF-Duet and subsequently pRSF-malZp::*rmlAB*::*rmlCD* was created.

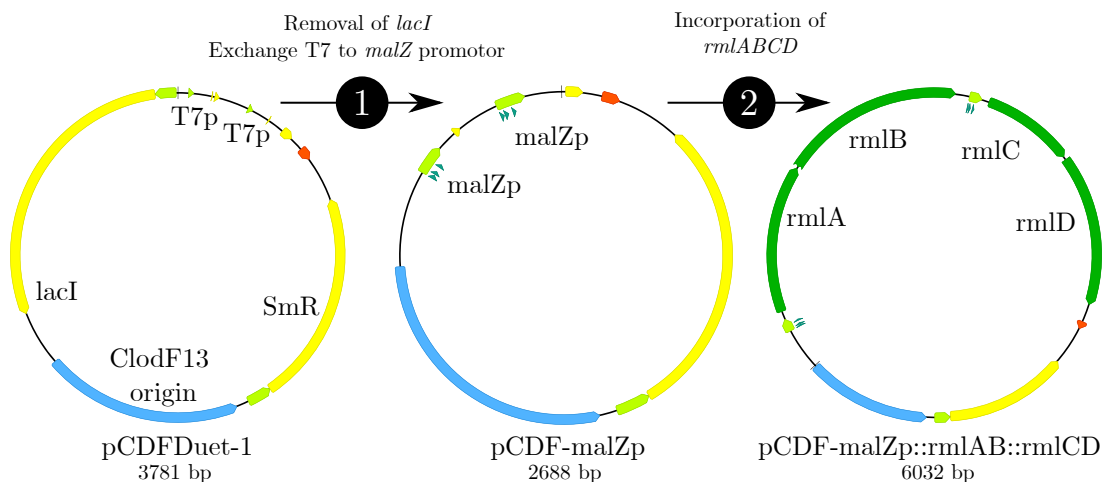


Figure 5.3.: Creation of Glyco-switch plasmid pCDF-malZp::*rmlAB*::*rmlCD*. A synthetic DNA fragment was cloned into pCDFDuet-1, exchanging its T7-promotor regions with maltodextrin glucosidase (*malZ*) promoter regions and simultaneously removing the *lac* repressor *lacI*. The ribosome binding sites, multiple cloning sites, and terminator sequences were left unchanged. pCDF-malZp can be used to express NDP-sugar synthesis pathways starting from glucose-1-phosphate, as shown for the *rml* operon (*rmlABCD*) able to produce *d*TDP-rhamnose from glucose-1-phosphate.

5.3. Naringenin rhamnosylation using Glyco-switch and

GT-module

GtfD was selected as the model glycosyltransferase, derived from *Dyadobacter fermentans*. In contrast to GtfC used within Part I, GtfD has a higher product specificity for 5-OH group of the A-ring of flavonoids, which was at that time, the main focus of new product development. GtfD was codon-optimized for *E. coli* K-12, denoted GtfD(Opt). Naringenin was used as a model substrate for the optimization and development of the platform technology. A list of production strains and their genotypes used within Part II is given in table table 5.2.

Table 5.2.: *E. coli* production strains created and used within Part II

<i>E. coli</i> strain	Genotype
<i>E. coli</i> UHH_CR11-A	$\Delta pgi, \Delta galU, recA::G6\text{-amylase}, pK44::GtfD(opt), pCDF\text{-malZp}::rmlAB::rmlCD$
<i>E. coli</i> UHH_CR11-B	$\Delta pgi, \Delta galU, recA::G6\text{-amylase}, pK44\text{-MalT}::GtfD(opt), pCDF\text{-malZp}::rmlAB::rmlCD$
<i>E. coli</i> UHH_CR11-C	$\Delta pgi, \Delta galU, recA::G6\text{-amylase}, pK44\text{-MalT}::GtfD(opt)$
<i>E. coli</i> UHH_CR12-A	$\Delta pgi, \Delta galU, recA::G6\text{-amylase}, \Delta rmlBDACX, pK44\text{-MalT}::GtfD(opt)$
<i>E. coli</i> UHH_CR12-B	$\Delta pgi, \Delta galU, recA::G6\text{-amylase}, \Delta rmlBDACX, pK44\text{-MalT}::GtfD(opt), pCDF\text{-malZp}::rmlAB::rmlCD$
<i>E. coli</i> UHH_CR13-A	$\Delta pgi, \Delta galU, recA::G6\text{-amylase}, \Delta rmlBDACX, \Delta glgC, pK44\text{-MalT}::GtfD(opt), pCDF\text{-malZp}::rmlAB::rmlCD$
<i>E. coli</i> UHH_CR14-A	$\Delta pgi, \Delta galU, recA::G6\text{-amylase}, \Delta rmlBDACX, \Delta glgC, \Delta ushA, pK44\text{-MalT}::GtfD(opt), pCDF\text{-malZp}::rmlAB::rmlCD$
<i>E. coli</i> UHH_CR14-B	$\Delta pgi, \Delta galU, recA::G6\text{-amylase}, \Delta rmlBDACX, \Delta glgC, \Delta ushA, pK44\text{-MalT}::GtfD(opt), pRSF\text{-malZp}::rmlAB::rmlCD$
<i>E. coli</i> UHH_CR14-C	$\Delta pgi, \Delta galU, recA::G6\text{-amylase}, \Delta rmlBDACX, \Delta glgC, \Delta ushA, pK44\text{-MalT}::GtfW, pCDF\text{-malZp}::galU$
<i>E. coli</i> UHH_CR14-D	$\Delta pgi, \Delta galU, recA::G6\text{-amylase}, \Delta rmlBDACX, \Delta glgC, \Delta ushA, pK44\text{-MalT}::RhaGT, pCDF\text{-malZp}::galU::MUM4$
<i>E. coli</i> UHH_CR14-E	$\Delta pgi, \Delta galU, recA::G6\text{-amylase}, \Delta rmlBDACX, \Delta glgC, \Delta ushA, pK44\text{-MalT}::AmUGT, pCDF\text{-malZp}::galU::ugd$
<i>E. coli</i> UHH_CR14-F	$\Delta pgi, \Delta galU, recA::G6\text{-amylase}, \Delta rmlBDACX, \Delta glgC, \Delta ushA, pK44\text{-MalT}::VVUGT, pCDF\text{-malZp}::galU::ugd$

5.3.1. Proof of principle experiment by *rml* operon complementation

To test the functionality of the modular concept two proof of principle experiments were performed. Firstly, the effect of overexpressing the transcriptional activator MalT was investigated, and secondly the functionality of the Glyco-switch is shown through a complementation experiment of the deleted *rml* operon, leading to the formation of *d*TDP-rhamnose from glucose-1-phosphate. The experiments were performed in 48 h shake flask experiments using TB-Dex medium containing 5 % dextrins of starch as carbon source.

To assess the effect of the transcriptional activator MalT, expressed on the GT-module, *E. coli* UHH_CR11-A, expressing codon-optimized GtfD on pK44::GtfD(opt) and the *d*TDP-rhamnose forming Glyco-switch pCDF-malZp::*rmlAB*::*rmlCD*, was compared to *E. coli* UHH_CR11-B, containing pK44-MalT::GtfD(opt) instead of pK44::GtfD(opt) (figure 5.4).

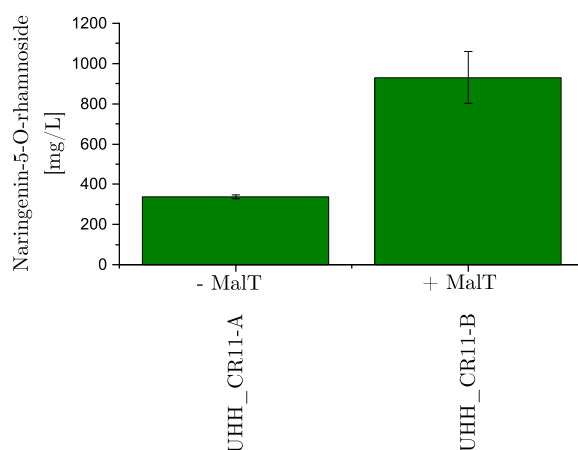


Figure 5.4.: Production of Naringenin-5-O-rhamnoside by auto-induced GtfD. *E. coli* production strains were grown in 10 mL TB-Dex media at 28 °C and 170 rpm. 5 g/L Naringenin were added as aglycone. N5R production was monitored after 48 hrs. Production strains are listed in table 5.2. (n=3) N4'R is produced as a minor side-product.

Using naringenin as model substrate UHH_CR11-A produced 338 ± 10 mg/L naringenin-5-O-rhamnoside (N5R). Incorporation of the transcriptional activator MalT in UHH_CR11-B led to a substantial increase of N5R production to 930 ± 129 mg/L, which corresponds to a nearly three-fold production increase. The *malT* gene product was firstly identified by Raibaud and Schwartz [131] showing a constitutive expression of *mal* operons when *malT* is expressed on a PBR322 plasmid. The constitutive nature of *mal* expression at increased MalT expression levels was shown by a genomic mutation in the regulation of MalT at the

5. Results & Discussion

transcriptional and translational level [132]. The increased rhamnosylation of naringenin is likely not only an effect of increased glycosyltransferase expression but furthermore can be attributed to an increased level of *mal* operon expression, enabling a constant supply of the maltodextrin degradation machinery, including maltodextrin phosphorylase (MalP) leading to the formation of the essential precursor G1P. The created system may not be, as initially intended, an “auto-induction” system but rather a constitutive expression system due to the incorporation of *malT*. The constitutive nature of *mal* expression could be revealed by a transcriptomics analysis, comparing the growth of *E. coli* UHH_CR11-A and UHH_CR11-B utilizing dextrin or glucose as carbon source. If constitutively expressed, all *mal* genes should be transcribed when utilizing glucose, and therefore, should be detectable via methods like quantitative PCR.

The *rml* operon of *E. coli* UHH_CR11 was deleted (creating *E. coli* UHH_CR12), to reduce the formation of side-products when working with promiscuous GTs. Nevertheless, this strain can be used to show the functionality of the Glyco-switch plasmid in a complementation assay, in which the *rml* operon deletion is complemented on by a synthetic *rml* operon, expressed on the Glyco-switch plasmid. *E. coli* UHH_CR11-C, containing pK44-MalT::GtfD(opt) GT-module, but not containing the *d*TDP-rhamnose forming Glyco-switch, relies on its genomic *rml* operon for *d*TDP-rhamnose synthesis. The genomic *rml* operon is deleted in *E. coli* UHH_CR12-A, containing pK44-MalT::GtfD(opt), which is complemented via the pCDF-malZp::*rmlAB*::*rmlCD* Glyco-switch in *E. coli* UHH_CR12-B (figure 5.5).

E. coli UHH_CR11-C, only containing the GT-module and the genomic *rml* operon, produced 361 ± 58 mg/L. The *rml* operon deletion mutant *E. coli* UHH_CR12-A, only containing pK44-MalT::GtfD(opt), did not produce N5R. The Glyco-switch complemented *E. coli* UHH_CR12-B strain resulted in the production of 907 ± 32 mg/L N5R, showing the successful complementation of the *rml* operon on the Glyco-switch pCDF-malZp::*rmlAB*::*rmlCD*.

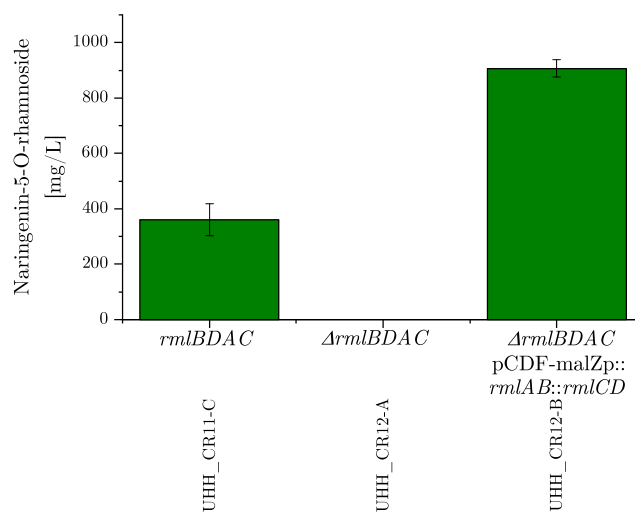


Figure 5.5.: Complementation of the *rml* operon on the Glyco-switch plasmid pCDF-malZp::*rmlAB*::*rmlCD*. *E. coli* production contain pK44-MalT::GtfD(opt) and strains were grown in 10 mL TB-Dex media at 37 °C and 150 rpm. 5 g/L Naringenin were added as aglycone. N5R production was monitored after 48 hrs. Production strains are listed in table 5.2. (n=3) N4'R is produced as a minor side-product.

5.3.2. Deletion of *glgC* and *ushA*

In order to create a modular system with reduced flux towards alternative NDP-sugars that might be transferred by promiscuous GTs, competing NDP-sugar synthesis pathways were deleted. The deletion of the *rml* operon was complemented on the Glyco-switch pCDF-malZp::*rmlAB*::*rmlCD* by *E. coli* UHH_CR12-B in a proof of principle experiment performed in shake flask experiments (figure 5.4). To inhibit the formation of storage glycogen in *E. coli* the *glgC* gene was deleted, creating *E. coli* UHH_CR13. Subsequently, *E. coli* UHH_CR14 was created by the deletion of *ushA*, which is a UDP-sugar hydrolase shown to increase glycosylation reactions in *E. coli* utilizing UDP-sugars. The created strains were transformed with the Glyco-switch pCDF-malZp::*rmlAB*::*rmlCD* and the GT-module pK44-MalT::*GtfD*(opt). The production of naringenin-5-O-rhamnoside was monitored in solid fed-batch fermentations for 72 h (figure 5.6).

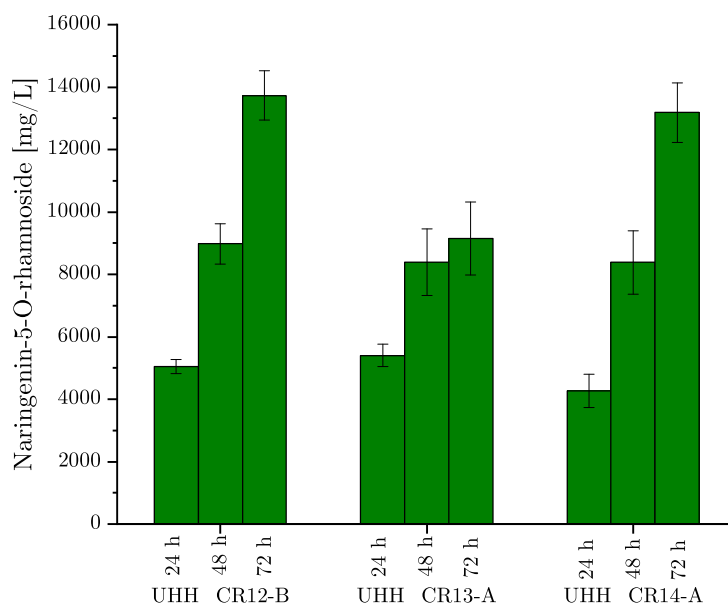


Figure 5.6.: Effect of *glgC* and *ushA* gene deletions. Naringenin-5-*O*-rhamnoside production in *E. coli* solid fed-batch fermentations. All *E. coli* strains expressed GT-module pK44-MalT::*GtfD*(opt) and Glyco-switch pCDF-malZp::*rmlAB*::*rmlCD* leading to the formation of *d*TDP-rhamnose. *E. coli* UHH_CR12 has a deleted *rml* operon; UHH_CR13 has an additional deletion of the *glgC* gene; UHH_CR14 has an additional deletion of the *ushA* gene. Every 24 h, a 50 g/L of solid dextrins, and 5 g/L of naringenin was added. Production strains are listed in table 5.2. Fermentations were performed in quadruplicates, error bars indicate confidence intervals based on Students t-distribution ($\alpha=0.05$, $n=4$). N4'R is produced as a side-product.

5.3. Naringenin rhamnosylation using Glyco-switch and GT-module

E. coli UHH_CR12 is a *pgi*, *galU* and *rml* operon deficient strain, expressing the G6-amylase genomically integrated for the *recA* gene, thereby combining beneficial traits, discovered in part I, with the deletion of the *rml* operon needed to create a modular system with reduced side-product formation (See design rationale in section 5.1 on page 47). After 24 h UHH_CR12-B produced 5.0 ± 0.2 g/L, which increased to 9.0 g/L ± 0.6 g/L and 13.7 ± 0.8 g/L after 72 h biotransformations. This is to the best of my knowledge the highest so far published flavonoid glycosylation, i.e. rhamnosylation, titer.

The additional deletion of *glgC* in *E. coli* UHH_CR13-A, leading to the formation of ADP-glucose from G1P, showed no significant difference after 24 and 48 h biotransformation, producing 5.4 ± 0.4 g/L and 8.4 ± 1.0 g/L N5R, respectively. However, the production of N5R only slightly increased during the last 24 h of biotransformation, leading to a final production titer of 9.1 ± 1.2 g/L N5R after 72 h.

The deletion of the *ushA* gene in *E. coli* UHH_CR14-A did not show the same reduced production after 72 h naringenin rhamnosylation, producing 13.2 ± 0.96 g/L N5R and 1.0 ± 0.13 g/L N4'R (figure 5.7). There was no observation of a significant difference in the production of N5R after 24 and 48 h, producing 4.3 ± 0.5 g/L and 8.3 ± 1.0 g/L, respectively. UshA is a UDP-sugar hydrolase, which is specific for UDP sugars and not able to hydrolyze dTDP-sugars [126]. The goal was to generate a glycodiversification platform able to produce high glycosylation titers, including UDP-sugars, i.e., UDP-glucose, UDP-rhamnose, and UDP-glucuronic acid. The deletion of *ushA* has been shown to be beneficial for UDP-sugar dependent glycosylation reactions [77, 86, 128, 129]. Therefore, *E. coli* UHH_CR14 was chosen as the base strain for the glycodiversification platform.

5.3.3. Comparison of medium and high copy-number Glyco-switch plasmids

E. coli UHH_CR14 was chosen as the base strain for the glycodiversification platform, which combines a glycosyltransferase expressed on a GT-module with a NDP-sugar synthesis pathway expressed on the Glyco-switch plasmid, producing a specific NDP-sugar form glucose-1-phosphate. The Glyco-switch plasmid was initially created on the medium copy plasmid pCDF-malZp (ClodF13 origin, 20-40 copies per cell). In contrast to pCDF-malZp, pRSF-malZp is derived from the pRSFDuet-1 vector, which has a high copy RSF1030 origin of replication with copy numbers beyond 100 copies per cell [116]. pRSF-malZp::*rmlAB*::*rmlCD* was created, to compare copy-number effects of the Glyco-switch plasmids. Solid fed-batch fermentations were performed using naringenin as aglycone and *E. coli* UHH_CR14 as base strain, containing the GT-module pK44-MalT::GtfD(opt) (figure 5.7).

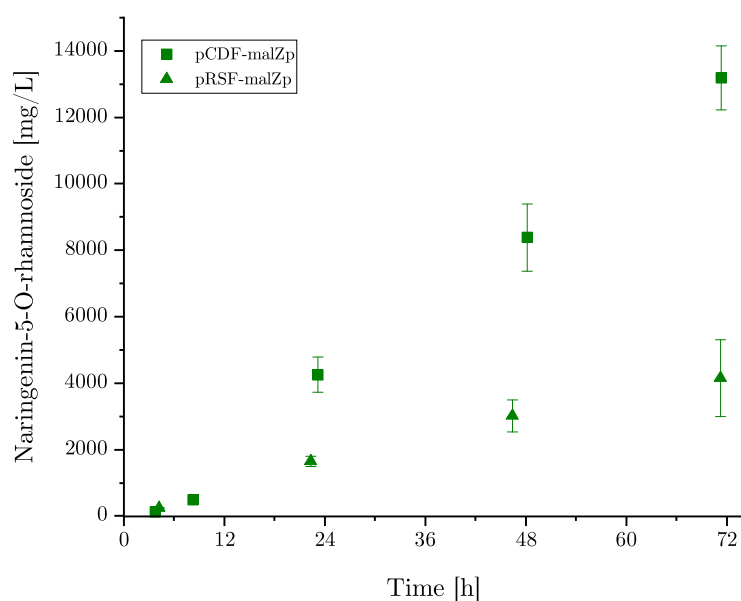


Figure 5.7.: Comparison of naringenin rhamnosylation using a high-copy (pRSF-malZp::*rmlAB*::*rmlCD*, UHH_CR14-B) and medium-copy (pCDF-malZp::*rmlAB*::*rmlCD*, UHH_CR14-A) Glyco-switch expressing *d*TDP-rhamnose synthesis pathway in *E. coli* UHH CR14 solid-fed-batch fermentations. Every 24 h, a 50 g/L of solid dextrins and 5 g/L of naringenin was added. Both *E. coli* strain expressed GtfD(opt) on pK44-MalT::GtfD(opt). Fermentations were performed in quadruplicates, error bars indicate confidence intervals based on Students t-distribution ($\alpha=0.05$, $n=4$). N4'R is produced as a side-product.

The naringenin rhamnosylation by medium-copy Glyco-switch containing *E. coli* UHH_CR14-A increased nearly linear from 24 h, producing 4.3 ± 0.53 g/L Naringenin-5-*O*-rhamnoside

5.3. Naringenin rhamnosylation using Glyco-switch and GT-module

(N5R) and 0.19 ± 0.03 g/L Naringenin-4'-*O*-rhamnoside (N4'R), to 13.2 ± 0.96 g/L N5R and 1.0 ± 0.13 g/L N4'R after 72 h of biotransformation. The linear increase did not reach a plateau phase until the end of the biotransformation, indicating that the production titers can be further increased with prolonged fermentation times.

E. coli UHH_CR14-B expresses the synthetic *rml* operon on a high-copy vector pRSF-malZp::*rmlAB*::*rmlCD*. The production rate of naringenin rhamnosides in *E. coli* UHH_CR14-B is strongly reduced, producing 1.64 ± 0.15 g/L N5R and 0.09 ± 0.007 g/L N4'R after 24 h. The production increases to a final production titer of 4.1 ± 1.2 g/L and 0.4 ± 0.1 g/L after 72 h, respectively. Both the glycosyltransferase GtfD and *rmlABCD* are expressed under the control of *malZ* promoter. Increasing the copy number of the Glyco-switch plasmid may lead to an increase of mRNA available for translation into RmlABCD in relation to the mRNA encoding glycosyltransferase GtfD and to the degradative enzymes of the maltodextrin systems, which are necessary for growth and glucose-1-phosphate production. The results show that balancing the expression of the GT-module and Glyco-switch is beneficial for the rhamnosylation of naringenin. pCDF-malZp was chosen as the backbone for the creation of further nucleotide sugar synthesis pathways, i.e., pathways leading to the formation of UDP-glucose, UDP-rhamnose, and UDP-glucuronic acid, to demonstrate the modularity of the platform.

5.4. Glycodiversification of flavonoids

E. coli UHH_CR14 was developed as a base strain to produce high levels of different flavonoid glycosides in a modular manner, as initially demonstrated with the production of naringenin-5-*O*-rhamnosides. Glyco-switches leading to the formation of rhamnosides, glucosides, and glucuronides were created to show that other NDP-sugar synthesis pathways starting from glucose-1-phosphate, can be efficiently expressed and coupled to glycosyltransferases in glycosylation reactions. Glycosyltransferases were selected according to literature concerning flavonoid GTs able to transfer the corresponding NDP-sugar synthesis pathways. The selected Glycosyltransferases were integrated into the GT-module pK44-MalT and the NDP-sugar pathways onto the Glyco-switch plasmid pCDF-malZp (figure 5.8). Using these plasmids production strains were created, which are given table 5.2 on page 52. The production strains were used in 100 mL solid-fed-batch experiments in TB-Dex media using the aglycones naringenin and quercetin. A summary of flavonoid glycodiversification produced in this study in comparison with literature is given in table 5.3.

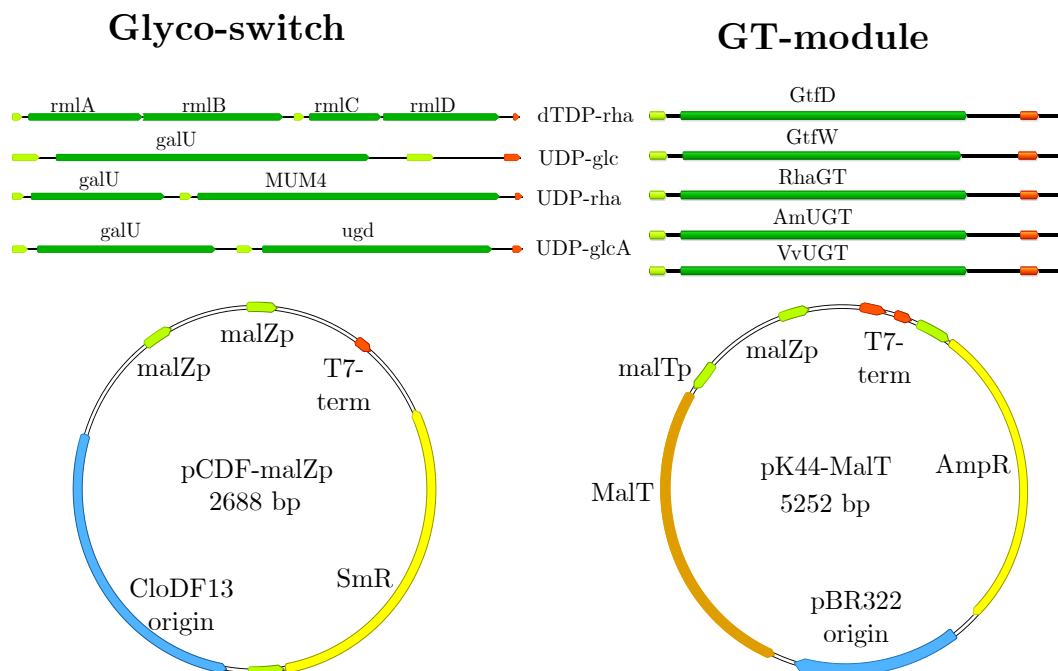


Figure 5.8.: Glyco-switch and GT-modules generated for glycodiversification experiments. The Glyco-switches encode pathways leading from glucose-1-phosphate to a desired NDP-sugar. The GT-modules encode glycosyltransferases that have been shown, in literature, to transfer the NDP-sugars produced by the Glyco-switches.

5.4.1. Rhamnosylation

Flavonoid rhamnosides can be produced in *E. coli* using either *d*TDP-rhamnose or UDP-rhamnose. As shown in this study repeatedly, *d*TDP-rhamnose can be synthesized by the *rml* operon, composed of four enzymatic steps, performed by RmlABCD. UDP-rhamnose is not naturally produced in *E. coli* but can be found in plants, synthesized from UDP-glucose by the UDP-rhamnose synthase (MUM4). Therefore, a Glyco-switch was created combining GalU, synthesizing UDP-glucose from glucose-1-phosphate, and MUM4 from *A. thaliana* to synthesize the desired UDP-rhamnose. De Bruyn et al. [78] had shown that the glycosyltransferase RhaGT from *A. thaliana* is able to rhamnosylate quercetin, kaempferol, fisetin, morin, and myricetin. Therefore, RhaGT was incorporated into the GT-module and tested for flavonoid rhamnosylation using UDP-rhamnose as the NDP-sugar donor (figure 5.9).

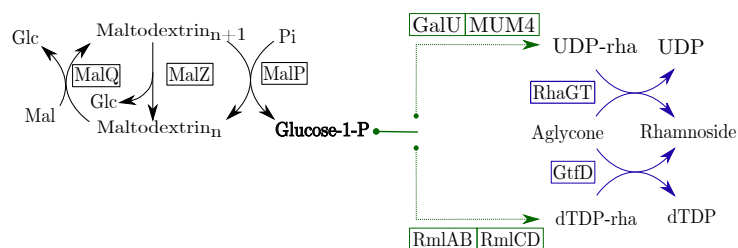


Figure 5.9.: Glyco-switch and GT-module combinations to produce rhamnosides. Two different pathways can be used to produce flavonoid rhamnosides, the bacterial derived *d*TDP-rhamnose synthesis pathway (RmlABCD) and the plant-derived UDP-rhamnose synthesis pathway, utilizing UDP-rhamnose synthase (MUM4).

The first Glyco-switch and GT-module combination leading to the formation of naringenin rhamnosides was UHH_CR14-A, containing *d*TDP-rhamnose producing Glyco-switch pCDF-malZp::*rmlAB*::*rmlCD* in combination with GtfD(opt) expressed on pK44-MalT. *E. coli* UHH_CR14-A was able to produce 13.2 ± 0.96 g/L N5R and 1.0 ± 0.13 g/L N4'R (table 5.3).

To see if rhamnosylation could be achieved by UDP-rhamnose instead of *d*TDP-rhamnose a Glyco-switch leading to the formation of UDP-rhamnose by the action of GalU and MUM4 was created. *E. coli* UHH_CR14-D combines the Glyco-switch with RhaGT from *A. thaliana* expressed on the GT-module, known from literature to produce flavonoid rhamnosides [78]. Indeed *E. coli* UHH_CR14-D was able to produce 1.41 ± 0.02 g/L Quercetin-3-*O*-rhamnoside (Q3R) in 48 h, which did not increase significantly after 72 h

Table 5.3.: Glycodiversification of flavonoids in *E. coli*. All UHH_CR14 substrains express the Glyco-switch and GT-module on pCDF-malZp and pK44-MalT, respectively. N, Naringenin; Q, Quercetin; L, Luteolin; BR, Bioreactor; SF, shake flask; TT, test tube

Product	Titer [g/L]	Time [h]	Mode	NDP-sugar	Glyco-switch	GT	Strain	Reference
Naringenin								
N-7-O-glc	4.9 ± 0.29	72	100 mL BR	UDP-glc	<i>galU</i>	<i>gtfW</i>	UHH_CR14-C	This study
N-5-O-rha	13.2 ± 0.96	72	100 mL BR	dTDP-rha	<i>mmlABCD</i>	<i>gtfD(opt)</i>	UHH_CR14-A	This study
N-4'-O-rha	1.0 ± 0.13	48	20 mL SF	UDP-rha	<i>galU-MUM4</i>	<i>RhaGT</i>	UHH_CR14-D	This study
-	-	48	20 mL SF	UDP-rha	<i>galU-MUM4</i>	<i>RhaGT</i>	UHH_CR14-D	This study
Quercetin (Q)								
Q-3-O-rha	4.32 ± 0.14	48	100 mL BR	dTDP-rha	<i>mmlOP</i>	<i>gtfC</i>	UHH_CR5-A	Ruprecht et al. [64]
Q-3-O-rha	1.41 ± 0.02	48	100 mL BR	UDP-rha	<i>galU-MUM4</i>	<i>RhaGT</i>	UHH_CR14-D	This study
Q-3-O-rha	1.18	30	1 L BR	UDP-rha	<i>ugpA-MUM4</i>	<i>RhaGT</i>	sRha3	De Bryn et al. [78]
Q-3-O-glcA	-	48	20 mL SF	UDP-glcA	<i>galU-ugd</i>	<i>AmUGT</i>	UHH_CR14-E	This study
Q-3-O-glcA	-	48	20 mL SF	UDP-glcA	<i>galU-ugd</i>	<i>VuUGT</i>	UHH_CR14-F	This study
Q-3-O-glcA	0.66	48	2 mL TT	UDP-glcA	<i>galU-ugd</i>	<i>VuUGT</i>	B509	Kim et al. [133]
L-7-O-glcA	0.30	48	2 mL TT	UDP-glcA	<i>galU-ugd</i>	<i>AmUGT</i>	B505	Kim et al. [133]

producing a final 1.53 ± 0.43 g/L Q3R. The sRha3 strain created by De Bruyn et al. [78] was able to produce 1.18 g/L of Q3R in 30 h using also a *galU* and *rml* operon deletion strain complemented with *ugpA* of *Bifidobacterium bifidum* and MUM4 from *A. thaliana*. Interestingly, *E. coli* UHH_CR5-A from Part I was already able to produce 4.32 ± 0.14 g/L Q3R using a bacterial GT, GtfC, and the bacterial *dTDP*-rhamnose synthesis genes, without having any of the modifications created in this part. These results demonstrate that it is necessary to screen a wide array of NDP-sugar synthesis pathways and glycosyltransferases for high production combinations. Even more so, pathways should ideally be balanced transcriptionally and translationally.

Secondly, RhaGT was evaluated for its ability to rhamnosylate naringenin. *E. coli* UHH_CR14-D was unable to produce naringenin rhamnosides in shake flask experiments. However, RhaGT was able to produce 3-OH rhamnosides of the flavanols quercetin, kaempferol, fisetin, morin, and myricetin [78]. RhaGT seems to be specific for the 3-OH function at the C-ring of flavanones and is therefore unable to rhamnosylate naringenin, which lacks this hydroxyl function.

5.4.2. Glucosylation

The vast majority of flavonoids occur as glycosides, often in the β -glycosidic form [46]. Glucosides are synthesized using mainly UDP-glucose as NDP-sugar. Therefore, *E. coli* UHH_CR14-C was created, combining the UDP-glucose forming Glyco-switch (pCDF-malZp::*galU*) with the glycosyltransferase GtfW from *Bacillus weihenstephanensis* expressed on the GT-module (figure 5.10).

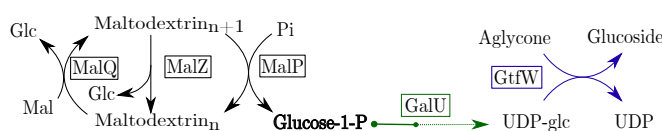


Figure 5.10.: Glyco-switch and GT-module combination to produce glucosides. GalU produces UDP-glucose from glucose-1-phosphate, which can be utilized by GtfW from *Bacillus weihenstephanensis* to produce glucosides.

GtfW was known in within our working group to produce Naringenin-7-*O*-glucoside (N7G). After 72 h biotransformation, *E. coli* UHH_CR14-C produced 4.9 ± 0.29 g/L N7G (table 5.3). In Part I, the *galU* deletion mutant proved to show the most substantial

5. Results & Discussion

effect of the single deletion mutants to increase the rhamnosylation of flavonoids by GtfC. The complementation by a pCDF-malZp::*galU* Glyco-switch might, therefore, reduce the glycosylation capability. The deletion of *galU* is known to create a deep rough phenotype, which might increase glycosylation through increased uptake of the hydrophobic aglycone molecules. A different strategy to create a reduced, truncated LPS could be to target the glycosyltransferase, transferring UDP-glucose for LPS elongation, when UDP-glucose forming GalU is required on a Glyco-switch. A candidate GT for deletion would be *waaG* transferring the first glucosidic residue in LPS formation from UDP-glc [134], which could lead to increased glucoside production rates. Indeed, the outer membrane permeability of *waaG* mutant *E. coli* strains have been shown to exhibit increased permeability of hydrophobic small molecules of nearly two-fold [135].

5.4.3. Glucuronidation

A great variety of drugs are quickly metabolized to their glucuronides for detoxification and excretion [136]. Glucuronides are needed in the scientific community as standard substances, as many drugs are found in their glucuronide form, formed by human UDP-glucuronyltransferases [137]. Furthermore, the glucuronides can be of great value to drug development to identify drugs with very high turn over rates (low efficacy) or for the identification of cytotoxic glucuronides [136].

Glucuronides can be produced from UDP-glucuronic acid, synthesized from UDP-glucose by the UDP-glucose dehydrogenase (Ugd). Flavonoid glucuronides are synthesized by AmUGT from *Antirrhinum majus* and VvUGT from *Vitis vinifera*, as shown in literature, producing Luteolin-7-*O*-glucuronic acid and Quercetin-3-*O*-glucuronic acid in test tubes [133]. Therefore, a Glyco-switch expressing *galU* and *ugd*, and the corresponding GT-modules were created to enable glucuronidation (figure 5.11).

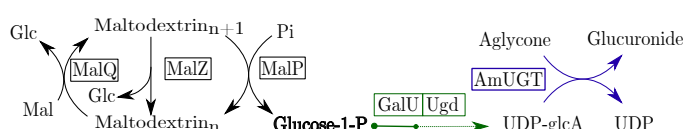


Figure 5.11.: Glyco-switch and GT-module combination to produce glucuronides. AmUGT from *Antirrhinum majus* is able to utilize UDP-glucuronic acid (UDP-glcA), which is produced from glucose-1-phosphate by the Glyco-switch expressing *galU* and *ugd* derived from *E. coli* K-12.

In contrast to literature, both glycosyltransferases did not show activity on quercetin, whereas luteolin was not assayed (table 5.3). To make a clear statement about the functional expression of AmUGT and VvUGT in *E. coli* UHH_CR14, the functionality of the Glyco-switch producing UDP-glucuronic acid and the glycosyltransferases need to be verified. The production of UDP-glcA could be monitored via HPLC methods for nucleotide sugar analysis. Alternatively, an *in vitro* assay for glycosyltransferase activity could be performed using commercially available UDP-glucuronic acid, thereby ensuring functionality of the GTs.

In this part, a modular system was successfully created enabling the glycodiversification of small molecules in *E. coli*. Already in part I the highest so far published rhamnosylation titers were created. Through the combination of a rearrangement of the *rml* operon and the incorporation of a new expression system for the glycosyltransferase and the NDP-sugar synthesis pathway, for the first time production titers beyond 10 g/L were shown. Furthermore, the glycosylation platform is capable of producing other glycosides in a g/L scale, as shown for glucosides. Nevertheless, the different production titers of the glycosides created, highlight the need to optimize and fine-tune expression and production systems for every specific product, including but not limited to the expression of the NDP-sugar synthesis pathways and the identification of suitable glycosyltransferases.

Part III.

Development of a
rhamnosyltransferase activity
screen

6. Introduction

The modular glycosylation platform developed in Part II is able to combine different glycosyltransferases with their corresponding nucleotide sugar donor to create various glycosides. Even though a large variety of combinations are possible, creating potentially novel glycosides, there might be a specific need to create a variant of glycosyltransferases with altered properties. Looking at the hesperetin rhamnosylation of GtfC (figure 3.2 on page 31) Hesperetin-3'-O-rhamnoside is formed as major glycosylation product, whereas Hesperetin-5-O-rhamnoside is formed as a side-product and no Hesperetin-7-O-rhamnoside is formed.

A pure production of only one of the rhamnosides is not possible with GtfC. Screening for a new glycosyltransferase performing the specific rhamnosylation of interest can be quite time consuming and does not give a certain outcome. A directed enzyme engineering approach of the glycosyltransferase could be an additional approach to tackle such a problem. Engineering of glycosyltransferases can be used to create new catalysts with improved functions, including broadening the acceptor range or increasing sugar donor specificity. In order to employ a successful enzyme engineering approach, usually, large libraries of newly created glycosyltransferase variants need to be screened and assessed for activity. As cultivation with subsequent HPLC analysis of all generated clones would be too laborious, a quick and easy to use first screening to assess the activity of a glycosyltransferase is required.

6.1. Glycosyltransferase activity screening

Several activity assays for glycosyltransferases have been published. Usually, these assays involve fluorescent substrates as, e.g., 4-methylumbelliferone (4-MU), which fluorescence

6. Introduction

is quenched upon glycosylation. Alternative methods involve the deglycosylation of the produced glycoside with subsequent detection of the glycosidic moiety.

Williams and Thorson [138] developed an *in vitro* 4-MU screening method for glycosyltransferase engineering. This screening method is rather laborious, involving the protein expression and purification via crude cell lysis and an *in vitro* activity assay with the fluorescent 4-MU as a primary screening method. A secondary screening of positive hits is required, to verify the results of the primary screening. The 4-MU assay was successfully applied to increase the substrate specificity of the *Streptomyces antibioticus* glycosyltransferase OleD, which catalyzes the glucosylation of oleandomycin using UDP-glucose [139].

A non-fluorescent screening method was developed by Weis et al. [140]. The screening method involves a three-stage process. Firstly, a biotransformation of scopoletin is performed in *E. coli*, recombinantly expressing glycosyltransferases. In a second stage, the glycosides are separated from the production media and the glycosidic residue is released by the action of a β -glucosidase. In a final detection stage, the released glucose is enzymatically detected. The results of the glucosidase assay were confirmed using a secondary detection via HPLC. Using this approach *Arabidopsis thaliana* glycosyltransferases were screened for increased scopoletin glycosylation. Furthermore, a regioselectivity shift for *trans*-resveratrol glucosylation (4'-OH to 3-OH) was engineered using this screening approach.

Both exemplary glycosyltransferase engineering approaches require in addition to their laborious primary screening method, a secondary analytical method for the validation of their results. The generation of glycosyltransferase variants involves the plating of *E. coli* cells, harboring the mutagenesis library, onto Agar plates. Therefore an agar plate-based activity screening, giving a qualitative assessment of glycosyltransferase activity would reduce the screening effort in glycosyltransferase engineering tremendously while creating a mutant library. The smaller number of positive hits in a primary assay, could then be screened in a secondary biotransformation, for the desired traits.

An initial attempt using the fluorescent 4-MU in agar plates was unsuccessful and did not result in colonies able to quench the fluorescence of 4-MU (data not shown). However, a secondary approach using an indigogenic 5-bromo-4-chloro-indoxyl substance was developed.

7. Results & Discussion

7.1. Blue/white screening for rhamnosyltransferase activity

Indigogenic substances, i.e. their esters and glycosides are useful chromogenic substances that can be used to detect enzymatic activity [141]. A variation of indigo blue screening widely used in molecular biology is the blue/white screening, firstly described by Vieira and Messing [142], developed to quickly assess an integration of a DNA fragment into plasmid DNA. The screening method is based on the function of the β -galactosidase (LacZ) and the galactoside 5-Brom-4-chlor-3-indoxyl- β -D-galactose (X-gal). A functional, plasmid-based, β -galactosidase gene, *lacZ*, is expressed and leads to the formation of β -galactosidase upon Isopropylthio- β -galactoside (IPTG) or lactose induction. The β -galactosidase is able to cleave the galactose moiety of the colorless X-gal. The resulting 5-bromo-4-chloro-indoxyl dimerizes in the presence of oxygen to form the blue colored 5,5'-dibromo-4,4'-dichloro-indigo. However, a successful integration of a DNA fragment into the plasmids *lacZ* gene perturbs the production of active β -galactosidase, thereby omitting the initial galactose cleavage. These colonies appear white on agar plates containing IPTG and X-gal, making the integration of DNA fragments screenable. In this part a new “twist” on the blue/white screening was developed (Figure 7.1).

E. coli K-12 possesses its native β -galactosidase gene *lacZ*, inducible by the addition of IPTG. The β -galactosidase cleaves the colorless X-gal releasing 5-bromo-4-chloro-indoxyl. The free 3-hydroxyl function of 5-bromo-4-chloro-indoxyl can now act as an acceptor for a potentially active glycosyltransferase. An active rhamnosyltransferase, which can utilize 5-bromo-4-chloro-indoxyl as a substrate, can potentially form the colorless 5-Brom-4-chlor-3-indoxyl- α -L-rhamnoside (X-rha), which cannot be hydrolyzed by the β -galactosidase.

7. Results & Discussion

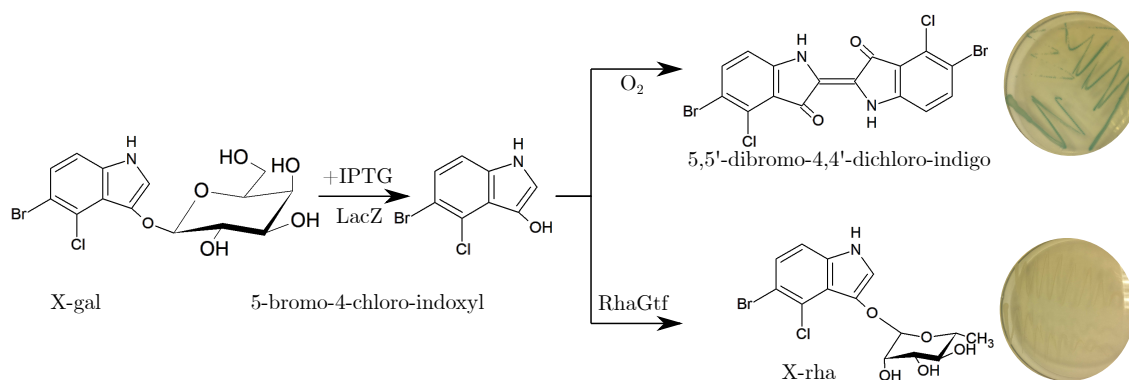


Figure 7.1.: Molecular basis of blue/white screening. Wildtype *E. coli* K-12 growing on agar plates containing IPTG produces a functional β -galactosidase gene able to hydrolyze the glycosidic bond of 5-Bromo-4-chloro-3-indoxyl- β -D-galactose (X-gal). The dimerization of the resulting aglycone leads to the formation of blue colonies. *E. coli* expressing GtfC forms uncolored, “white” colonies, which is hypothesized to be due to the rhamnosylation of 5-bromo-4-chloro-indoxyl, thereby omitting blue coloration from the indigo dye.

Therefore colonies with active rhamnosyltransferases remain white, whereas inactive rhamnosyltransferases colonies turn blue due to the formation of the blue indigo dye. The blue/white screening for GtfC revealed white colonies on agar plates, whereas *E. coli* K-12 not expressing GtfC revealed a blue coloration (Figure 7.1).

7.2. Application of blue/white screening

To assess the capability of the blue/white screening, 18 rhamnosyltransferases (Accession numbers are given in table 10.4 on page 99) were screened for their ability to glycosylate 5-bromo-4-chloro-indoxyl using *d*TDP-rha as nucleotide sugar donor (table 7.1). Eight of the screened glycosyltransferases, namely GtfC(opt), GtfD(opt), GtfF, GtfS(opt), Chim3b(opt), Chim4b(opt), Gtf33(opt) and Gtf34(opt) showed no coloration, indicating rhamnosyltransferase activity. The results of the blue/white screening were compared to biotransformations performed in 48 well plates using naringenin as aglycone. In the HPLC analysis of naringenin biotransformations, seven of the eight active rhamnosyltransferases were able to produce naringenin rhamnosides, with the exception of Gtf33. Additionally Gtf31 and Gtf 35 produced naringenin rhamnosides but showed a negative blue staining in the blue/white assay.

The differences in the blue/white screening compared to naringenin rhamnosylation may

7.3. Application potential for blue/white screening method

Table 7.1.: Blue/white screening of rhamnosyltransferases in *E. coli* UHH_CR14 expressing dTDP-rhamnose synthesis genes (pCDF-malZp::rmlAB::rmlCD). Blue colonies (B), White colonies (W) were compared to naringenin (N) rhamnoside formation analyzed by HPLC/MS.

	GtfC(opt)	GtfD(opt)	GtfF	GtfH	GtfJ	GtfL	GtfX	GtfS(opt)	Chim3b	Chim4b	Gtf31(opt)	Gtf32(opt)	Gtf33(opt)	Gtf34(opt)	Gtf35(opt)	Gtf36(opt)	GtfO	GtfN
W	+	+	+					+	+	+				+	+			
B				-	-	-	-					-	-			-	-	-
N	+	+	+	-	-	-	-	+	+	+	+	-	-	+	+	-	-	-

be attributed to different substrate promiscuity. The ability to identify small molecule rhamnosyltransferases seems strikingly good using the blue/white screening. The rhamnosyltransferases were identified via homology modeling to GtfC. Nevertheless, the similarity is quite low between the different glycosyltransferases (Appendix on page 128). Therefore, it would be intriguing to test a larger library of more, structurally diverse GTs for rhamnosyltransferase hits.

7.3. Application potential for blue/white screening method

The developed blue/white screening method is able to screen for rhamnosyltransferase activity. The blue/white screening can be used as a primary screen in a mutagenesis approach. The workflow of an envision mutagenesis approach (figure 7.2) includes two phases, the mutant library generation and secondary activity screen for desired properties. In the first stage, a mutant library is generated either in a random or in a structure-guided approach. After mutant library generation colonies are transferred onto blue/white agar and incubated for 24 hrs. Positive white colonies can then used in biotransformation approaches with the desired substrate and screened using HPLC for increased or altered production. Interesting colonies can then be used in another cycle of mutagenesis. In general, this screening method is not limited to rhamnosyltransferases. As shown in Part II, different Glyco-switches can be created, leading to the synthesis of various NDP-sugars. Using the different Glyco-switches in screening strains should enable a powerful method for glycosyltransferase screening. A similar approach seems possible to screen larger metagenomic

7. Results & Discussion

libraries for the identification of novel glycosyltransferases, not limited to rhamnose.

In addition to screening for glycosyltransferase activity, the assay could also be used to engineer NDP-sugar synthesis pathways. The *rml* operon consisting of the 4 step pathway, RmlABCD, is a potential target for further engineering approaches, as, e.g. *rmlA* is feedback inhibited. Generating pathway libraries with a direct method of screening for a functional pathway is of great value. In this way, the single enzymes of the *rml* operon could be exchanged for genes with homologous gene product functions for increased rhamnoside production by a GT that is active in blue/white screening. Mutations leading to unfunctional *d*TDP-rha synthesis pathways would stain blue, whereas a functional *d*TDP-rhamnose synthesis pathway would lead to white colonies.

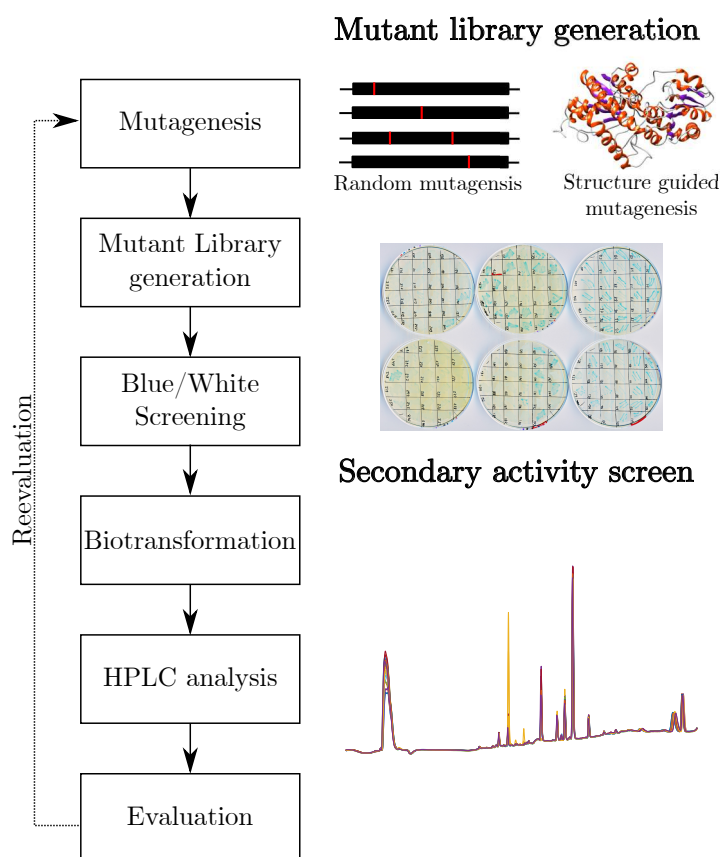


Figure 7.2.: Proposed workflow for a mutagenesis approach using blue/white screening. The blue/white screening can be used as a primary screening method to assert the functional state of glycosyltransferases. The reduction of a large amount of unfunctional mutant glycosyltransferases in the step of mutant library generation reduces the time needed for an enzyme engineering approach. The positive hits of a primary screen can be used for secondary screening using specific substrates.

Part IV.

Conclusion & Outlook

8. Conclusion & Outlook

The main goal of this work was to establish the production of flavonoid rhamnosides in a g/L scale. The developments taken throughout this work aimed continuously at increasing production titers, which were able to be increased from initially below 100 mg/L in 48 well plate experiments, to above 1 g/L. The high production titers were achieved by coupling the growth of *E. coli* K-12 on dextrans of starch, leading to a constant production of the central precursor G1P, to the rhamnosylation of flavonoids. Using a metagenomic rhamnosyltransferase, in concert with the overexpression of the *d*TDP-rhamnose synthesis pathway, and a G6-amylase expression for increased dextrin degradation, the production goal was exceeded nearly 5-fold. Furthermore, the creation of synthetic expression systems using the maltodextrin glucosidase promoter region increased the production of naringenin-5-O-rhamnoside in titers above 10 g/L which is the highest published glycosylation titer of flavonoids.

In order to further increase the glycosylation capabilities, the most crucial part is the identification of bottlenecks of the glycosylation reaction. The identification of such limitations is usually performed in a multi-omics approach. The multi-omics approach combines metabolomics, proteomics, and transcriptomics data. After identification of the bottlenecks, the next round of targeted strain and process development will likely increase the glycosylation further.

Obviously the glycosyltransferase itself is a candidate for optimization and likely shows different reaction kinetics for different aglycone substrates. The newly developed blue/white screening method might be used as a primary activity screen to engineer a GT with higher substrate specificity, reduced side-product formation, increased productivity of the enzymes towards its aglycone, or even altered nucleotide sugar acceptor of the GT. The GT is not the only possible bottleneck reducing potential production. Interestingly, less soluble agly-

8. Conclusion & Outlook

cone structures tend to lead to reduced production titers. Solubility and bioavailability enhancing molecules like cyclodextrins have shown to be effective in increasing glycosylation reactions *in vitro* [143], but have so far not been utilized in *in vivo* glycosylation reactions.

The developed platform is state of the art and able to produce high amounts of flavonoid glycosides, especially rhamnosides. In future research, the platform can be applied to produce flavonoid glycoside libraries. These libraries could be used in activity screens on a small scale to identify glycosides with a desired trait, as, e.g. anti-biofilm activities. After identification of the glycosidic molecule, the glycosyltransferase and the synthesis pathway can be balanced to produce larger quantities of the desired compounds. In a world in which sustainability becomes more and more important, a complete *de novo* synthesis approach, synthesizing the complete production of the glycoside in a heterologous host, is desirable; however, *de novo* titers of flavonoid glycosides remain low [25]. Additionally, the often promiscuous GTs might be able to glycosylate the precursor molecules of the synthesis pathway, as well as the desired aglycone, which would require highly specific GTs.

8.1. Future developments of the glycodiversification platform

Currently, the CAZY database GT Family 1, GTs transferring sugars moieties from activated sugar molecules onto small lipophilic acceptors, contains a total of 20781 (13276 bacterial) GTs, of which only 394 are characterized and 35 structures (2 crystal structures are available (<http://www.cazy.org/GT1.html> - accessed 30.10.2019)). There is a tremendous difficulty in predicting the precise function of these uncharacterized glycosyltransferase in regard to the NDP-sugars they can utilize, and the aglycone structures they can address. An impressive approach to elucidate and predict GT functionality by training a model of GT family 1 biotransformations of *A. thaliana* GTs was shown by Yang et al. [144]. Using a functional-based training set, a GT-Predict model was created, which was able to predict the functionality of GTs, which were not used in the training set of the model. However, the approach was “limited” to using 13 different mainly UDP-sugars with additional *d*TDP-glucose, -xylose, -rhamnose and GDP-glucose, -mannose, -fucose. Metacyc currently lists 224 different NDP sugars, comprised of 82 UDP-sugars, 76 *d*TDP-sugars, 15 ADP-sugars, 14 CDP-sugars and 37 GDP-sugars (<https://biocyc.org/compound?orgid=META&id=NDP-sugars#tab=showAll>, accessed 30.10.2019)[145]. The *d*TDP sugars are the most structurally diverse class of NDP-sugars, and all so far known synthesis pathways are derived from glucose-1-phosphate [146], making them producible by *E. coli* UHH_CR14 (Figure 8.1).

NDP-sugars, which are currently not derived from G1P and are therefore are not designed for the growth coupled system, include GDP-sugars, which are derived from mannose-1-phosphate and UDP-N-acetyl sugars which are derived from *N*-acetyl-glucosamine. Nevertheless, a wide variety of CDP-, UDP- and *d*TDP-sugars are producible by *E. coli* UHH_CR14. Especially the structurally diverse *d*TDP-sugars are interesting for the further expansion of the glycodiversification platform. *d*TDP-sugars are grouped into three different groups according to their structural traits [146]. As depicted in figure 8.1 *d*TDP-sugar groups share the intermediate *d*TDP-4-keto-6-deoxy-D-glucose, formed through the action of RmlA and RmlB in *E. coli* K-12.

Group I *d*TDP-sugars are all 6-deoxy sugars (e.g., *d*TDP- β -L-rhamnose, - β -L-pneumose and -4-O-demethyl- β -L-noviose). All of these sugars are synthesized from *d*TDP-4-dehydro-

8.1. Future developments of the glycodiversification platform

β -L-rhamnose formed by RmlC. The d TDP- β -L-rhamnose forming pCDF-malZp::*rmlAB*::*rmlCD*, therefore, could easily be adjusted by incorporation of *tll* gene from *Actinobacillus actinomycetemocomitans* and *novU* and *novS* genes from *Actinonallotichus cyanogriseus* to produce d TDP- β -L-rhamnose, d TDP- β -L-pneumose and d TDP-4-*O*-demethyl- β -L-noviose in one *E. coli* strain. This approach would enable the screening of multiple, related d TDP-sugars for glycosyltransferases that are able to transfer them onto small hydrophobic molecules. Direct NMR identification of glycosides present in the culture supernatant should be possible (personal communication Dr. Thomas Hackl, University Hamburg, Head of NMR division). After the identification of novel glycosides, dedicated Glyco-switches can be created to increase productivity and reduce byproduct formation. Ultimately it might be possible to screen a pool of aglycones simultaneously.

Similarly, additional Glyco-switches can be created that share large parts of the same synthesis pathways (Figure 8.1). A key intermediate is 3,4,-didehydro-2,6-dideoxy- α -D-glucose, which is the branching point between group II and group III d TDP-sugars. When looking at these structures, it must be kept in mind that some further modifications of sugar structure like methylation (*S*-adenosylmethionine), acetylation (acetyl-CoA), or transamination (L-glutamate) require new co-substrates that might pose bottlenecks for high-level glycosylation and might, therefore, require further strain engineering. In contrast, a great variety of group III 2,6-dideoxy sugars do not require additional co-substrates and high-level glycoside production by *E. coli* UHH_CR14 seems possible. These sugars are formed as building blocks for antibiotic synthesis. I propose to create a “grouped” Glyco-switch for these sugars to screen for GTs able to transfer these sugars. The developed blue/white screening method could be used to aid in GT engineering if no suitable GTs are found producing group II/III glycosides. This approach should enable the creation of a large variety of novel glycosides with interesting, potentially new functions and applications.

Part V.
Materials & Methods

9. Bacterial strains & Cultivation

9.1. Strains used within the study

Within this study, *E. coli* DH5 α was used for cloning and maintenance of plasmids. Deletion strains were generated from *E. coli* K-12 (MG1655) which was acquired from DSMZ (Braunschweig, Germany). Genotypes of the strains are given in table 9.1. If not stated otherwise, *E. coli* strains harbouring plasmids were grown in LB medium for 18 h using the corresponding antibiotics (ampicillin 100 $\mu\text{g}/\text{mL}$, chloramphenicol 25 $\mu\text{g}/\text{ml}$, streptomycin 50 $\mu\text{g}/\text{ml}$) at 37 °C.

Genedeletions in *E. coli* K-12 (MG1655)

E. coli K-12 MG1655 gene deletions (Table 9.1) were constructed using the “Quick and Easy *E. coli* Gene Deletion Kit” (Gene Bridges, Germany) according to manufacturer’s protocol. The gene deletions were verified using control PCR reactions.

An example of the design and control of *malZ* deletion in *E. coli* UHH_CR1 is shown in figure 9.1. In a first *in silico* design phase, the genomic region of *malZ* is extracted from the genome of *E. coli* K-12 (MG1655) (accession number NC_000913) including upstream and downstream regions. After the design of the primer sequences, they are blasted against the *E. coli* genome to check for unspecific binding. Special care should be taken to avoid any repeating sequences within the genome. Afterwards, a knockout fragment is PCR amplified using the FW/RV_malZ_KO primer pair, containing 50 bp overhangs with homologous regions to the chromosomal *malZ* gene region. A strain of interest is transformed with the pRedET(Amp) plasmid containing λ -red recombination genes. The linear knockout fragment is electroporated in *E. coli* strains with induced λ -

9. Bacterial strains & Cultivation

red genes to facilitate homologous recombination and plated on LB-agar plates containing kanamycin. Single kanamycin resistance colonies are checked via colony PCR for correct localization of the kanamycin resistance cassette. Therefore, a PCR with the external primer FW-malZ_ext and the P2_Kan primer is performed. A successful incorporation results in a PCR product of 500 bp. After correct localization is verified, the resistance cassette is “flipped” using FLP mediated excision at the FRT sites. Using kanamycin sensitive clones and the external primer pair FW/RV_malZ_ext, the excision can be monitored. Finally, the removal of *malZ* is confirmed by using the internal primer pair FW/RV_malZ_int, which should not result in a PCR product. All other deletion mutants were designed and verified in a similar manner (Data not shown); primer sequences are given in table 10.2.

Table 9.1.: Bacterial strains used and created in this study

Strain	Genotype	Source
<i>E. coli</i> DH5 α	<i>F</i> ⁻ <i>endA1 glnV44 thi-1 recA1 relA1 gyrA96</i> <i>deoR nupG purB20 ϕ80dlacZΔM15</i> Δ (<i>lacZYA-argF</i>)U169, <i>hsdR17</i> (<i>r_K</i> ⁻ <i>m_K</i> ⁺), λ	Invitrogen (Karlsruhe, Germany)
<i>E. coli</i> K-12 (MG1655)	<i>F</i> ⁻ , λ ⁻ , <i>rph-1</i> , <i>Fnr</i> ⁺	DSM #18039
<i>E. coli</i> UHH_CR1	<i>F</i> ⁻ , λ ⁻ , <i>rph-1</i> , <i>Fnr</i> ⁺ , Δ <i>malZ</i>	This Study
<i>E. coli</i> UHH_CR2	<i>F</i> ⁻ , λ ⁻ , <i>rph-1</i> , <i>Fnr</i> ⁺ , Δ <i>agp</i>	This Study
<i>E. coli</i> UHH_CR3	<i>F</i> ⁻ , λ ⁻ , <i>rph-1</i> , <i>Fnr</i> ⁺ , Δ <i>pgm</i>	This Study
<i>E. coli</i> UHH_CR4	<i>F</i> ⁻ , λ ⁻ , <i>rph-1</i> , <i>Fnr</i> ⁺ , Δ <i>galU</i>	This Study
<i>E. coli</i> UHH_CR5	<i>F</i> ⁻ , λ ⁻ , <i>rph-1</i> , <i>Fnr</i> ⁺ , Δ <i>pgm</i> , Δ <i>galU</i>	This Study
<i>E. coli</i> UHH_CR6	<i>F</i> ⁻ , λ ⁻ , <i>rph-1</i> , <i>Fnr</i> ⁺ , Δ <i>agp</i> , Δ <i>pgm</i>	This Study
<i>E. coli</i> UHH_CR7	<i>F</i> ⁻ , λ ⁻ , <i>rph-1</i> , <i>Fnr</i> ⁺ , Δ <i>agp</i> , Δ <i>malZ</i>	This Study
<i>E. coli</i> UHH_CR8	<i>F</i> ⁻ , λ ⁻ , <i>rph-1</i> , <i>Fnr</i> ⁺ , Δ <i>pgm</i> , Δ <i>malZ</i>	This Study
<i>E. coli</i> UHH_CR9	<i>F</i> ⁻ , λ ⁻ , <i>rph-1</i> , <i>Fnr</i> ⁺ , Δ <i>pgi</i>	This Study
<i>E. coli</i> UHH_CR10	<i>F</i> ⁻ , λ ⁻ , <i>rph-1</i> , <i>Fnr</i> ⁺ , Δ <i>pgi</i> , Δ <i>galU</i>	This Study
<i>E. coli</i> UHH_CR11	<i>F</i> ⁻ , λ ⁻ , <i>rph-1</i> , <i>Fnr</i> ⁺ , Δ <i>pgi</i> , Δ <i>galU</i> , <i>recA::G6-amylase</i>	This Study
<i>E. coli</i> UHH_CR12	<i>F</i> ⁻ , λ ⁻ , <i>rph-1</i> , <i>Fnr</i> ⁺ , Δ <i>pgi</i> , Δ <i>galU</i> , <i>recA::G6-amylase</i> , Δ <i>rmlBDACX</i>	This Study
<i>E. coli</i> UHH_CR13	<i>F</i> ⁻ , λ ⁻ , <i>rph-1</i> , <i>Fnr</i> ⁺ , Δ <i>pgi</i> , Δ <i>galU</i> , <i>recA::G6-amylase</i> , Δ <i>rmlBDACX</i> , Δ <i>glgC</i>	This Study
<i>E. coli</i> UHH_CR14	<i>F</i> ⁻ , λ ⁻ , <i>rph-1</i> , <i>Fnr</i> ⁺ , Δ <i>pgi</i> , Δ <i>galU</i> , <i>recA::G6-amylase</i> , Δ <i>rmlBDACX</i> , Δ <i>glgC</i> , Δ <i>ushA</i>	This Study

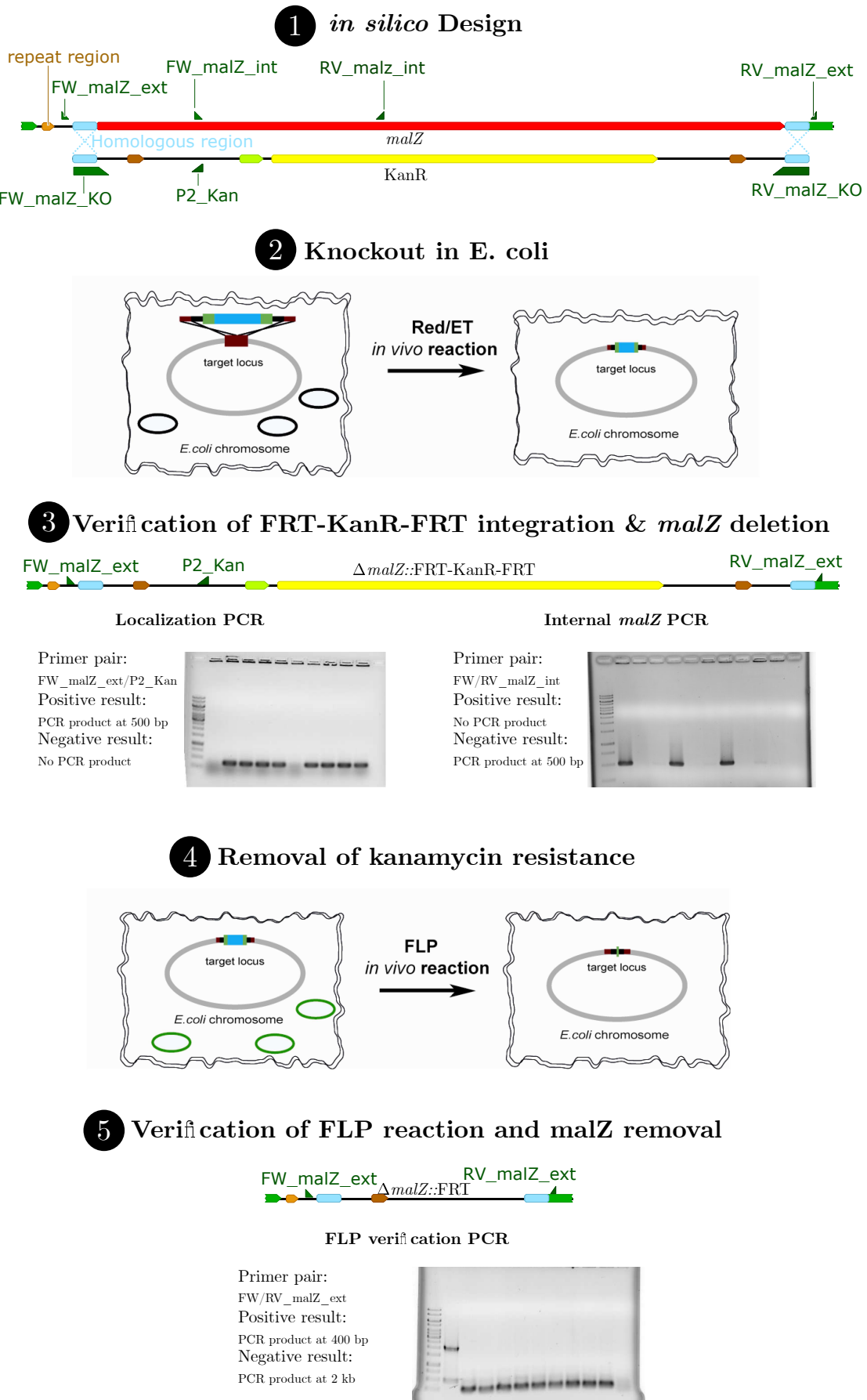


Figure 9.1.: Design and deletion of *malZ* in *E. coli* K-12(MG1655). Depictions of steps 2 & 4 are derived from the manufacturer's protocol of the "Quick & Easy *E. coli* Gene Deletion Kit".

9. Bacterial strains & Cultivation

9.2. Cultivation media

The following media were used for cultivation and deviations from the recipes are given at the appropriate sections. For the preparation of agar plates, 1.5 % agar was added to the cultivation media. When appropriate growth media was supplemented with antibiotics (table 9.2). Antibiotics were prepared in 1000 fold Stock concentration and sterile-filtered. Additionally, IPTG was added, when induction of T5 or *trc* promoters was required, in a concentration of 100 mg/L from a 100 g/L stock solution.

Table 9.2.: Antibiotics stock solution and working concentrations used within this study

Antibiotic	working concentration [mg/L]	Stock [g/L]	Solvent
Ampicillin	100	100	H ₂ O
Chloramphenicol	25	25	70 % Ethanol
Streptomycin	50	50	H ₂ O
Spectinomycin	50	50	H ₂ O
Kanamycin	25	25	H ₂ O

M9 media

For convenient M9 media preparation, stock solutions of M9 salts, carbon source, MgSO₄, CaCl₂, biotin, thiamin, and trace elements were prepared and mixed according to table 9.3.

LB (Lennox) media

LB (Lennox) powder was acquired from Roth (Germany), and 20 g/L LB powder was used for 1 L medium, composed of 10 g/L tryptone, 5 g/L yeast extract, 5 g/L sodium chloride at a pH value of 7.0.

Terrific Broth (TB) media

Terrific broth medium powder was acquired from Roth (Germany), and 50.8 g was dissolved for 1 L TB media. The TB powder was composed of 12 g/L casein (enzymatic digestion), 24 g/L yeast extract, 12.54 g/L K₂HPO₄, and 2.31 g/L KH₂PO₄ at pH 7.2.

Table 9.3.: M9 composition for 1 L medium, containing glucose as carbon source

V [ml]	Stock solution	Components	C
100	M9 salt solution (10X)	Na ₂ HPO ₄	33.7 mM
		KH ₂ PO ₄	22 mM
		NaCl	8.55 mM
		NH ₄ Cl	9.35 mM
20	20 % glucose	glucose	0.4 %
1	1 M MgSO ₄	MgSO ₄	1 mM
0.3	1 M CaCl ₂	CaCl ₂	0.3 mM
1	biotin (1 mg/ml)	biotin	1 µg
1	thiamin (1 mg/ml)	thiamin	1 µg
10	trace elements (100X)	trace elements	1X
fill up to 1000 ml with H ₂ O			
Trace Elements 100X			
	Component	C	M
	EDTA	5 g/L	13.4 mM
	FeCl ₃ * 6 H ₂ O	0.83 g/L	3.1 mM
	ZnCl ₂	84 mg/L	0.62 mM
	CuCl ₂ * 2 H ₂ O	13 mg/L	76 µM
	CoCl ₂ * 2 H ₂ O	10 mg/L	42 µM
	H ₃ BO ₃	10 mg/L	162 µM
	MnCl ₂ * 4 H ₂ O	1.6 mg/L	8.1 µM

SOC media

To increase transformation efficiencies in electroporation and heat shock transformations, SOC media was used for the regeneration of *E. coli* cells. SOC media is composed of 20 g/L peptone (Roth, Germany), 5 g/L yeast extract (Roth, Germany), 4.8 g/L MgSO₄ *H₂O, 3.6 g/L glucose (Acros Organics, Belgium), 0.5 g/L NaCl, 0.18 g/L KCl.

2-YT media

2-YT media was composed of 16 g/L peptone (Roth, Germany), 10 g/L yeast extract (Roth, Germany) and 5 g/L NaCl (Roth, Germany).

9. Bacterial strains & Cultivation

Blue/white agar plates

Blue/white screening for rhamnosyltransferase activity was performed on LB-agar plates, containing an additional 5 % dextrans of starch, to ensure sufficient induction of GT-module and Glyco-switch for activity screening. Additionally, the *E. coli* β -galactosidase (LacZ) was induced by supplementation of 100 mM IPTG, and the galactoside 5-Brom-4-chlor-3-indoxyl- β -D-galactose (X-gal) was dissolved in DMSO as stock solution in a concentration of 50 mg/mL. The stock solution was diluted 1000 fold for use in blue/white agar plates. When first plating the cells, a blue smear on the agar plate created by dead and lysed cells may be observed. If this was the case single colonies were restreaked on blue/white agar plates to screen their blue/white activity without interference. This background staining can be avoided in future work by creating a *lacZ* gene deletion mutant of the screening strain and complementing it on the plasmid which is used for library generation.

Cryocultures

For cryopreservation of bacterial cultures, a fresh overnight culture was mixed 1:3 with 87 % glycerol (Roth, Germany) and stored at -80 °C for long term storage.

9.3. Glycosylation in whole cell biotransformations

The production strains were generally recultivated overnight from cryopreservation preceding a biotransformation using the same media and growth conditions.

Aglycones & glycosides

Hesperetin (>98 %) was purchased from Willols Ingredients (Ireland), kaempferol (>98 %) and naringenin (>98 %) from Molekula (United Kingdom) and quercetin dihydrate (>98 %) from Alfa Aesar (Germany). Analytical standards of quercetin-3-*O*-rhamnoside, quercetin-3-*O*-glucuronic acid, naringenin-7-*O*-glucoside and kaempferol-3-*O*-rhamnoside for glycoside quantification were purchased from Extrasynthese (France). The 3-*O*-rhamnoside, 5-*O*-rhamnosides of hesperetin and naringenin were self-produced and purified by Tanja Heyer (>95 % UV 254 nm) as no analytical standards were available.

Biotransformation in 48 well plates

E. coli strains were inoculated from an overnight culture to an optical density at 600 nm (OD₆₀₀) of 0.1 in 1 mL M9 media, containing 1% dextrans of starch (Sigma-Aldrich) as sole carbon source (M9-Dextrin), in 48 well FlowerPlates (M2PLabs). The FlowerPlates were incubated at 1000 rpm and 28 °C. After 6 hours 100 µM of IPTG and 250 µM hesperetin was added. After 24 h of cultivation, the supernatant was harvested by centrifugation (3 min, 14000 rpm), and hesperetin rhamnosylation was analyzed via HPLC.

Biotransformations in shake flasks

For shake flask experiments performed in Part II no IPTG was supplemented. In general, if not stated otherwise, 20 mL of growth medium were inoculated using 200 µL of fresh *E. coli* over-night cultures and 5 g/L aglycone was added. The shake flasks were incubated at 150 rpm at 37 °C. The supernatant was analyzed via HPLC.

Biotransformations in a bioreactor

A 5 ml *E. coli* preculture was inoculated in shake flasks from cryopreservation with the appropriate antibiotics and grown overnight at 28 °C and 150 rpm. The biotransformation was performed in a 250 mL stirred parallel bioreactor system (DAS-Box, DASGIP, Germany) with a working volume of 100 mL at a constant pH of 7.2, a stirrer controlled dissolved oxygen (DO) of 30 %, and a temperature of 28 °C. The growth medium consisted of Terrific Broth (Roth), containing 5 % dextrans of starch, 100 µM IPTG, and 500 mg hesperetin was inoculated to an OD₆₀₀ of 1 from the preculture. The pH value was controlled using 25 % ammonia and 2.5 M phosphoric acid. The supernatant was analyzed using HPLC over a time span of 48 h if not stated otherwise.

For bioreactor experiments performed in Part II the aglycone varied, and no IPTG induction was performed. Additionally the DO concentration was reduced to 20 % and the temperature increased to 37 °C. The inoculum was reduced to an OD₆₀₀ of 0.2 and the run-time of the bioreactors was increased to 72 h.

10. Molecular Biology

10.1. Primers and Plasmids

A list of all plasmids used within this study is given in table 10.1. A list of primers used for the generation and verification of deletion mutants is given in table 10.2, a list of primers used to generate plasmids is given in table 10.3. The glycosyltransferases cloned into the GT-module used in the rhamnosyltransferase activity screen were mostly generated by Dr. Friedericke Bönisch and Kerstin Wolff and are given in table 10.4.

Table 10.1.: Plasmids used within this study, excluding the platform glycosyltransferases used in blue/white screening which are given in table 10.4.

Plasmid	Source
pRedET(Amp)	Gene Bridges
pFLP2	Friedericke Haack, AG Streit
pCC1Fos	Epicentre
pCC1Lig	This Study
pCC1Lig::Mhex-FRT-Kan-FRT	This Study
pTrcHisA	Thermo Fisher Scientific
pTrcHisA::GtfC(opt)	This Study
pTrcHisA::GtfD(opt)	This Study
pK44::GtfD(opt)	Max Konersmann
pK44-MalT::GtfD(opt)	This Study
pK44-MalT::GtfC(opt)	This Study
pK44-MalT::AmUGT(opt)	This Study
pK44-MalT::VvUGT(opt)	This Study
pK44-MalT::GtfW	This Study
pK44-MalT::RhaGT	This Study
pCDFDuet-1	Novagen
pCDF-T5:: <i>rmlOP</i>	This Study
pCDF-malZp	This Study
pCDF-malZp:: <i>rmlAB::rmlCD</i>	This Study
pCDF-malZp:: <i>galU</i>	This Study
pCDF-malZp:: <i>galU::MUM4</i>	This Study
pCDF-malZp:: <i>galU::ugd</i>	This Study

Table 10.2.: Primers used to generate and verify deletion or insertion mutants

Name	Sequence
P2_Kan	CGAGACTAGTGAGACGTGCTAC
<i>ΔmalZ</i>	
FW_malZ_KO	TGCATTAGGCTATGGCAAGGTGATCAGATTTTCATCACAGGGGAATTATGAATT AACCCCTCACTAAAGGGCGG
RV_malZ_KO	GTTTTATCCGCGGATGATGGCGCAGGCGTCACGCAAGGCGTTATAAAACGTAA TACGACTCACTATAGGGCTCG
FW_malZ_Int	GATCGCCAGCGTTGGTTTAC
RV_malZ_Int	CCACTGTGGTTAAACACGCC
FW_malZ_ext	CAGATGATGAGTGATCC
RV_malZ_ext	GCTCATTATGACGCC
<i>Δagp</i>	
FW_agp_KO	CATATTTCTGTCCACTCTTTAGTGATTGATAACAAAAGAGGTGCCAGGAAATTAACCCCTCACT AAAGGGCGG
RV_agp_KO	TAAAAACGTTTAAACCAGCGACTCCCCGCTTCTCGCGGGGAGTTTTCTGTAATACGACTCACT ATAGGGCTCG
FW_agp_Int	ACTCGCTTCAAACGCTCAGG
RV_agp_Int	GGTAGCTGTCGGTAAGCTGG
FW_agp_Ext	CTGTTCCCGGAAAAAAGT
RV_agp_Ext	CGAACAGACCATCGAAC
<i>Δpgm</i>	
FW_pgm_KO	TGAGAAGGTTTGCGGAACCTATCTAAAACGTTGCAGACAAAAGGACAAAAGCAAATTAACCCCTCACT AAAGGGCGG
RV_pgm_KO	ATACGTAAAAAAGGGCGATCTTGCGACCGCCCTTTTTTTTATAAATGTGTTAATACGACTCACTA TAGGGCTC
FW_pgm_Int	GCAGTGGGGCAAAGATGTTG
RV_pgm_Int	ACCAGCCGTTGTGTCAGTCATC
FW_pgm_Ext	ATTCCCGCGGAATTGAT
RV_pgm_Ext	TCAGGCAATTCTGTGTTTGTC
<i>ΔgalU</i>	
FW_galU_KO	ATACAGAAATATGAACACGTTCAAACACGAAACAGTCCAGGAGAATTTAAAATTAACCCCTCACT AAAGGGCGG
RV_galU_KO	AACGGCGTCGATTGCTCAACGCCGTTTCGTGGATAACACCGATACGGATGTAATACGACTCACT ATAGGGCTC
FW_galU_Int	CCAGGATGTTGCCGGC
RV_galU_Int	TTTGCCAGCAACGGCC
FW_galU_Ext	ACCGGTGGTCGACTGC
RV_galU_Ext	GCCAAGGCCGTACTCC
<i>Δpgi</i>	
FW_pgi_KO	CGCTACAATCTTCCAAAGTCACAATTCTCAAAATCAGAAGAGTATTGCTAAATTAACCCCTCACT AAAGGGCGG
RV_pgi_KO	TCGTGCTATGTATTAATTGCCGAATACGATGTACATATCGGCATCGACCTTAATACGACTCACT ATAGGGCTC
FW_pgi_Int	CCCGGAAACCACGCTG
RV_pgi_Int	CAACGCACCCAGGCTG
FW_pgi_Ext	TCCACTCCTGGCGGTC
RV_pgi_Ext	ACGTCGGCATTGTTATTAAGG

Table 10.2 continued.

Name	Sequence
P2_Kan	CGAGACTAGTGAGACGTGCTAC
<i>ΔrecA::G6-amylase</i>	
FW_recA(Mhex)	AAAAAAGCAAAGGGCCGAGATGCGACCCTTGTGTATCAAACAAGACGACTGACAGCTA GCTCAGTC
RV_recA(Mhex)	TACTGTATGAGCATACAGTATAATTGCTTCAACAGAACATATTGACTATCATTGTTCCT ACTCAGGAGAGC
FW_recA_Int	CCTCTTTCACCGCGCC
RV_recA_Int	GCTGCAGGTGATCGCC
FW_recA_Ext	CATATGCCGGGCGACG
RV_recA_Ext	CCGGCGGAATGCTTC
RV_MHex_int	GCGCCCTTCCATGCTG
RV_Mhex_veri	GGCCCTTACCATTTTCAG
<i>ΔrmlBDACX</i>	
FW_rmlOP_KO	CGATTAAGAACAAGCGTACTTGATATTCCTGGGTATATTGCTTGGGT GATAATTAACCCCTACTAAAGGGCGG
RV_rmlOP_KO	GTGAAAATACTTGTACTGGTGGCGCAGGATTTATTGGTTCAGCTGT AGTTAATACGACTCACTATAGGGCTCG
FW_rmlC	CATATGAATGTGATTAGAAGTAAAT
RV_rmlC	CTCGAGAGATAATTTATTGCTATTCATGCA
FW_wzxB_ext	GCAGAATTAATGAAAAGCACCACC
FW_rmlOP_ext	GGTAGCTGTAAAGCCAGGGG
<i>ΔglgC</i>	
FW_glgC_KO	ATGGTTAGTTTLAGAGAAGAACGATCACTTAATGTTGGCGGCCAGCTGCCAATTAACCCCTC ACTAAAGGGCG
RV_glgC_KO	TTATCGCTCCTGTTTATGCCCTAACTTCGGTAGCATTTCGCGCCTTACCATAATACGACT CACTATAGGGCTC
FW_glgC_Int	CCAATAAGCGAGCAAAACCG
RV_glgC_Int	TCGCTTCCAGTAAGCTTCC
FW_glgC_Ext	CGGATTGTGTGTGTTCCAGA
RV_glgC_Ext	TTAAGCAGCGGGAACATCTC
<i>ΔushA</i>	
FW_ushA_KO	ATGAAATTATTGCAGCGGGGCGTGGCGTTAGCGCTGTTAACCACATTTAC
RV_ushA_KO	TTACTGCCAGCTCACCTCACCTTTCGGTTCATAAACACTCACATCCAGCG
FW_ushA_Int	ATTCAGGAGCTGCAACAGAC
RV_ushA_Int	GGCGGTCAGGTAATCAATCA
FW_ushA_Ext	TGGGGTTGTTCACTCATTGC
RV_ushA_Ext	TCGATGCCAAATTTGCTGATATC

Table 10.3.: Primers used within this study to generate and verify production plasmids

Name	Sequence
Glycosyltransferases	
FW_malZp_RBS	GCCCATGGTATCCGC
RV_malZp_RBS	ATGCGGATCCTYCTKATC
RBS_TOP	CCGGAATAATTTGTTTAACTTTAATACGRGCAGAAAGGCTCCAGGGATMAGRAG GATCCGCAT
malZp_BOT	TTAAAGTTAAACAAAATTATTCCGGCTGATCACCTTGCCATAGCCTAATGCAGGATCACTC ATCATCTGAAGGATATTTGGGGGAGGAGGACGGGGGCGGATACCATGGGC
FW_malT_PaeI	TATGCATGCAATTGTGACACAGTGCAAATTCA
RV_malT_PciI	ATAACATGTTTACACGCCGTACCCCAT
FW_GTD_BamHI	GCGGATCCATGACGAAATACAAAATGAATTAACAGG
RV_GTD_SalI	GCGTGGACTTAACCGCAAACAACCCG
FW_RhaGT	ATCGGATCCATGACCAAATTTCTCCGAGCC
RV_RhaGT	ATCCTCGAGCTAAACTTTTACAATTTTCGTCCAAC
Glycoswitches	
FW_CDF_NotI	AGCTGCGGCCGCCCTCAGGCATTTGAGAAGC
RV_CDF_EcoRI	CGGAATTCGCAATTAATGTAAGTTAGCTCACTC
FW_malZp_veri	GTCCCTCCTCCCCCAAATATC
FW_malZp_Duett	ACTCTAGATTTTCAGTGCAATTTATCTC
RV_malZp_Duett	ACCAGACTCGAGGGTACC
FW_rmlA_NcoI	ATGAAAATGCGTAAAGGTATTTATTTAGC
RV_rmlA_EcoRI	CTCGAATTCTTAATTTGAATCCTTCGT
FW_rmlB_EcoRI	AAGAATTCATGAAAATACTTGTTACTGGTGCC
RV_rmlB_PstI	ACCTGCAGTTACTGGCGGCCCTCATAG
FW_rmlB_insA	CGTAAAACGGTGAATGGTACCTGTCC
RV_rmlB_insA	GGACAGGTACCATTCCACCGTTTTACG
rmlC_for_E_NdeI	CATATGAATGTGATTAGA ACTGAAAT
rmlC_rev_E_XhoI	CTCGAGAGATAATTTATTCGTATTCATGCA
FW_rmlD_infu	TGAATACGAATAAATTATCTCTCGAATGAATATCCTCCTTTTTGGCAAAAC
RV_rmlD_infu	GCAGCGGTTTCTTTACCAGACTCGATTAAATTGCTGTAGTCGTAAATAATTCATTG
FW_galU_NcoI	ATACCATGGGCATGGCTGCCATTAATACGAAAGTC
RV_galU_BamHI	TCGGATCCTTACTTCTTAATGCCCATCTCTTCTTC
FW_ugd_RF	AGGAGATATACATATGGCAGATCTCATGAAAATCACCATTTCCGG
RV_ugd_RF	CAGCGGTTTCTTTACCAGACTCGAGTTAGTCGCTGCCAAAGAGATC

Table 10.3 continued.

Name	Sequence
Sequencing primer	
RV_MalT_ext	ATCCCTCATGCCATCTGCTG
FW_pK44_seq	GTTCGCGCCGGAAAGTTTAG
RV_CC1Lig_seq	ACCACGGTCCCCTCG
FW_CC1Lig_seq2	GTCTGATTATCGGTCTGGGAC
Trc_RBS_seq	CAGACAAGCTGTGACCGTCT
FW_CDF-Lig_seq	TCGAGATCCCGGTGCC
RV_CDF-Lig_seq	TCGGTTCAGGGCAGGG
G6-amylase	
FW_prom_rrnb_Pci	CATGACATGTGAATTCGC
RV_prom_rrnb_Not	AGCTGCGGCCG
FW_CC1Lig	GCCCCACCTGACCCCAT
RV_CC1Lig	GCCGGATCCCACGTGAAG
FW_RBS_Mhex	AACGAGAATACACAGAGTAAGGAGAGTAAACATGAGCGGCTGCCGCTGATT
RV_Mhex	TTATTTGTTGACCCAAATAGAAACTGACCCCTCC
FW_Kan-FRT	AATTAACCCTCACTAAAGGGCG
RV_Kan-FRT	TAATACGACTCACTATAGGGCTC
BO1_CC1_Mhex	GCAAGCTTCACGTGGGATCCGGCAACGAGAATACACAGAGTAAGGAGA GTAAACATGAGCG
BO2_Mhex_Kan	GAATGGAGGGTCAGTTTCTATTTGGGTCAACAAATAAAATTAACCCTCAC TAAAGGGCGGCCG
BO3_Kan_CC1	GTATAGGAACTTCTCGAGCCCTATAGTGAGTCGTATTAGCCCCACCTGAC CCCATGCC

Table 10.4.: Glycosyltransferases used within this study with their accession numbers if available.

Glycosyltransferase	Origin	Accession number
GtfC(opt)	metagenome (river Elbe, Germany)	JX157627
GtfD(opt)	<i>Dyadobacter fermentans</i>	CP001619.1
GtfW	<i>Bacillus wheinestephanensis</i>	CP011145.1
RhaGT	<i>Arabidopsis thaliana</i>	AEE31240.1
AmUGT(opt)	<i>Antirrhinum majus</i>	AB362988.1
VvUGT(opt)	<i>Vitis vinifera</i>	CBI40488.3
GtfF	<i>Fibrosoma limi</i>	CAIT01000004
GtfH	<i>Helicobacter pylori</i>	HP0421
GtfJ	<i>Bradyrhizobium japonicum</i>	CP009692.1
GtfL	<i>Spirosoma linguale</i>	CP001737.1
GtfX	<i>Xanthomonas campestris</i>	NC_003902.1
GtfS(opt)	<i>Segetibacter koreensis</i>	NZ_KB893315.1
Chim3b	Chimera of GtfC and GtfD	-
Chim4b	Chimera of GtfC and GtfD	-
Gtf31(opt)	<i>Flaviumibacter solisilvae</i>	KIC94899.1
Gtf32(opt)	<i>Cesiribacter andamanensis</i>	EMR00735.1
Gtf33(opt)	<i>Niabella aurantiaca</i>	WP_018628482.1
Gtf34(opt)	<i>Spirosoma radiotolerans</i>	AKD55267.1
Gtf35(opt)	<i>Fibrella aestuarina</i>	CCH02745.1
Gtf36(opt)	<i>Aquimarina macrocephali</i>	WP_024771218.1
GtfN	<i>Sinorhizobium fredii</i>	WP_015887755.1
GtfO	<i>Streptomyces coelicolor</i>	WP_011026800.1

10.2. Molecular biology methods

Various standard methods for molecular biology, as e.g. agarose gel electrophoresis can be obtained from Sambrook and Russell [147].

Polymerase chain reaction (PCR)

Proof reading polymerases were used to amplify genes of interest for cloning into specific vectors, or amplifying knockout fragments for gene deletions in *E. coli*. To enhance the sensitivity of a PCR reaction without having to optimize the annealing temperature a touch-down (TD) PCR was generally performed. In contrast to regular PCRs the annealing temperature of TD PCRs is decreased each cycle by e.g. 1 °C. The melting temperature (T_M) of the annealing step was started 7 °C above the primer annealing temperatures and reduced by 10 °C in 10 cycles, followed by 20 cycles of elongation 3 °C below calculated T_M .

Colony PCR

To verify the correct insertion of inserts into plasmids, or to verify deletion mutants, colony PCRs were performed. Single colonies were picked and transferred onto fresh agar plates using a 100 µL pipette tip and subsequently added into a PCR tube containing 25 µL of PCR master mix including a specific primer pair and usually TAQ polymerase. To reduce *E. coli* background signals in the verification process of *E. coli* genes, commercial DNase treated commercial polymerases were used. The colony PCRs were generally performed as a touch-down PCR.

DNA purification

Plasmids were isolated from *E. coli* DH5α strains using Presto™ Mini Plasmid Kit. If necessary PCR or restriction digested DNA fragments were purified using GenepHlow™ Gel/PCR kit. For specific sized DNA fragments agarose gel purification using the same kit was performed. All procedures were performed to the manufacturers protocol.

Heat Shock

Heat shock competent cells were created according to Sambrook and Russell [147]. Heat-shock competent cells were thawed on ice for 30 min, after which DNA for transformation was added, followed by incubation for 30 min. A preheated thermocycler (42 °C) was used to heat-shock the transformation mix for 45 seconds, followed by 2 min incubation on ice. Subsequently 250 µL SOC medium was added and regeneration was performed at the appropriate temperature for 30 min to 3 h. Afterwards different amounts of the transformation mix were plated onto agar plates with the appropriate antibiotics.

Electroporation

To obtain higher transformation efficiencies, electroporation was used. To transform a plasmid or a linear DNA fragment the designation strain was inoculated from cryopreservation or from an agar plate and cultured over night, at the appropriate temperature in 3 mL of LB medium. 10 mL LB medium was inoculated with 1 mL preculture and incubated for approximately 1-3 hrs at 37 °C. 1.5 mL of culture were harvested in a pre-cooled centrifuge and washed three times with ice-cold glycerol. The cells were resuspended in 100 µl 10 % glycerol, and the DNA for electroporation was added and transferred into 1 mm pre-cooled electroporation cuvettes. The electroporation was performed in BioRad GenePulser Xcell (Voltage 1350 V, Capacity 10 µF, Resistance 600 Ω, Cuvette 1 mm) and after electroporation, the cells were directly resuspended in 1 mL pre-warmed SOC media and regenerated for a minimal time of 30 min up to 3 hrs. The cells were plated on LB-agar plates containing the appropriate antibiotics.

Sequencing

Sequencing of created production plasmids was performed by Eurofins Genomics (Ebersberg), using dideoxy chain termination cycle sequencing (Sanger sequencing). Samples were generally sent premixed, using 15 µl of the DNA of interest mixed with 2 µl of sequencing primer, prepared in concentrations according to Eurofins Genomics.

10.3. Molecular cloning methods

Restriction cloning

Restriction cloning was performed according to Sambrook and Russell [147].

Ligase cycling reaction (LCR)

LCR makes use of thermostable Ligase and so called bridging oligonucleotides enabling the assembly and cloning of multiple DNA fragments. Although highly effective, larger costs through the necessity of phosphorylated primers make this method fall behind in comparison to other restriction-free cloning methods. For detailed information on LCR please refer to Kok et al. [148].

In-Fusion HD cloning (TaKaRa Biotech)

Infusion cloning is a ligase independent cloning technology. One or multiple inserts can be cloned into a linearized vector if they possess complementary ends of approximately 15 bp. The enzymes contained in Infusion cloning generate 5' overhangs of the complementary regions. These complementary overhangs anneal and are “rescued” in *E. coli* cells. The advantage of such a method is scarless cloning and the independence of unique restriction sites that can become limiting in larger constructs. For more detailed information on the In-Fusion cloning kit refer to the manufacturers guide. (<https://www.takarabio.com/learning-centers/cloning/in-fusion-cloning-faqs>)

Restriction free cloning

Restriction free cloning is a PCR based cloning method developed by Ent and Löwe [149]. In a first PCR reaction the fragment of interest is amplified, containing homologous regions to a plasmid of interest. In a second PCR reaction the primary PCR is used as primer sequence thereby directly creating the plasmid of interest containing single strand nicks at the insertions sites. These nicks are repaired by *E. coli* upon transformation. The negative background of “empty” plasmid is removed by restriction digestion of methylated DNA by DpnI.

QuickChange™

The QuickChange™ (Stratagene) protocol is closely related predecessor to the restriction free cloning procedure. A mutagenic primer pair is ordered containing a minor exchange or deletion of nucleotides from the template sequence. A PCR amplifying the complete plasmid containing the introduced mutation is performed followed by a DpnI digestion to remove unaltered template DNA.

10.4. Construction of production plasmids

The nucleotide sequences of the fragments used to generate the production plasmids are shown in the appendix in FASTA format.

pTrcHisA::GtfC(opt)

Glycosyltransferase C was ordered codon optimized for *E. coli* K-12 and sub-cloned by Eurofins Genomics (Germany) into pTrcHisA. The sequence of pTrcHisA::GtfC(Opt) was deposited in Genbank under the accession number MK802894.

pCDF-T5::rmlOP

The *rml* operon was initially cloned by Nele Ilmberger into pCDFDuet-1 under the control of a T7 promotor. In order to have a compatible plasmid under the control of a promotor expressible in *E. coli* K-12 the *rml* operon was firstly cloned into pQE30 under the control of a T5 promotor using BamHI and SacI as restriction enzymes. Using XhoI and PstI restriction enzymes the *rml* operon was reintegrated into the compatible pCDFDuet-1 plasmid. The sequence was deposited in Genbank under MK8002895.

pCC1Lig::G6-amylase

The backbone of pCC1Lig::G6-amylase is originally pCC1Fos. pCC1Fos was digested using NotI and PciI and ligated to a synthetic fragment composed of a promotor from the Anderson collection and terminator sequences, creating pCC1Lig. The newly generated pCC1Fos vector does not contain the *lacZ* gene used for blue-white screening or the lambda

10. Molecular Biology

cos site required for phage packaging. The G6-amylase was ordered codon optimized for *E. coli* K-12 from Eurofins Genomics and the natural export signal was replaced by an engineered FhuD secretion signal. Using the ligase cycling reaction the G6-amylase and a resistance cassette flanked by FRT sites for genomic integration were incorporated to form pCC1Lig::G6-amylase. The sequence was deposited under accession number MK802894 in Genbank.

pTrcHisA::GtfD(opt)

GtfD(opt) was synthesized by Eurofins Genomics (Germany) and delivered in a standard pK4 vector. GtfD(opt) was PCR amplified using FW_GTD_BamHI and RV_GTD_SalI primer pair and cloned using restriction cloning with BamHI and SalI into pTrcHisA.

pK44-MalT::GtfD(opt)

To further improve the auto-induced glycosylation system, the transcriptional activator MalT was amplified containing its natural promotor and RBS from *E. coli* K-12 (MG1655) genomic DNA using FW_malT_PaeI and RV_malT_PciI primer pair. The PCR product was cloned using restriction cloning with PaeI and PciI. GTs were cloned into pK44-MalT by a digestion using BamHI/XhoI.

pCDF-malZp & pRSF-malZp

The synthetic fragment malZp-Duet was ordered from Eurofins Genomics (Germany) and amplified using the primer pair FW_malZp_Duett and RV_malZp_Duett. The PCR fragment and the pCDF-Duet vector were cloned using restriction cloning with XbaI/XhoI yielding pCDF-malZp. The same procedure was performed using pRSF-Duet-1 as backbone, thereby creating pRSF-malZp.

pCDF-malZp::rmlAB::rmlCD

In a first step *rmlA* was cloned into pCDF-malZp using restriction cloning with NcoI and EcoRI after PCR amplification of *rmlA*, with FW_rmlA_NcoI and RV_rmlA_EcoRI primer pair. Secondly *rmlC* was incorporated using NdeI/XhoI restriction cloning from

pCDF-Duet::rmlA::rmlC. Thirdly *rmlB* was cloned using restriction cloning using EcoRI/PstI after PCR amplification with simultaneous replacement of a GTG starting codon to an ATG. A detected frameshift mutation in *rmlB* was corrected using a quick exchange protocol with the primer pair FW_rmlB_insA/RV_rmlB_insA. Finally *rmlD* was incorporated using Infusion cloning.

pCDF-malZp::galU

The primer pair FW_galU_NcoI and RV_galU_BamHI was used to amplify the *galU* gene and restriction cloning using NcoI and BamHI was performed to create pCDF-malZp::*galU*.

pCDF-malZp::galU::MUM4

Digestion of pCDF-malZp::galU with EcoRI/XhoI and pCDF-malZp::rmlA::MUM4 (Created in Bachelor Thesis of Carina Niemann) using EcoRI/XhoI. The pCDF-malZp::galU::MUM4 plasmid was created by Clara Vie during her internship.

pCDF-malZp::galU::ugd

The *ugd* gene was amplified from genomic *E. coli* K-12 (MG1655) DNA using the FW_ugd_RF and RV_ugd_RF primer pair. Afterwards restriction free cloning was performed using the primary PCR as template, for a secondary PCR using pCDF-malZp::galU as template.

11. Analytical Methods

11.1. High Performance Liquid Chromatography (HPLC)

For quantification of the produced Glycosides an analytical high-pressure liquid chromatography method was implemented using an Agilent ZORBAX SB-C18 column (4.6 mm internal diameter x 250 mm length, 5 μ m particle size) on a Hitachi Elite LaChrome HPLC system. Analysis was performed with acetonitrile (A) and water with 0.1 % trifluoroacetic acid (B) gradient (1. 0 min 15:85 (A:B), 2. 17 min 100:0, 3. 22 min 100:0, 4. 22.1 min 5:95, 5. 30 min 5:95) at a constant flow rate of 1 mL/min. For sample preparation, the cells were separated by centrifugation, and the cell-free supernatant was diluted appropriately. Glycosides were quantified using linear regression of the corresponding standard substances. Quercetin and kaempferol glycosylation was analyzed on a Nucleoshell RP18 column (2 mm internal diameter x 100 mm length, 2.7 μ m particle size) running an acetonitrile/water gradient (acetonitrile (A) and water (B) both containing 0.1 % acetic acid, 1. 0 min 10:90 (A:B) - 5 min 100:0, 2. 5-7 min 100:0, 3. 7-9 min 10:100) using an Thermo Scientific Ultimate 3000 UHPLC system at a flow rate of 0.5 mL/min. Absorption was monitored at 254 nm.

11.2. Thin Layer Chromatography

900 μ l of culture broth was extracted with 900 μ l ethyl acetate for 1 minute followed by centrifugation at 10 000 rpm for 5 min. 20 μ l of supernatant was applied by the ATS 4 (CAMAG, Switzerland) on (HP)TLC silica 60 F254 plates (20x10, Merck). The TLC plates were run in a TLC chamber using a mobile phase composed of ethyl acetate, formic acid, glacial acetic acid and water in a ratio of 100:11:11:27, respectively. The TLC plates

11. Analytical Methods

were dried using a hair dryer for approximately one minute. Absorption at 330 nm were acquired using a TLC Scanner 3 (CAMAG, Switzerland).

12. Acknowledgments

Firstly, I want to thank the German Federal Ministry of Education and research for the financial funding of this work (Grant number 031A376). Furthermore, I want to thank Prof. Wolfgang R. Streit for his support and guidance throughout this work. I am especially thankful for the “long leash,” enabling me to pursue my ideas and make my own mistakes, which have contributed significantly to my development as a scientist. I want to thank Prof. Dr. Nina Schützenmeister for taking over the position of the second examiner and all other members of the examination committee.

Furthermore, I want to thank Dr. Ulrich Rabausch for providing me with the opportunity to work in my research area of interest. The topic of metabolic engineering, especially the application and economic focus of Glyconic, has taught me so many priceless lessons. Thank you for the best research topic I could have ever imagined for my Ph.D. thesis, our countless discussions and the opportunity and responsibilities you have provided for me.

I want to thank the whole working group Rabausch, for the fantastic working atmosphere you created. Primarily working with Kerstin Wolff, the by far best technician one can have, and Dr. Friedericke Bönisch was a daily delight with lots of laughs and good discussion, work-wise, and personal. Furthermore, I want to thank Petra von Wiegen and Christiane Debus for all their help.

I would like to thank all members of the AG Streit. I will miss the working atmosphere, the discussions, crazy scientific ideas and crazy non-scientific ideas in numerous coffee breaks.

Finally, I want to thank my family for their constant support. No matter what I need, I can always count on you to help me without any questions asked. Thank you, without you, this would not have been possible.

Glossary

4-MU	4-methylumbelliferone
Aglycones	Specific structure of glycosides without the sugar moiety
Agp	Glucose-1-phosphatase
BaSP	Sucrose phosphorylase
CAZymes	Carbohydrate-Active enZymes
CHS	Chalcone synthase
CoA	Coenzyme A
COG	Cost of goods
DHA	Dihydroxyascorbate
<i>d</i> TDP-rha	<i>d</i> TDP-rhamnose
EC	Enzyme Classification number
G1P	Glucose-1-phosphate
GalU	UTP-1-phosphate uridylyltransferase
GH	Glycoside hydrolase
GlgC	Glucose-1-phosphate adenylyltransferase
GP	Glycoside phosphorylases
GS	Glycogen/starch synthase
GSH	Glutathione
GSSG	Glutathione disulfide
GT	Glycosyltransferase
IPTG	Isopropylthio- β -galactoside
Lac-Z	β -galactosidase
LPS	Lipopolysaccharides
MalP	Maltodextrin phosphorylase
MalQ	Amylomaltase
MalT	Transcriptional activator of the maltodextrin system

MalZ	Maltodextringlucosidase
MUM4	UDP-rhamnose synthase
N4'R	Naringenin-4'-O-rhamnoside
N5R	Naringenin-5-O-rhamnoside
N7G	Naringenin-7-O-glucoside
N7Ru	Naringenin-7-O-rutinoside
NDP	Nucleotide diphosphate
NHDF	Normal human dermal fibroblasts
NHEK	Normal human epidermal keratinocytes
NHEM	Normal human epidermal melanocytes
Pgi	Glucose-6-phosphate isomerase
Pgm	Phosphoglucomutase
PTS	Glucose specific phosphotransferase system
Q3R	Quercetin-3-O-rhamnoside
QQ	Quercetin quinone
RBS	Ribosome binding site
RecA	DNA recombination and repair protein
ROS	Reactive oxygen species
SC	<i>Stratum corneum</i>
STY	Space-time yield
TB	Terrific broth growth medium
TG	Transglycosidase
Ugd	UDP-glucose dehydrogenase
UshA	UDP-sugar hydrolase
VEGF	Vascular endothelial growth factor
WT	Wildtype
X	5-Brom-4-chloro-indoxyl
X-gal	5-Brom-4-chloro-indoxyl- β -D-galactose
Zwf	NADP ⁺ -dependent glucose-6-phosphate dehydrogenase

Bibliography

- [1] U. Rabausch et al. "Functional Screening of Metagenome and Genome Libraries for Detection of Novel Flavonoid-Modifying Enzymes". In: *Applied and Environmental Microbiology* (2013). DOI: 10.1128/AEM.01077-13.
- [2] P. M. Coutinho et al. "An Evolving Hierarchical Family Classification for Glycosyltransferases". In: *Journal of Molecular Biology* (2003). DOI: 10.1016/S0022-2836(03)00307-3.
- [3] V. Lombard et al. "The carbohydrate-active enzymes database (CAZy) in 2013". In: *Nucleic Acids Research* (2014). DOI: 10.1093/nar/gkt1178.
- [4] L. Lairson et al. "Glycosyltransferases: Structures, Functions, and Mechanisms". In: *Annual Review of Biochemistry* (2008). DOI: 10.1146/annurev.biochem.76.061005.092322.
- [5] E. Cid et al. "Glycogen synthase: towards a minimum catalytic unit?" In: *FEBS Letters* (2002). DOI: 10.1016/S0014-5793(02)03313-6.
- [6] R. A. Laine. "A calculation of all possible oligosaccharide isomers both branched and linear yields 1.05×10^{12} structures for a reducing hexasaccharide: the *Isomer Barrier* to development of single-method saccharide sequencing or synthesis systems". In: *Glycobiology* (1994). DOI: doi.org/10.1093/glycob/4.6.759.
- [7] P. Lapébie et al. "Bacteroidetes use thousands of enzyme combinations to break down glycans". In: *Nature Communications* (2019). DOI: 10.1038/s41467-019-10068-5.
- [8] J. M. Cote and E. A. Taylor. "The Glycosyltransferases of LPS Core: A Review of Four Heptosyltransferase Enzymes in Context". In: *International Journal of Molecular Sciences* (2017). DOI: 10.3390/ijms18112256.
- [9] D. A. Wesener et al. "Recognition of microbial glycans by human intelectin-1". In: *Nature Structural & Molecular Biology* (2015). DOI: 10.1038/nsmb.3053.
- [10] I. Benz and M. A. Schmidt. "Never say never again: protein glycosylation in pathogenic bacteria". In: *Molecular Microbiology* (2002). DOI: 10.1046/j.1365-2958.2002.03030.x.
- [11] H. Li et al. "Understanding protein glycosylation pathways in bacteria". In: *Future Microbiology* (2016). DOI: 10.2217/fmb-2016-0166.
- [12] Z. Yao et al. "Characterization of human UDP-glucuronosyltransferases responsible for glucuronidation and inhibition of norbakuchinic acid, a primary metabolite of hepatotoxicity and nephrotoxicity component bakuchiol in *Psoralea corylifolia* L." In: *RSC Advances* (2017). DOI: 10.1039/C7RA10376J.
- [13] B. Poppenberger et al. "Detoxification of the *Fusarium* Mycotoxin Deoxynivalenol by a UDP-glucosyltransferase from *Arabidopsis thaliana*". In: *Journal of Biological Chemistry* (2003). DOI: 10.1074/jbc.M307552200.
- [14] X. Li et al. "A barley UDP-glucosyltransferase inactivates nivalenol and provides *Fusarium* Head Blight resistance in transgenic wheat". In: *Journal of Experimental Botany* (2017). DOI: 10.1093/jxb/erx109.

- [15] R. Delgoda and J. Murray. “Evolutionary Perspectives on the Role of Plant Secondary Metabolites”. In: *Pharmacognosy*. Elsevier, 2017. Chap. 7. DOI: 10.1016/B978-0-12-802104-0.00007-X.
- [16] D. N. Bolam et al. “The crystal structure of two macrolide glycosyltransferases provides a blueprint for host cell antibiotic immunity”. In: *Proceedings of the National Academy of Sciences* (2007). DOI: 10.1073/pnas.0607897104.
- [17] J. Wang and B. Hou. “Glycosyltransferases: key players involved in the modification of plant secondary metabolites”. In: *Frontiers of Biology in China* (2009). DOI: 10.1007/s11515-008-0111-1.
- [18] J. He and M. M. Giusti. “Anthocyanins: Natural Colorants with Health-Promoting Properties”. In: *Annual Review of Food Science and Technology* (2010). DOI: 10.1146/annurev.food.080708.100754.
- [19] V. Křen and L. Martinkova. “Glycosides in Medicine: “The Role of Glycosidic Residue in Biological Activity””. In: *Current Medicinal Chemistry* (2001). DOI: 10.2174/0929867013372193.
- [20] V. Křen and T. Řezanka. “Sweet antibiotics – the role of glycosidic residues in antibiotic and antitumor activity and their randomization”. In: *FEMS Microbiology Reviews* (2008). DOI: 10.1111/j.1574-6976.2008.00124.x.
- [21] A. Bentsáth, S. Rusznyák, and A. Szent-Györgyl. “Vitamin Nature of Flavones”. In: *Nature* (1936). DOI: 10.1038/138798a0.
- [22] V. Bruckner and A. Szent-Györgyl. “Chemical Nature of Citrin”. In: *Nature* (1936). DOI: 10.1038/1381057b0.
- [23] Y. Nakamura et al. “KNAPSAcK Metabolite Activity Database for Retrieving the Relationships Between Metabolites and Biological Activities”. In: *Plant and Cell Physiology* (2014). DOI: 10.1093/pcp/pct176.
- [24] M. L. Falcone Ferreyra, S. P. Rius, and P. Casati. “Flavonoids: biosynthesis, biological functions, and biotechnological applications”. In: *Frontiers in Plant Science* (2012). DOI: 10.3389/fpls.2012.00222.
- [25] J. Zha et al. “Pathway enzyme engineering for flavonoid production in recombinant microbes”. In: *Metabolic Engineering Communications* (2019). DOI: 10.1016/j.mec.2019.e00104.
- [26] J.-L. Ferrer et al. “Structure and function of enzymes involved in the biosynthesis of phenylpropanoids”. In: *Plant Physiology and Biochemistry* (2008). DOI: 10.1016/j.plaphy.2007.12.009.
- [27] L. Lepiniec et al. “Genetics and Biochemistry of Seed Flavonoids”. In: *Annual Review of Plant Biology* (2006). DOI: 10.1146/annurev.arplant.57.032905.105252.
- [28] P. V. A. Babu, D. Liu, and E. R. Gilbert. “Recent advances in understanding the anti-diabetic actions of dietary flavonoids”. In: *Journal of Nutritional Biochemistry* (2013).
- [29] G. Williamson, C. D. Kay, and A. Crozier. “The Bioavailability, Transport, and Bioactivity of Dietary Flavonoids: A Review from a Historical Perspective”. In: *Comprehensive Reviews in Food Science and Food Safety* (2018). DOI: 10.1111/1541-4337.12351.
- [30] J. Boyer and R. H. Liu. “Apple phytochemicals and their health benefits”. In: *Nutrition Journal* (2004). DOI: 10.1186/1475-2891-3-5.

-
- [31] A. W. Boots et al. "Oxidized quercetin reacts with thiols rather than with ascorbate: implication for quercetin supplementation". In: *Biochemical and Biophysical Research Communications* (2003). DOI: 10.1016/S0006-291X(03)01438-4.
- [32] H. M. Awad et al. "Quenching of Quercetin Quinone/Quinone Methides by Different Thiolate Scavengers: Stability and Reversibility of Conjugate Formation". In: *Chemical Research in Toxicology* (2003). DOI: 10.1021/tx020079g.
- [33] H. Jacobs et al. "An essential difference in the reactivity of the glutathione adducts of the structurally closely related flavonoids monoHER and quercetin". In: *Free Radical Biology and Medicine* (2011). DOI: 10.1016/j.freeradbiomed.2011.09.013.
- [34] G. Galati et al. "Glutathione-Dependent Generation of Reactive Oxygen Species by the Peroxidase-Catalyzed Redox Cycling of Flavonoids". In: *Chemical Research in Toxicology* (1999). DOI: 10.1021/tx980271b.
- [35] K. Lemmens et al. "The Minor Structural Difference between the Antioxidants Quercetin and 4'-O-Methylquercetin Has a Major Impact on Their Selective Thiol Toxicity". In: *International Journal of Molecular Sciences* (2014). DOI: 10.3390/ijms15057475.
- [36] A. Hopia and M. Heinonen. "Antioxidant activity of flavonol aglycones and their glycosides in methyl linoleate". In: *Journal of the American Oil Chemists' Society* (1999). DOI: 10.1007/s11746-999-0060-0.
- [37] M. J. Chung et al. "Water-Soluble Genistin Glycoside Isoflavones Up-Regulate Antioxidant Metallothionein Expression and Scavenge Free Radicals". In: *Journal of Agricultural and Food Chemistry* (2006). DOI: 10.1021/jf060510y.
- [38] A. Lepak et al. "Creating a Water-Soluble Resveratrol-Based Antioxidant by Site-Selective Enzymatic Glucosylation". In: *ChemBioChem* (2015). DOI: 10.1002/cbic.201500284.
- [39] H.-J. Woo et al. "Synthesis and characterization of ampelopsin glucosides using dextransucrase from *Leuconostoc mesenteroides* B-1299CB4: Glucosylation enhancing physicochemical properties". In: *Enzyme and Microbial Technology* (2012). DOI: 10.1016/j.enzmictec.2012.07.014.
- [40] R. Roscher, W. Schwab, and P. Schreier. "Stability of naturally occurring 2,5-dimethyl-4-hydroxy-3 [2H]-furanone derivatives". In: *Zeitschrift für Lebensmitteluntersuchung und -Forschung A* (1997). DOI: 10.1007/s002170050109.
- [41] A. Vidal et al. "Stability of DON and DON-3-glucoside during baking as affected by the presence of food additives". In: *Food Additives & Contaminants: Part A* (2018). DOI: 10.1080/19440049.2017.1401741.
- [42] I. Yamamoto et al. "Collagen Synthesis in Human Skin Fibroblasts is Stimulated by a Stable Form of Ascorbate, 2-O- α -D-Glucopyranosyl-L-Ascorbic Acid". In: *The Journal of Nutrition* (1992).
- [43] L. Mäkilä et al. "Stability of Hydroxycinnamic Acid Derivatives, Flavonol Glycosides, and Anthocyanins in Black Currant Juice". In: *Journal of Agricultural and Food Chemistry* (2016). DOI: 10.1021/acs.jafc.6b01005.
- [44] C. Manach et al. "Bioavailability and bioefficacy of polyphenols in humans. I. Review of 97 bioavailability studies". In: *The American Journal of Clinical Nutrition* (2005). DOI: 10.1093/ajcn/81.1.230S.
-

Bibliography

- [45] I. L. F. Nielsen et al. "Bioavailability Is Improved by Enzymatic Modification of the Citrus Flavonoid Hesperidin in Humans: A Randomized, Double-Blind, Crossover Trial". In: *The Journal of Nutrition* (2006). DOI: 10.1093/jn/136.2.404.
- [46] P. C. H. Hollman. "Absorption, Bioavailability, and Metabolism of Flavonoids". In: *Pharmaceutical Biology* (2004).
- [47] K. Nemeth et al. "Deglycosylation by small intestinal epithelial cell β -glucosidases is a critical step in the absorption and metabolism of dietary flavonoid glycosides in humans". In: *European Journal of Nutrition* (2003). DOI: 10.1007/s00394-003-0397-3.
- [48] G. Corona et al. "The Impact of Gastrointestinal Modifications, Blood-Brain Barrier Transport, and Intracellular Metabolism on Polyphenol Bioavailability". In: *Polyphenols in Human Health and Disease*. Elsevier, 2014. DOI: 10.1016/B978-0-12-398456-2.00044-X.
- [49] E. Diaz et al. "Biodegradation of Aromatic Compounds by *Escherichia coli*". In: *Microbiology and molecular Biology Reviews* (2001).
- [50] S.-Y. Chuang et al. "Elucidating the Skin Delivery of Aglycone and Glycoside Flavonoids: How the Structures Affect Cutaneous Absorption". In: *Nutrients* (2017). DOI: 10.3390/nu9121304.
- [51] W. Koenigs and E. Knorr. "Ueber einige Derivate des Traubenzuckers und der Galactose". In: *Berichte der deutschen chemischen Gesellschaft* (1901). DOI: 10.1002/cber.190103401162.
- [52] K. Igarashi. "The Koenigs-Knorr Reaction". In: *Advances in Carbohydrate Chemistry and Biochemistry*. Elsevier, 1977. DOI: 10.1016/S0065-2318(08)60326-1.
- [53] F. De Bruyn et al. "Biotechnological advances in UDP-sugar based glycosylation of small molecules". In: *Biotechnology Advances* (2015). DOI: 10.1016/j.biotechadv.2015.02.005.
- [54] X. Zhu and R. R. Schmidt. "New Principles for Glycoside-Bond Formation". In: *Angewandte Chemie International Edition* (2009). DOI: 10.1002/anie.200802036.
- [55] T. Desmet et al. "Enzymatic Glycosylation of Small Molecules: Challenging Substrates Require Tailored Catalysts". In: *Chemistry - A European Journal* (2012). DOI: 10.1002/chem.201103069.
- [56] K. Corbett et al. "Tailoring the substrate specificity of the β -glucosidase from the thermophilic archaeon *Sulfolobus solfataricus*". In: *FEBS Letters* (2001).
- [57] C. Liang et al. "Engineering a Carbohydrate-processing Transglycosidase into Glycosyltransferase for Natural Product Glycodiversification". In: *Scientific Reports* (2016). DOI: 10.1038/srep21051.
- [58] T. Desmet and W. Soetaert. "Enzymatic glycosyl transfer: mechanisms and applications". In: *Biocatalysis and Biotransformation* (2011). DOI: 10.3109/10242422.2010.548557.
- [59] K. De Winter et al. "Biphasic Catalysis with Disaccharide Phosphorylases: Chemoenzymatic Synthesis of α -D-Glucosides Using Sucrose Phosphorylase". In: *Organic Process Research & Development* (2014). DOI: 10.1021/op400302b.
- [60] J. Seibel, H.-J. Jördening, and K. Buchholz. "Glycosylation with activated sugars using glycosyltransferases and transglycosidases". In: *Biocatalysis and Biotransformation* (2006). DOI: 10.1080/10242420600986811.

-
- [61] T. M. Gloster. "Advances in understanding glycosyltransferases from a structural perspective". In: *Current Opinion in Structural Biology* (2014). DOI: 10.1016/j.sbi.2014.08.012.
- [62] D.-M. Liang et al. "Glycosyltransferases: mechanisms and applications in natural product development". In: *Chemical Society Reviews* (2015). DOI: 10.1039/C5CS00600G.
- [63] S. S. Lee et al. "Mechanistic evidence for a front-side, S_Ni-type reaction in a retaining glycosyltransferase". In: *Nature Chemical Biology* (2011). DOI: 10.1038/nchembio.628.
- [64] C. Ruprecht et al. "High level production of flavonoid rhamnosides by metagenome-derived Glycosyltransferase C in *Escherichia coli* utilizing dextrans of starch as a single carbon source". In: *Metabolic Engineering* (2019). DOI: 10.1016/j.ymben.2019.07.002.
- [65] J.-X. Liao et al. "Highly efficient synthesis of flavonol 5-O-glycosides with glycosyl *ortho*-alkynylbenzoates as donors". In: *Organic & Biomolecular Chemistry* (2015). DOI: 10.1039/C5OB02313K.
- [66] K. R. Choi et al. "Systems Metabolic Engineering Strategies: Integrating Systems and Synthetic Biology with Metabolic Engineering". In: *Trends in Biotechnology* (2019). DOI: 10.1016/j.tibtech.2019.01.003.
- [67] S. Y. Park et al. "Metabolic Engineering of Microorganisms for the Production of Natural Compounds". In: *Advanced Biosystems* (2017). DOI: 10.1002/adbi.201700190.
- [68] J. Bailey. "Toward a science of metabolic engineering". In: *Science* (1991). DOI: 10.1126/science.2047876.
- [69] S. Y. Lee and H. U. Kim. "Systems strategies for developing industrial microbial strains". In: *Nature Biotechnology* (2015). DOI: 10.1038/nbt.3365.
- [70] H.-P. Meyer, W. Minas, and D. Schmidhalter. "Industrial-Scale Fermentation". In: *Industrial Biotechnology: Products and Processes*. 2017. DOI: 10.1002/9783527807833.ch1.
- [71] T. Escherich. "Die Darmbakterien des Neugeborenen Säuglings". In: *Fortschritte der Medizin* (1885).
- [72] D. Steverding. "Die Geschichte der Kolibakterien. Vom Darmbewohner zum Bioreaktor". In: *Biologie in unserer Zeit* (2010). DOI: 10.1002/biuz.201010423.
- [73] J. Lederberg. "*E. coli* K-12". In: *Microbiology Today* (2004).
- [74] I. M. Keseler et al. "The EcoCyc database: reflecting new knowledge about *Escherichia coli* K-12". In: *Nucleic Acids Research* (2016). DOI: 10.1093/nar/gkw1003.
- [75] S. Pontrelli et al. "*Escherichia coli* as a host for metabolic engineering". In: *Metabolic Engineering* (2018). DOI: 10.1016/j.ymben.2018.04.008.
- [76] J.-A. Yoon et al. "Production of a Novel Quercetin Glycoside through Metabolic Engineering of *Escherichia coli*". In: *Applied and Environmental Microbiology* (2012). DOI: 10.1128/AEM.00275-12.
- [77] F. De Bruyn et al. "Development of an *in vivo* glucosylation platform by coupling production to growth: Production of phenolic glucosides by a glycosyltransferase of *Vitis vinifera*". In: *Biotechnology and Bioengineering* (2015). DOI: 10.1002/bit.25570.

- [78] F. De Bruyn et al. “Metabolic engineering of *Escherichia coli* into a versatile glycosylation platform: production of bio-active quercetin glycosides”. In: *Microbial Cell Factories* (2015). DOI: 10.1186/s12934-015-0326-1.
- [79] E.-K. Lim, D. A. Ashford, and D. J. Bowles. “The Synthesis of Small-Molecule Rhamnosides through the Rational Design of a Whole-Cell Biocatalysis System”. In: *ChemBioChem* (2006). DOI: 10.1002/cbic.200600193.
- [80] D. Simkhada, H. C. Lee, and J. K. Sohng. “Genetic Engineering Approach for the Production of Rhamnosyl and Allosyl Flavonoids from *Escherichia coli*”. In: *Biotechnology and Bioengineering* (2010). DOI: 10.1002/bit.22782.
- [81] D. Simkhada et al. “Metabolic Engineering of *Escherichia coli* for the Biological Synthesis of 7-*O*-Xylosyl Naringenin”. In: *Molecules and Cells* (2009). DOI: 10.1007/s10059-009-0135-7.
- [82] D. B. Kell and S. G. Oliver. “How drugs get into cells: tested and testable predictions to help discriminate between transporter-mediated uptake and lipoidal bilayer diffusion”. In: *Frontiers in Pharmacology* (2014). DOI: 10.3389/fphar.2014.00231.
- [83] D. Smith et al. “Passive Lipoidal Diffusion and Carrier-Mediated Cell Uptake Are Both Important Mechanisms of Membrane Permeation in Drug Disposition”. In: *Molecular Pharmaceutics* (2014). DOI: 10.1021/mp400713v.
- [84] M.-F. Giraud and J. H. Naismith. “The rhamnose pathway”. In: *Current Opinion in Structural Biology* (2000). DOI: 10.1016/S0959-440X(00)00145-7.
- [85] G. Stevenson et al. “Structure of the O Antigen of *Escherichia coli* K-12 and the Sequence of Its *rfb* Gene Cluster”. In: *Journal of Bacteriology* (1994).
- [86] R. P. Pandey et al. “Glucosylation of Isoflavonoids in Engineered *Escherichia coli*”. In: *Molecules and Cells* (2014). DOI: 10.14348/molcells.2014.2348.
- [87] R. P. Pandey et al. “Biosynthesis of amino deoxy-sugar-conjugated flavonol glycosides by engineered *Escherichia coli*”. In: *Biochemical Engineering Journal* (2015). DOI: 10.1016/j.bej.2015.05.017.
- [88] N. H. Thuan et al. “Microbial production of astilbin, a bioactive rhamnosylated flavanone, from taxifolin”. In: *World Journal of Microbiology and Biotechnology* (2017). DOI: 10.1007/s11274-017-2208-7.
- [89] T. Xia and M. A. Eiteman. “Quercetin Glucoside Production by Engineered *Escherichia coli*”. In: *Applied Biochemistry and Biotechnology* (2017). DOI: 10.1007/s12010-017-2403-x.
- [90] W. Boos and H. Shuman. “Maltose/Maltodextrin System of *Escherichia coli*: Transport, Metabolism, and Regulation”. In: *Microbiology and molecular Biology Reviews* (1998).
- [91] T. Ferenci. “The Recognition of Maltodextrins by *Escherichia coli*”. In: *European Journal of Biochemistry* (1980). DOI: 10.1111/j.1432-1033.1980.tb04758.x.
- [92] S. Freundlieb and W. Boos. “ α -Amylase of *Escherichia coli*, Mapping and Cloning of the Structural Gene, *malS* and Identification of Its Product as a Periplasmic Protein”. In: *The Journal of Biological Chemistry* (1985).
- [93] L. Rosales-Colunga and A. Martínez-Antonio. “Engineering *Escherichia coli* K12 MG1655 to use starch”. In: *Microbial Cell Factories* (2014). DOI: 10.1186/1475-2859-13-74.

-
- [94] R. Kanai et al. "Biochemical and Crystallographic Analyses of Maltohexaose-Producing Amylase from Alkalophilic *Bacillus* sp. 707". In: *Biochemistry* (2004). DOI: 10.1021/bi048489m.
- [95] S. Samant et al. "Effect of codon-optimized *E. coli* signal peptides on recombinant *Bacillus stearothermophilus* maltogenic amylase periplasmic localization, yield and activity". In: *Journal of Industrial Microbiology & Biotechnology* (2014). DOI: 10.1007/s10295-014-1482-8.
- [96] M. Hofnung and M. Schwartz. "Mutations allowing growth on maltose of *Escherichia coli* K12 strains with a deleted *malT* gene". In: *Molecular & General Genetics* (1971). DOI: 10.1007/BF00267490.
- [97] K. Watson et al. "The crystal structure of *Escherichia coli* maltodextrin phosphorylase provides an explanation for the activity without control in this basic archetype of a phosphorylase". In: *The EMBO Journal* (1997). DOI: 10.1093/emboj/16.1.1.
- [98] S. Adhya and M. Schwartz. "Phosphoglucomutase Mutants of *Escherichia coli* K-12". In: *Journal of Bacteriology* (1971).
- [99] T. Brautaset, S. Petersen, and S. Valla. "An experimental study on carbon flow in *Escherichia coli* as a function of kinetic properties and expression levels of the enzyme phosphoglucomutase". In: *Biotechnology and Bioengineering* (1998). DOI: 10.1002/(SICI)1097-0290(19980420)58:2/3<299::AID-BIT27>3.0.CO;2-6.
- [100] R. A. Roehl and R. T. Vinopal. "New Maltose Blu Mutations in *Escherichia coli* K-12". In: *Journal of Bacteriology* (1979).
- [101] A. H. Delcour. "Outer membrane permeability and antibiotic resistance". In: *Biochimica et Biophysica Acta (BBA) - Proteins and Proteomics* (2009). DOI: 10.1016/j.bbapap.2008.11.005.
- [102] P. Genevaux et al. "Identification of Tn10 insertions in the *rfaG*, *rfaP*, and *galU* genes involved in lipopolysaccharide core biosynthesis that affect *Escherichia coli* adhesion". In: *Archives of Microbiology* (1999). DOI: 10.1007/s002030050732.
- [103] P. Gustafsson, K. Nordström, and S. Normark. "Outer Penetration Barrier of *Escherichia coli* K-12: Kinetics of the Uptake of Gentian Violet by Wild Type and Envelope Mutants". In: *Journal of Bacteriology* (1973).
- [104] C. A. Schnaitman and J. D. Klena. "Genetics of Lipopolysaccharide Biosynthesis in Enteric Bacteria". In: *Microbiological Reviews* (1993).
- [105] R. L. Bernstein and P. W. Robbins. "Control Aspects of Uridine 5'-Diphosphate Glucose and Thymidine 5'-Diphosphate Glucose Synthesis by Microbial Enzymes". In: *The Journal of Biological Chemistry* (1965).
- [106] S. Zuccotti et al. "Kinetic and crystallographic analyses support a sequential-ordered bi bi catalytic mechanism for *Escherichia coli* glucose-1-phosphate thymidyltransferase". In: *Journal of Molecular Biology* (2001). DOI: 10.1006/jmbi.2001.5073.
- [107] K. Kimura et al. "Cloning of a gene for maltohexaose producing amylase of an alkalophilic *Bacillus* and hyper-production of the enzyme in *Bacillus subtilis* cells". In: *Applied Microbiology and Biotechnology* (1988). DOI: 10.1007/BF00251771.
- [108] G. Eydallin et al. "Genome-wide screening of genes affecting glycogen metabolism in *Escherichia coli* K-12". In: *FEBS Letters* (2007). DOI: 10.1016/j.febslet.2007.05.044.

Bibliography

- [109] P. Parajuli et al. “Synthetic sugar cassettes for the efficient production of flavonol glycosides in *Escherichia coli*”. In: *Microbial Cell Factories* (2015). DOI: 10.1186/s12934-015-0261-1.
- [110] B.-G. Kim, H. J. Kim, and J.-H. Ahn. “Production of Bioactive Flavonol Rhamnosides by Expression of Plant Genes in *Escherichia coli*”. In: *Journal of Agricultural and Food Chemistry* (2012). DOI: 10.1021/jf302123c.
- [111] T. H. Adair and J.-P. Montani. *Angiogenesis. Integrated Systems Physiology: from Molecule to Function to Disease*. 2010.
- [112] L. A. Sullivan and R. A. Brekken. “The VEGF family in cancer and antibody-based strategies for their inhibition”. In: *mAbs* (2010). DOI: 10.4161/mabs.2.2.11360.
- [113] K. Yano, L. F. Brown, and M. Detmar. “Control of hair growth and follicle size by VEGF-mediated angiogenesis”. In: *Journal of Clinical Investigation* (2001). DOI: 10.1172/JCI11317.
- [114] V. Yadav et al. “ α -L-Rhamnosidase: A review”. In: *Process Biochemistry* (2010). DOI: 10.1016/j.procbio.2010.05.025.
- [115] S Blanchard and J Thorson. “Enzymatic tools for engineering natural product glycosylation”. In: *Current Opinion in Chemical Biology* (2006). DOI: 10.1016/j.cbpa.2006.04.001.
- [116] *User Protocol TB340 Rev. F 0211JN - Duet Vectors*. Novagen.
- [117] A. Schlegel et al. “Network Regulation of the *Escherichia coli* Maltose System”. In: *Journal of Molecular Microbiology and Biotechnology* (2002).
- [118] L. Notley and T. Ferenci. “Differential expression of *mal* genes under cAMP and endogenous inducer control in nutrient-stressed *Escherichia coli*”. In: *Molecular Microbiology* (1995). DOI: 10.1111/j.1365-2958.1995.tb02397.x.
- [119] W. Boos. “Learning new tricks from an old dog: MalT of the *Escherichia coli* maltose system is part of a complex regulatory network”. In: *Trends in Genetics* (2000). DOI: 10.1016/S0168-9525(00)02086-2.
- [120] N. Joly et al. “The Aes Protein Directly Controls the Activity of MalT, the Central Transcriptional Activator of the *Escherichia coli* Maltose Regulon”. In: *Journal of Biological Chemistry* (2002). DOI: 10.1074/jbc.M200991200.
- [121] P. Charusanti et al. “Genetic Basis of Growth Adaptation of *Escherichia coli* after Deletion of *pgi*, a Major Metabolic Gene”. In: *PLoS Genetics* (2010). DOI: 10.1371/journal.pgen.1001186.
- [122] G. A. L. Gonçalves et al. “De novo creation of MG1655-derived *E. coli* strains specifically designed for plasmid DNA production”. In: *Applied Microbiology and Biotechnology* (2013). DOI: 10.1007/s00253-012-4308-5.
- [123] S. Flores et al. “Growth-rate recovery of *Escherichia coli* cultures carrying a multi-copy plasmid, by engineering of the pentose-phosphate pathway”. In: *Biotechnology and Bioengineering* (2004). DOI: 10.1002/bit.20137.
- [124] C. M. Radding. “Recombination activities of *E. coli* RecA protein”. In: *Cell* (1981). DOI: 10.1016/0092-8674(81)90224-5.
- [125] D. P. Biek and S. N. Cohen. “Identification and Characterization of *recD*, a Gene Affecting Plasmid Maintenance and Recombination in *Escherichia coli*”. In: *Journal of Bacteriology* (1986).

-
- [126] L. Glaser, A. Melo, and R. Paul. "Uridine Diphosphate Sugar Hydrolase". In: *The Journal of Biological Chemistry* (1967).
- [127] D. Innes, I. R. Beacham, and D. M. Burns. "The role of the intracellular inhibitor of periplasmic UDP-sugar hydrolase (5'-nucleotidase) in *Escherichia coli*: cytoplasmic localisation of 5'-nucleotidase is conditionally lethal". In: *Journal of Basic Microbiology* (2001).
- [128] R. P. Pandey et al. "Production of 3-*O*-xylosyl quercetin in *Escherichia coli*". In: *Applied Microbiology and Biotechnology* (2013). DOI: 10.1007/s00253-012-4438-9.
- [129] S. Malla et al. "Regiospecific modifications of naringenin for astragalin production in *Escherichia coli*". In: *Biotechnology and Bioengineering* (2013). DOI: 10.1002/bit.24919.
- [130] M. Konersmann. "Untersuchung zur Substratspezifität und heterologen Expression von Glykosyltransferasen in *Escherichia coli*". 2016.
- [131] O. Raibaud and M. Schwartz. "Restriction Map of the *Escherichia coli* *malA* Region and Identification of the *malT* Product". In: *Journal of Bacteriology* (1980).
- [132] C. Chapon. "Expression of *malT*, the regulator gene of the maltose regulon in *Escherichia coli*, is limited both at transcription and translation". In: *The EMBO Journal* (1982).
- [133] S. Y. Kim et al. "Metabolic engineering of *Escherichia coli* for the biosynthesis of flavonoid-*O*-glucuronides and flavonoid-*O*-galactoside". In: *Applied Microbiology and Biotechnology* (2015). DOI: 10.1007/s00253-014-6282-6.
- [134] J. A. Yethon et al. "Mutation of the Lipopolysaccharide Core Glycosyltransferase Encoded by *waaG* Destabilizes the Outer Membrane of *Escherichia coli* by Interfering with Core Phosphorylation". In: *Journal of Bacteriology* (2000). DOI: 10.1128/JB.182.19.5620-5623.2000.
- [135] Z. Wang et al. "Influence of Core Oligosaccharide of Lipopolysaccharide to Outer Membrane Behavior of *Escherichia coli*". In: *Marine Drugs* (2015). DOI: 10.3390/md13063325.
- [136] C. H. Brierley and B. Burchell. "Human UDP-glucuronosyl transferases: Chemical defence, jaundice and gene therapy". In: *BioEssays* (1993). DOI: 10.1002/bies.950151108.
- [137] R. H. Tukey and C. P. Strassburg. "Human UDP-Glucuronosyltransferases: Metabolism, Expression, and Disease". In: *Annual Review of Pharmacology and Toxicology* (2000). DOI: 10.1146/annurev.pharmtox.40.1.581.
- [138] G. J. Williams and J. S. Thorson. "A high-throughput fluorescence-based glycosyltransferase screen and its application in directed evolution". In: *Nature Protocols* (2008). DOI: 10.1038/nprot.2007.538.
- [139] G. J. Williams, C. Zhang, and J. S. Thorson. "Expanding the promiscuity of a natural-product glycosyltransferase by directed evolution". In: *Nature Chemical Biology* (2007). DOI: 10.1038/nchembio.2007.28.
- [140] M. Weis et al. "Regioselective Glucosylation of Aromatic Compounds: Screening of a Recombinant Glycosyltransferase Library to Identify Biocatalysts". In: *Angewandte Chemie International Edition* (2006). DOI: 10.1002/anie.200504505.
- [141] J. Kiernan. "Indigogenic substrates for detection and localization of enzymes". In: *Biotechnic & Histochemistry* (2007). DOI: 10.1080/10520290701375278.
-

Bibliography

- [142] J. Vieira and J. Messing. “The pUC plasmids, an M13mp7-derived system for insertion mutagenesis and sequencing with synthetic universal primers”. In: *Gene* (1982). DOI: 10.1016/0378-1119(82)90015-4.
- [143] L. Bungaruang, A. Gutmann, and B. Nidetzky. “ β -Cyclodextrin Improves Solubility and Enzymatic C-Glucosylation of the Flavonoid Phloretin”. In: *Advanced Synthesis & Catalysis* (2016). DOI: 10.1002/adsc.201500838.
- [144] M. Yang et al. “Functional and informatics analysis enables glycosyltransferase activity prediction”. In: *Nature Chemical Biology* (2018). DOI: 10.1038/s41589-018-0154-9.
- [145] R. Caspi et al. “The MetaCyc database of metabolic pathways and enzymes and the BioCyc collection of Pathway/Genome Databases”. In: *Nucleic Acids Research* (2014). DOI: 10.1093/nar/gkt1103.
- [146] C. J. Thibodeaux, C. E. Melançon, and H.-w. Liu. “Natural-Product Sugar Biosynthesis and Enzymatic Glycodiversification”. In: *Angewandte Chemie International Edition* (2008). DOI: 10.1002/anie.200801204.
- [147] J. Sambrook and D. W. Russell. *Molecular cloning: a laboratory manual*. 3rd ed. Cold Spring Harbor, N.Y: Cold Spring Harbor Laboratory Press, 2001.
- [148] S. d. Kok et al. “Rapid and Reliable DNA Assembly via Ligase Cycling Reaction”. In: *ACS Synthetic Biology* (2014). DOI: 10.1021/sb4001992.
- [149] F. van den Ent and J. Löwe. “RF cloning: A restriction-free method for inserting target genes into plasmids”. In: *Journal of Biochemical and Biophysical Methods* (2006). DOI: 10.1016/j.jbbm.2005.12.008.
- [150] J. M. Carceller et al. “Selective synthesis of citrus flavonoids prunin and naringenin using heterogeneized biocatalyst on graphene oxide”. In: *Green Chemistry* (2019). DOI: 10.1039/C8GC03661F.
- [151] A. Espah Borujeni, A. S. Channarasappa, and H. M. Salis. “Translation rate is controlled by coupled trade-offs between site accessibility, selective RNA unfolding and sliding at upstream standby sites”. In: *Nucleic Acids Research* (2014). DOI: 10.1093/nar/gkt1139.
- [152] A. Espah Borujeni and H. M. Salis. “Translation Initiation is Controlled by RNA Folding Kinetics via a Ribosome Drafting Mechanism”. In: *Journal of the American Chemical Society* (2016). DOI: 10.1021/jacs.6b01453.

Part VI.
Appendix

HPLC analysis of *E. coli* deletion strains

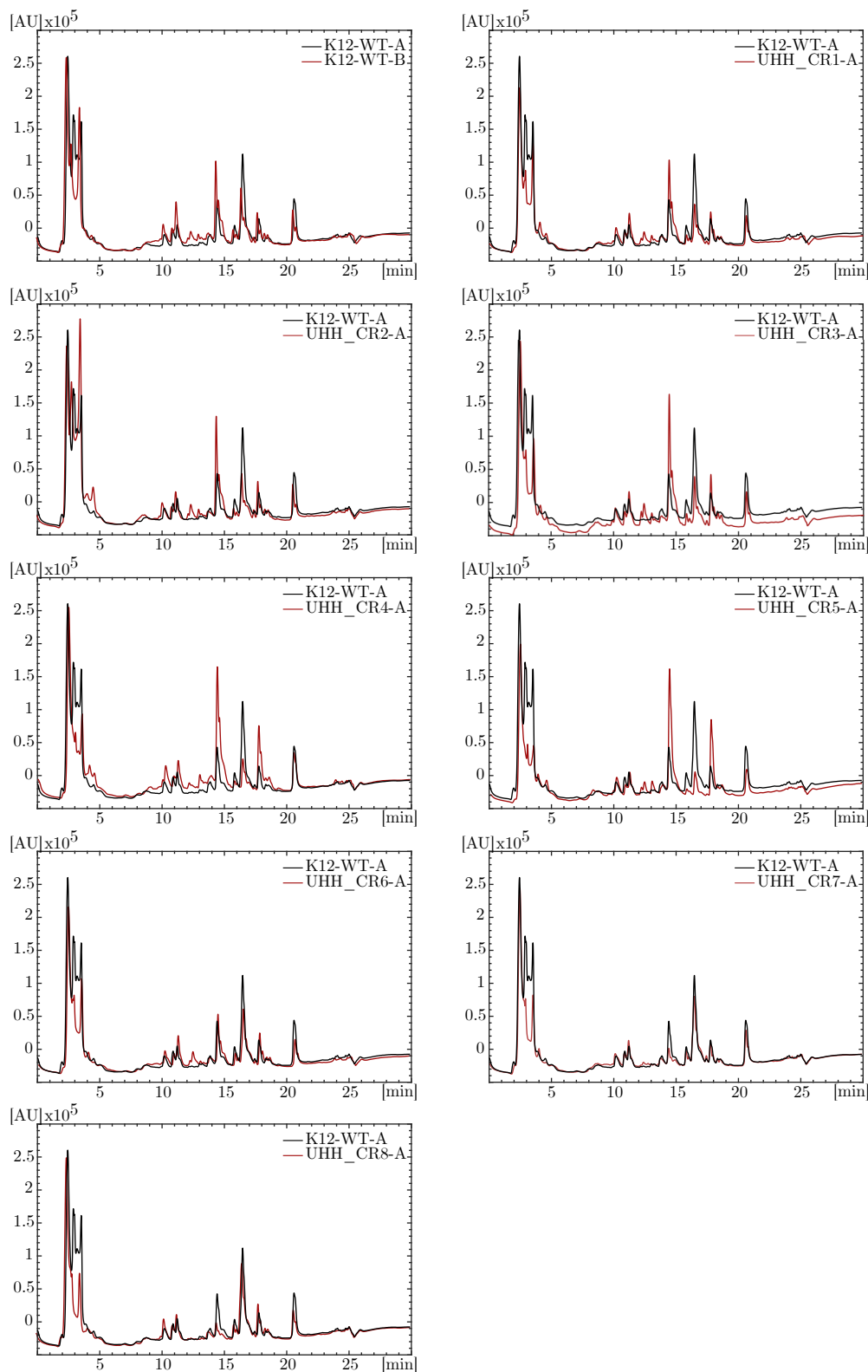
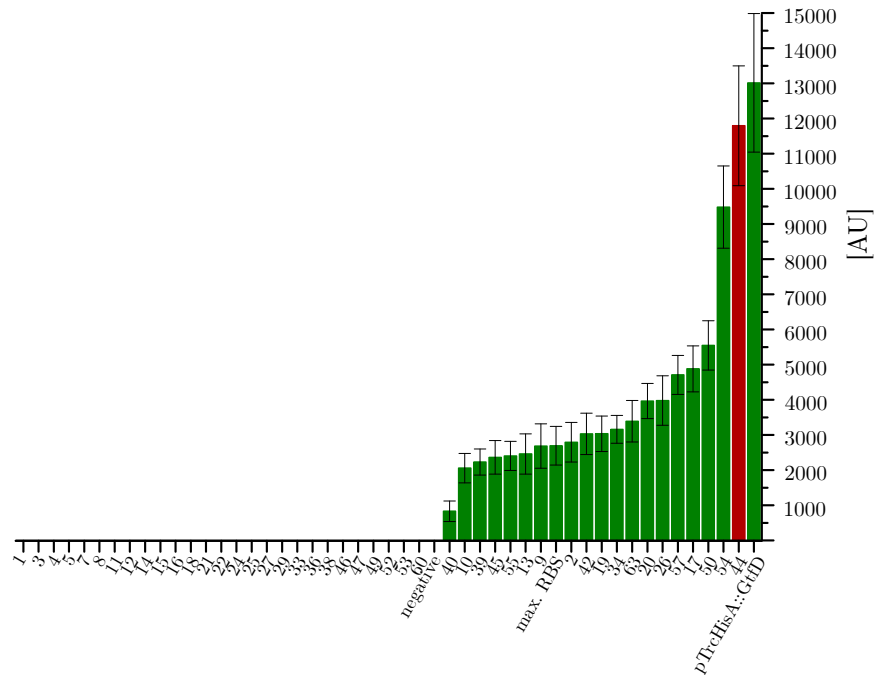


Figure 12.1.: HPLC analysis of hesperetin rhamnosylation in 48 well plates. Biotransformations performed in M9 media (48 well FlowerPlates) containing 1 % dextrans as carbon source. Production strains heterologously expressed Glycosyltransferase C (pTrcHisA::GtfC) and the G6-amylase (pCC1Lig::G6-amylase), all strains except K-12-WT-A overexpressed the native *E. coli* rml-operon (*rmlBDAC*), regulated by a T5 promoter (pCDF-T5::*rmlOP*). Genotypes of the production strains is given in table 3.1.

Proof of principle: Autoinduction of GtfD



Phylogenetic tree of Glycosyltransferases

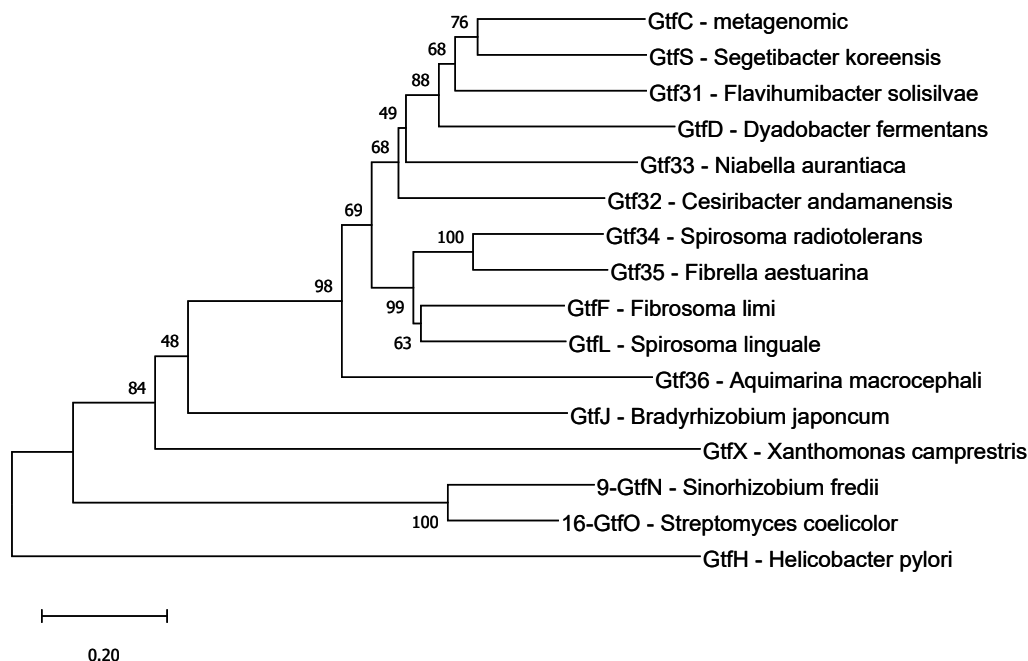


Figure 12.3.: Phylogenetic tree of the glycosyltransferases used in blue/white screening. The evolutionary history was inferred using the Minimum Evolution method [1]. The optimal tree with the sum of branch length = 7.80912602 is shown. The percentage of replicate trees in which the associated taxa clustered together in the bootstrap test (500 replicates) are shown next to the branches [2]. The tree is drawn to scale, with branch lengths in the same units as those of the evolutionary distances used to infer the phylogenetic tree. The evolutionary distances were computed using the Poisson correction method [3] and are in the units of the number of amino acid substitutions per site. The ME tree was searched using the Close-Neighbor-Interchange (CNI) algorithm [4] at a search level of 1. The Neighbor-joining algorithm [5] was used to generate the initial tree. This analysis involved 16 amino acid sequences. All ambiguous positions were removed for each sequence pair (pairwise deletion option). There were a total of 493 positions in the final dataset. Evolutionary analyses were conducted in MEGA X [6].

1. Rzhetsky A. and Nei M. (1992). A simple method for estimating and testing minimum evolution trees. *Molecular Biology and Evolution* 9:945-967.
2. Felsenstein J. (1985). Confidence limits on phylogenies: An approach using the bootstrap. *Evolution* 39:783-791.
3. Zuckerkandl E. and Pauling L. (1965). Evolutionary divergence and convergence in proteins. Edited in *Evolving Genes and Proteins* by V. Bryson and H.J. Vogel, pp. 97-166. Academic Press, New York.
4. Nei M. and Kumar S. (2000). *Molecular Evolution and Phylogenetics*. Oxford University Press, New York.
5. Saitou N. and Nei M. (1987). The neighbor-joining method: A new method for reconstructing phylogenetic trees. *Molecular Biology and Evolution* 4:406-425.
6. Kumar S., Stecher G., Li M., Knyaz C., and Tamura K. (2018). MEGA X: Molecular Evolutionary Genetics Analysis across computing platforms. *Molecular Biology and Evolution* 35:1547-1549.

Nucleotide sequences

Synthetic fragments

>Promotor-rnrB terminator for pCC1Lig generation

```
CATGACATGTGAATTCGCATGCGTTAACGTGACACCTGACAGCTAGCTCAGTCCTAGGTATAATGCTAGCAAGCTTCAAGTGG
GATCCGGCGCCCCACCTGACCCCATGCGGAACCTCAGAAAGTGAACCGCGTAGCGCCGATGGTAGTGTGGGGTCTCCCCAT
GCGAGAGTAGGGGAGGCCCGGCAGTACCCAAATAAACGAAAGGCTCAGTCGAAAGACTGGGCCCTTTCGTTTTATCTG
TTGTTTGTCCGGTGAACGCTCTCCTGAGTAGGACAAATCAGACTGCTTCGGGTAGTCAATAAACCGGTAAACAGCAATAG
ACATAAGCGGTATTTAACGACCCTGCCCTGAACCGACGACCGGGTCAAGAAGGCCATCTGACGGATGGCCCTTTGCGG
CCGCAGCT
>malzp Duett
CTAGATTTTCAGTGCAATTTATCTCTCAAATGTAGCACCTGAAGTCAGCCCCATACGATATAAGTTGTAATTTCTCATGTTAG
TCATGCCCGCGCCACCAGGAGAGCTGACCTGGGTTGAAGGCTCTCAAGGGCATCGGTGAGATCCCGGTGCCTAATG
AGTGAGCTAACCTTACATTAATTGCGTTGCGCCGGAGGATCTCGACGCTCTCCCTTATGCGACTCCTGCATAGGAAATTA
TCCGCCCCCGTCTCCTCCCCAAATATCCTTCAGATGATGAGTGATCCTGCATTAGGCTATGGCAAGGTGATCAGCGCTGA
GAAATAATTTGTTTAACTTTAATAAGGAGATATACCATGGGACGACCATCCCATCATCCACAGCCAGGATCCGAA
TTCCGACTCCGGCGCCTGACAGTTCGACAAGCTTGGCGCCGATAAATGCTTAAGTCGAAACAGAAAGTAATCGTATTGTA
CAGCGCCGATAAATCGAAATATCCGCCCCCGTCTCCTCCCCCAAATATCCTTCAGATGATGAGTGATCCTGCATTAGGCT
ATGGCAAGGTGATCAGCCATCTTAGTATATTAGTTAAGTATAAGAAGGAGATATACATATGCGAGATCTCAATGGATATC
GGCCGCCACCGATCGCTGACGTCCGTACCCCTCGA
```

Glycosyltransferases

>GtfC(opt)

```
ATGTCAAACCTGTTCTCATCTCAAACAAACCTGGCCTCGGTAAACCCGTTAAAAGGTCGTAATAATCCTTTTCGCAAATTT
TCCCGCTGATGGACACTTTAATCCGTTAACTGGGTTAGCAGTCCATTTACAAATGGCTTGGTTGCGATGTGCGTGTGGTAC
CTTCAAATAAGTACGCGATAAGCTTCGTGCGCTTAAACATCCCTCACTTCCCTTTTCGTAAGGCCATGGATATTGTGAC
TTAGAAAACATGTTTCCCTGAGCGTGATGCCATCAAAGGACAGGTCGCAAAACTGAAGTTCGACATATTTAATGCTTTTCA
CTGCGCGGCCCTGAGTACTACGTGACCTTACAAGAAATTCATAAATCCTTCCCTTTGACGTTATGTCGCTGATGGCG
CGTTTACCGGAAATCCCGTTTCGTAACGACAAAATGATATTTCCGTCGATCGGTCCGGGTCCTTCCACTGACCCGAGCT
CFTAAAGATTTTCCTCCGGCCGATTGGGTTACTCCCTCGTTTTCCTTGGCAGGTAAGTTCAGAACTCGATTTTACG
CAGTGTGGCCGATTTGGTGTATTTCTGTGAGAGCAATAAGGTCATGCGCAAAATGTTGACTGAGCATGGTATTGACCAC
TTTACACAAAACGTTATTTGATCTTATGGTTAAAATAACACTTACTGTTGTCAGTCCAGGACTCCGGGCTTCGAGTATTAC
CGTAGTGATCTTGGTAAGAATATTCGTTTATCGGAAGCTTGGCTTCCCTATCAGAGCAAAAACAGACTACTGCTTGGAG
TGATGAGCGTCTGAATCGCTATGAAAAAATCGTCTGACTCAGGGAAGTGTAGAGAAAAACATCGAAAAAGATTTTGG
TGCCAAACCTTGAGGCTTTCCGCGACACTGACCTGCTTGTGATCGCGACGACGGGAGTTTCAGGAACCGCTGAATTTGAA
AAACGTTACCTCAGGGCAACTTAATCATTGAGGACTTTCATTCATTTGGTGACATTATGCCATACGCTGATGTATATAT
CACCAATGGTGGTTACGGCGGAGTTATGCTTGGCATCGAAAATCAACTGCCCTTGTGCTAGCCGGCATCCACGAAGGAA
AGAAAGAGATCAACGCACGTTATGGGTACTTTGAGCTTGGAAATCAATCTGAAAACGGAGTGGCCGAAAGCCAGAGCAGATG
AAAAAAGCGATTGACGAAGTTATCGGTAATAAGAAAGTACAAAGAGAAATATCAAAAACTGGCGAAGGAATTTCTCAAAC
CCATCTAACGAATTTGTCGCCCAATACATCTCTGAAGCTTTCACAGAAGACCGGCCGCTTGTACATTTTCGTTCAAAGAAG
AAGAAGAAAAGATTTACTAA
```

>GtfD(opt)

```
ATGACGAAATACAAAATGAATTAACAGGTAAGAATACTCTTTGGTACCGTTCCCGGAGACGGTCAATTTAATCCCTT
TACCGGGCTGTGTAATATTTACAGGAATTAGGGTGGGATGTCAGGTTGGTATGCTTCTGATGTTTCAAATGCAAGCTTG
AAAAATTTGCTGATACCACATTTATGGCTTCAA AAAAGCATGGGATGTCACCGTGTGAATGTAACAGATCTTCCCGGAG
CGACAAAATTAACAGATCCCGCGGAAA AACTGAGCTTTGACTTGTATCCACATTTTCGGAACCGGGCACCCTGAGTATTA
TGAGGATATTTTCGAAATACACGAATCGTTCCCATTCGATGTGTTTCATTGCTGACAGCTGCTTTCCGCGATTCCGTTAG
TTAGCAAGCTGATGAGCATCCCGTTGTTGCCGTTGGCGTAAATTCCTCTGGCGGAAGAACTGTGATCTGGCCGCTTAT
GGAACAGGATTTGCCCTGCGCGACGGAGGCAACGTCGATGTTTGGTATGAAAGATGCTTTGGCAACGTTGTTG
TTTCAAACACTGCCATTGACTCTTTTTCGCGCATTCTGGACCGGTACCAGGTACCGCACGAAAAAGCAATTTTATTCGATA
CATTGATCCGTC AATCCGACTTGTTCGCAAAATGGCGCAA AAGCAATTTGAGTATGACCCGACCGACCTGGCGGAAAA
GTCGCTTTTTCGCGCATTGCTGCGCTACTCGGAAAGTAAATCCCGGACGCTGTTTGTATCAGAACTTTTACAATA
TGGCAGGATTTGCTGGTTACCCAGGGCAGCTGTGAGCAGATATCAACAAGATACTTGTACCCAGCTGGAAGCTTTCA
AAAATTTCTGAGCGCTGGTAAATGCCACACAGGGCGTAAATGGGACAGCGGAATTTCCGCGCTTTTCTTTTCGAAAA
CTGATCATCGAAGATTTTCATTCGTTTACGATGTGATGCCAGAGCAGACGTTTATGTTACCAATGGTGGCTATGAGG
CACCTTGCTCAGCATACATAATCAGTTGCCAATGGTAGCGCGGGCGTGCATGAGGGTAAAATGAAGTTTGTCCAGTA
TCGGCCACTTCCGCTGTGGGATTAATCTGGAACCGTAACACACTCCCGAGATCAGATACCGGAAAGTTCACAAAATC
CTGTCTAATGACATCTTCAA AAGAATGTCTTCAGATTTTCGACGCACTTGGATGTGGATGCGAATGAAAAAGCGCGG
TCACATTTCTGACTTGTGGAAGAGCGGTTGTTTCCGCTAA
```

>GtfW

```
ATGGCAAAATGTACTCGTAATAAATTTCCCTGGAGAGGTCATATAAATCCGACTTTAGCTATTGTAAGTGAATTAATCG
GCGAGGGGAAACAGTTGTTTCGATTTGATTTGAAGATTATAGAAAGAAGATTGAAGCAACAGGTGCAGAATTCGAGTGT
TTGAGAATTTCTCTCTCAAATTAATATTTGAACGAGTAAATGAAGTGGGAGTCTTTGACAGTGTCTATCTCATATG
ATTTGAAGCATCAGAGCGTATTTGTTACTCAAATTTGTAAGAAACAAAAGGGGAAA AAGTACGATTTACTTGTATCCGATA
TCATTTTCCAGTAGGACGTTATATAGCGAATGTTTAAATTAACCTAGCGTTTCTTCTGTACACGTTTGTCTTTAATC
AGTACATTTACTTTAATGATGAACAAGAATCGAGCAAGTAGTAACTAATCCATTTATCAATCTTTGTTTTCGCGGGA
ATGGAAAATGGAATAGGCAGTATGGAATGA AATGTATTAATGTATGATATTTGAATCATCCTGGTGATATTACTAT
TGTATATACTTCAAAGGAATATCAGCCGCTTCAGATGTATTCGATGAATCGTATAAGTTTGTCCGTCATCAATTGCTA
CTCGAAAAGAAGTAGATAGCTTTTCCTATGGAAGATTAAAAGATAAACAATTTGATTTTCATTTCTATGGGAACAGTTT
AATGAACAACCTGAGTTATATGAAAAATGTTTGAAGCGTTTTAAAGATGTAGAACGACAGTTCGATTTAGTTGTTGGTAA
GAAGATAAATATAAGTCAATTTGAAAACATTTCCGAATAACTTTAAGTTGTATAATTTATGTCGCCAATTTAGAAGTATTAC
AGTACGCTGATGATTTCTGACACACGGTGGTATGAATAGTTTCGAGTGAAGCACTATATACGGTGTCCCGTTAGTTGTA
ATTCGCTTAACAGGAGATCAGCCTTTAGTTGCGAAACGAGTAGTGAAGTAGGAGCTGGAATAAGGCTTAATCGTAAAGA
ATTA ACTTCTGAATTTACGTTGAGCTGTAAAGAAAGTAATGTATGATGTAACGTTTAAAGGAAAATAGTCGAAAGTTG
GAGAGTCACTTCGAAATGCTGGTGGGTATAATAGGGCAGTTGATGAAATATTTAAAATGAAGTGAATTCATACTTAAAA
CTTAAATAA
```

>AmUGT(opt)

```
ATGGAAGATACCATTTGTGCTGTATGCAAGCGCAGAACATCTGAATAGCATGTTACTGCTGGGCAAACGTATTAATAAACA
TCATCCGACCATTAGCGTTGCAATTTAGCACCGCCCGCAATGCCGACGCAAGCTCAGTTGCGAGATTTGCGACGCCATTA
GCTATCAGCAGTTAAAACCGGCAACCTTACCGAGCGATCTGACCAA AATCCGATTGAACTGTTTTTTTGAATCCCGCCG
TTACATAATCCGAATCTGCTGGAAGCCCTGGAAGAATTATCACTGAAATCTAAAAGTTCCGCGCCTTTGTGATTTGATTTTT
TTGTAATCCGGCAATTTGAAGTGAAGTACCTCACTGAATTTCCGACCTATTTTATGTGCTTTCAGGCGCCTTTGGCCCTGT
GTGGCTTTCTGCATTTTCCGACCATTTGAAACCGCTGGA AAAAGATATTGGCGA ACTGATTTGGA AATTTCCG
GGTTGTCGCGCGGTGCTGAGTAGCGATTTTCCGAAAGGTATGTTTTTCGTAATCTAATACCTATAAACAATTTTCGGA
TACCGCCAAAATAATGCGTTCGCGCCAAAGGTATTTGGTTAATGCTTTGATGCAATGGAATTTCTGTCGCAAGAAGCC
TGGTTAATAAATTTATGTTTCCGAATAGTCCGACCCCGGGTGTCTTGGTGGCCCGCTTAGTGGGTGCCCTACACCAC
ACCAAACCAACCAATGAACAGCATGATGCTGAAATGGTTAGATGTTTCAGCCGATCGTAGCGTTATTTCTGTGTTT
TGGTCGTCGCGGCTGTTTAGTGCAGATAGTTAAAAGAAATGGCATTGGCTTAGAAAATAGGTCATCGCTTTCTGTG
GGAGTGTTCGCTGTCGCGCTTAAACCGAATAGCTATAATCCGATCCGGATTTAGATGAACCTGCTCCGGAAAGGCTTT
CTGTCAAGTACCGAAACCCGCGCTTTGTGATTAATCTTTGGCCACCGCAGAAAGAAGTGTCTCATGCGCGCAGTGGG
```

CGGCTTTGTGACCCATTGTGGTCCGCTCTTCAATTCTGGAAGCCGTGAGCTTTGGCGTCCGATGATTGGCTGGCCGATTT
ATGCAGAACAGCGCATGAATCCGGTGTATTATGGTGGAAAGAAATGAAAGTTGCCTTACAGTTAGATGAAGTTGAAGAAGCGT
TTTGTTCAGCAGTGGAACTGGAAAAACGGGTTAAAGAACTGATGGATAGTAAAAATGGTCCGTCGCGTTCAGCGCT
TAAAGAAATGAAAGTGGCCGAGAAAGTTGCCGTTGAAAAAGGCGGTAGTAGCGTGGTTGCCCTTACAGCGCTTTGTTGATA
TGTTGGTGGACTAA
>VvUGT(opt)
ATGGCAGAAAAACCGCCGCATATTGCAATTTCTGCCACACCAGGTATGGGTCATCTGATTCCGCTGATTGAACTGGCCAA
ACGCTTAGTGACCCATCATGGCTTTACCGTGACCTTTATTTATTTCCGAATGATAATAGTTCACTGAAAGCACAGAAAGCAG
TGTTACAGTCTCTGCCGCCGTCTATTGATAGCATTCTTCTGCCGCCGTGAGCTTTGATGATCTGCCGCCGAGAAACCCAAA
ATTGAAACCATGATTCACTGACCGTGTGGCTCACTGTCAATTTACGTAGTAGCTTAGAACTGCTGGTGGAGTAAAAAC
CCGCGTTGCAGCCCTGGTTGTGGATCTGTTGGGACAGATGCATTTGATGTGGCAGTGGAAATTTGGTGTTCGCCGTATA
TTTTTTTTCCGAGTACCGCGATGGCACTGTCTATTTCTGTTTCTGCCGAAACTGGATGAAATGGTTGCATGTGAATTT
CGCATATGAATGACCCGTGGCCATTTCCGGGCTGTGTTCCGGTTCATGGCTCTCAGCTGCTCGACCCGGTTCAGGATCG
TCGTAATGATGCCTATAAATGGGTGTACATCATACCAAACGGCTATCGCTTAGCAGAAGGTATTATGGTTAATAGCTTTA
TGGAACTGGAACCCGGTCCGTTAAAAGCCTTACAGACCCCGGAAACCCGGGCAACCCGCCGTGTATCCGGTGGTCCGTTA
ATTAACCGCAATCAGAAATGGGCTCAGGCGGAAAATGAATGTTTAAAATGGTTAGATGATCAGCCGTAGGTAGCGTGCT
GTTTGTGGCTTTGGCTCAGGCGGCACCTTACCGAGCGAACAGTTAGATGAACTGGCCTTAGGTCTGGAATGAGCGAAC
AGGCTTTCTGTGGGTTGTGGCTCTCCAAGCCGGTGGCAGATAGTTTCAATTTTATAGCGTGCATAGTCAAGATGATCCG
TTTTAGTTTTCTGCCCGAGGGCTTTTGGATCGCACCAAAAGGTCGCGGCCGCTGCTGGTGTCTTCTTGGCCCCCGAGGCCCA
GATTATTTACATGCAAGTACCGGCCGCTTTCTGTACATTTGTGGTTGGAATAGTACCTTAGAATCAGTTGATGTGGCG
TTCCGATGATTGCCGTGGCCGTTATATGCAGAACAGAAAATGAATGCAATTACCCTGACCGATGATTTAAAAGTTGCCCTG
CGTCCGAAAGTTAATGAAATGGTTTAAATGATCGCAATGAAATGACAGCATTGTTAAAAGGCCGTGATGGAAGCGGAAAG
AGGTAAGATGTTCCGTAGTGTGATGAAGATCTGAAAGATGACAGCGCCAAAAGTGCTGATGATGTTAGCTCTACCA
AAGCCTTAGCCACCGTGGCCGAGAAATGGAAAGCACATAAAAATTATTA
>RhaGT
ATGACCAAAATTTCCGAGCCAAATCAGAGACTCCACGTTGGCAGTTCTCCGCTTTTCCCGGTTGGCGCTCATGCCCCTCC
TCTCTTAGCCGCTCCTCGCCGCTCTCGCCCGGCTTCTCCCTCCACCATCTTTTCTTCTCAACCCGCAAGATCAAACG
CGTCGTTGTCTCCTCTGATCATCCGAGAACATCAAGGTCACAGCCTCTCTGACGGTGTTCGGGAGGGAACCATGCTC
GGGAATCACTGGAGATGGTTCGAGCTGTTTCTCGAAGCGGCTCCACGTATTTCCGGAGCGAAATCGCGCCGCGAGAGAT
AGAAGTTGGAAAGAAAGTGACATGCATGCTACAGATGCTTCTTCTGGTTCCGAGCGGACATAGCCGGCTGAGCTGAACG
CGACTTGGGTTGCCTTCTGGGCGCGGAGCAAACTCACTCTGTGCTCATCTCTACACTGATCTCATCAGAGAAACCTC
GGTCTCAAAGATGTAGTATGGAAGAGACATTTAGGGTTTATACCAGGAATGGAGAATACAGAGTTAAAGATATACCAGA
GGAAGTTGATTTGAAGATTTGGACTCTGTTTTCCCAAGGCTTATACCAATGAGTCTTGGCTTACCTCGTCCCTCTG
CTGTTTTCACTCAGTTCTTTGAAGAGTTAGAACCTACATTTGAACATAACCTAAGATCCAAACTTAAACGTTTCTTGGAA
ATCGCCCTCTCAGTTATTTACTACATCGGAGAAAGAGATGGTGGTGGTCCATGCTTCTGGATGCTTTGGTGGGAA
GAGATCAGCTGCTTCTGTAGCGTACATTAGCTTCCGGCACCGTTCATGGAACCTCCTCTGAAGAGCTTGTGGCGATAGC
AAGGTTGGAAATCAAGCAAGTGGCGTTGTTGGTGGTGGTGAAGGAGAAAGAAATGGTTCATCTACCAAAAGGTTTGG
GATCGGCAAGAGCAAGGATAGTGGTTCCTTGGGCTCCCAAGTGGAACTGCTGAACACGAGGCAATGGTGGTGGGAA
TGTGACACATTTGGATGGAAGTCTGTTGGAGAGTGTGTCGGCAGGTGTACCGATGATCGGCAGACCGATTTTGGCGG
ATAATAGGCTCAACGGAAGAGCAGTGGAGGTTGTGTGAAGGTTGGAGTGTGATGATGATAATGGAGTCTTACGAAAGAA
GGATTTGAGAAGTGTGTAATGATGTTTTGTTTATGATGATGGTAAGACGATGAAGGCTAATGCCAAGAAGCTTAAAGA
AAAACCTCAAAGAAGATTTCTCCATGAAAGAAAGCTCTTTAGAGAATTTCAAATAATTTGTTGGACGAAATTTGAAAGTTT
AG

MUM4

>MUM4

ATGGCAGATCTCAATTGGATATCGGCCGGCCACGGATCGCTGACGTGGTACCATGGATGATACTACGTATAAGCCAAA
GAACATCTCATTACTGGAGCTGCTGGATTTATTGCTTCTCATGTTGCCAACAGATTAATCCGTAACATCTCTGATTACA
AGATCGTTGTTCTTGACAAGCTTGATTACTGTTCCAGATCTGAGAAGAACTTGTATCCTTCTTTTCTTCAACAAATTTCAAG
TTTTGCAAAAGGAGATATCGCGAGTGTATGATCTCGTTAACTACCTTCTCATCTGAAAACATTGATACGATAATGCAATTT
TGCTGCTCAAACCTCATGTTGATAACTCTTTGGTAATAGCTTTGAGTTTACCAAGAACAAATATTTATGTACTCATCTTCT
TTTTGGAAAGCCTGTAAAGTTACAGGACAGATCAGGAGGTTTATCCCATGTGAGTACCGATGAAGTCTATGGAGAAACCGAT
GAGGATCTGCTGTAAGAAACCATAGCTTCTCAGCTTCCAGCAGAACTCCTTACTCTGCAACTAAAGCTGGTGGTGA
GATGCTTGTGATGGCTTATGGTAGATCATATGGATTGCCCTGTTATTAAGACTCGCGGGAACAATGTTTATGGCCCTAAC
AGTTTTCTGAAAAATGATTTCTTAAAGTTTCTGTTGGCTATGAGTGGGAAGCCGCTTCCCATCCATGGAGATGGATCT
AATGTCGGAGTTACTTGTACTCGAAGACGTTGCTGAGGCTTTTGGAGTTGTTCTTCAACAAAGGAAATCGGTCATGT
CTACAATGTCCGCACAAAAGAGAAAGGAGAGTATCGATGTGGCTAGAGACATCTGCAAACTTTTCCGGAAAGACCCCTG
AGTCAAGATTTGCTGGAGAACCCGGCCCTTAAATGATCAAAAGTACTTCTTGTGATGATCAGAAGCTGAAGAAATG
GGTGGCAAGAGCAACAATGGGAAGATGGATTGAAGACAATGGACTGGTACACTCAGAACTCCTGAGTGGTGGGG
TGATGTTTCTGGAGCTTTGCTCCTCATCCGAGAAATGCTTATGATGCCCGTGGGAAGACTTTCTGATGGATCTAGTGAGA
AGAAAGACGTTTCAAGCAACACGGTCCAGACATTTACGTTGTAACACCTAAGAATGGTGGATTCTGGTGACAAAGCTTCTG
TTGAAGTTTTTGTATGTTGTAAGACTGGTTGGCTTGGTGGCTTCTTAGGGAACATATGTGAGAAGCAAGGATTACATA
TGAGTATGGGAAGGAGCTCTGGAGGATAGAGCTTCTTGTGGCGGATATTCGTAGCATCAACAACTCACTCATGTGTTA
ATGCTGCTGGTTAACTGTGCAGACCAACGTTGACTGGTGTGAATCTCACAACCCAGAGACCATCGTGTAAATGTGCGCA
GGTACTTTGACTCTAGCTGATGTTTGCAGAGAAATGATCTTGTATGATGAACTTCCGACCCGTTGATCTTCTTGAATG
TGACGCTACACATCTGAGGGTTCGGGTATAGGTTTCAAGGAAGAAGACAAGCCAAATTTCTTGGTCTTCTTACTCGA
AAACCAAAAGCCATGGTAGAGGAGCTCTTGAAGAAATTTGACAATGTATGTACTTGGAGTCCGGATGCCAATCTGCTCA
GACCTAAACAACCCGAGAAACTTCAACAGAAATCTCGCGCTCAACAAAGTGGTGGACATCCCGAACAGCATGACCGT
ACTGACGAGCTTCTCCCAATCTTATCGAGATGGCGAAGAGAAACCTAAGAGGCATATGGAATTTCAACCAACCCGAGG
TGGTAGCCACAACAGAGATTTGGAGATGTACAAAGAAATACATCGAGCCAGGTTTTAAATGGTCCAACTTACAGTGGAA
GAACAAGCAAAGGTCATTTGCTGCTCGAAGCAACACGAAATGGATGGATCTAAACTAAGCAAGGAGTCCAGAGAT
GCTCTCCATCAAAGAGTCACTGCTCAAAATACGCTTTTGAACCAACAAGAGAACCTAA

FhuD-G6-amylase

>FhuD-G6-amylase

ATGAGCGCCGCTGCCGCTGATTAGCCGCGCCGCTGCTGACCCGATGGCGCTGAGCCGCTGCTGTGGCAGATGAACAC
CGCGCATGCCATCATAACCGTACGAACCGGCAATGATGCAATACTTTGAATGGTATCTACCTAATACCGGAAATCAT
GGAATCGATTAACCTGTGATCGAGTAACCTTAAAGCAAAGGATTACAGCGGTGTGGATTTCTCCAGCATGGAAGGGC
GCTTCTCAA AATAGCTAGTACGAGGAGCCTATGACCTGTATGATCTGGGAGAAATTAATCAA AAAGTACCGTCCGTA
AAAATATGGAACAGTGTAGTCAAGCTGCGGTAACCTCCTTAAAAATAATGGAATTCAGTATATGGTGACGTTG
TTATGAATCACA AAGGTGGCGCAGACGCTACTGAAATGGTAAAGGGCCGTTGAGTGAATCCCAATAACCGTAACCAAGAA
GTGACTGGTGA AATATACCATTTGAAGCTTGGACTAGATTTGATTTCCAGGGCGAGGAAATACATCTTCTAGCTTTAAAT
GAGATGGTATCATTTTGTATGGTGTGGATGGGATCAGTCACTGACTGAAACAATCGCATCTATAAATTTAGAGGTCATG
GCAAAGCTTGGGACTTGGAAAGTTGATACGGGAAATGGTAATTTATGATTTTAAATGATGATGATGATGATGATGATGAT
CCAGAAAGTAGTAAATGAATTAAGAAATTTGGGTTGTTGGTACACAACACATTAGGACTCGATGATTTAGAAATAGATGC
GGTTAAACATATAAGTATAGCTTTACCGCGGATTTGGATTAATCAGTTAGAAAGTGAACAGGTA AAAAATGTTTGGG
TTGCTGAGTTTTGGGAAAGATTTAGTGCAATTTGAAACTATCTGCAAGAAACA AACTGGAACCATTTAGCTTTGAT
GTGCCGTTACATTTAATCTTTATAATGCATCAAAAAGCGGAGGAACTATGATATGCAACATATTTAATGGAACCGT
TGTTCAACGACATCCAAAGTCACTGCTGTAACATTTGTTGATAATCATGATTCGCGAGCCTGAAGAAGCATTAATGATCTTTG

ATAGCCCGGAATCGTCCAGTCAAACGACCTCACTGAGGCGGCATATAGTCTCTCCCGGGATCAAAAACGTATGCTGTAT
CTGTTTCGTTGACCAGATCAGAAAATCTGATGGCACCTACAGGAACATGACGGTATCTGCGAGATCCATGTTGCTAAATA
TGCTGAAATATTGGATTGACCTCTGCGGAAGCCAGTAAGGATATACCGCAGGCATTGAAGAGTTTCGCGGGGAAGGAAG
TGGTTTTTTATCGCCCTGAAGAGGATGCCGGCGATGAAAAAGGCTATGAATCTTTTCCCTGGTTTATCAAACGTGCCGAC
AGTCCATCCAGAGGGCTTTACAGTGTACATATCAACCCATATCTCATTCCCTTCTTTATCGGGTTACAGAACCGGTTTAC
GCAGTTTCGGCTTAGTGAAACAAAAGAAATCACCAATCCGTATGCCATGCGTTTATACGAATCCCTGTGTACGTATCGTA
AGCCGGATGGCTCAGGCATCGTCTCTGAAAATCGACTGGATCATAGAGCGTTACCAGCTGCCTCAAAGTTACCAGCGT
ATGCCTGACTTCCGCCCGCTTCTCGCAGGCTGTGTAAATGAGATCAACAGCAGAACTCCAATCGCCCTCTCATACAT
TGAGAAAAGAAAGGCCGCCAGACGACTCATATCGTATTTTCCCTCCCGGATATCACTTCCATGACGACAGGATAGTCTG
AGGGTTATCTGTACAGATTTGAGGGTGGTTCGTCACATTTGTTCTGACCTACTGAGGGTAAATTTGTACAGTTTTGCTG
TTTTCTTCAGCCCTGCATGGATTTTCTCATACTTTTTGAACTGTAATTTTAAAGGAAGCCAAATTTGAGGGCAGTTTGTCA
CAGTTGATTTCCCTTCTTTTCCCTTCGTATGTGACCTGATATCGGGGGTTAGTTCTCATCATTTGATGAGGGTTGATTA
TCACAGTTTATTACTCTGAATTTGGCTATCCGCGTGTGTACCTCTACCTGGAGTTTTCACAGGTGGATATTTCTTCTTG
CGCTGAGCGTAAGAGCTATCTGACAGAACAGTTCTTTTGTCTCTCGCCAGTTCCGCTCGCTATGCTCGGTTACACGGC
TGCGCGAGCGCTAGTGATAATAAGTGACTGAGGTATGTGCTCTTCTTATCTCCTTTTGTAGTGTGCTCTTATTTTAAA
CAACTTTGCGGTTTTTTGATGACTTTGCGATTTTGTGTTGCTTTGCGAGTAAATTGCAAGATTTAATAAAAAACGCAAA
GCAATGATTAAGGATGTTTCAGAAATGAAACTCATGAAACACTTAACCAGTGCATAAACGCTGGTCAATGAAATGACGAAG
GCTATCGCCATTGCACGATTTAATGATGACAGCCCGGAAGCGAGGAAAATAACCCGGCGCTGGAGAAATAGGTGAAGCAGC
GGATTTAGTTGGGGTTTTCTTCTCAGGCTATCAGAGATGCCGAGAAAGCAGGGCGACTACCGCACCCGGATATGAAATTC
GAGGACGGGTTGAGCAACGTGTTGGTTTATACAATTGAACAAATTAATCATATGCGTGATGTGTTTGGTACGCGATTGCGA
CGTGCTGAAGACGTATTTCCACCGGTGATCGGGGTTGCTGCCATAAAGGTGGCGTTTACAAAACCTCAGTTTCTGTTCA
TCTTGTCTCAGGACTCGGCTCTGAAGGGCTACGTTGTTTTGCTCGTGAAGGTAACGACCCCGAGGAAACAGCCTCAATGT
ATCACGGATGGGTACCAGATCTTCATATTCATGACAGAAAGACACTCTCCTGCCTTTCTATCTTGGGGAAAAGGACGATGTC
ACTTATGCAATAAAGCCACTTGTCTGGCCGGGGCTTGACATTTATCCCTTCTCTGTCTGGCTCTGCACCGTATTTGAAACTGA
GTTAATGGGCAAATTTGATGAAGGTAAACTGCCACCGATCCACACCTGATGCTCCGACTGGCCATTGAAACTGTTGCTC
ATGACTATGATGTCATAGTTATTGACAGCGCGCCTAACCTGGGTATCGGCACGATTAATGTCGTATGTGCTGCTGATGTG
CTGATTTGTTCCACGCTGCTGAGTTGTTTACTACACTCCGCACTGCAGTTTTTTCGATATGCTTCGTGATCTGCTCAA
GAACGTTGATCTTAAAGGGTTCGAGCCTGATGTACGTATTTTGTACTACAAATACAGCAATAGTAATGGCTCTCAGTCCC
CGTGGATGGAGGAGCAAATTCGGGATGCCTGGGGAAGCATGGTTCTAAAAAATGTTGTACGTGAAACGGATGAAGTTGGT
AAAGGTCAGATCCGGATGAGAACTGTTTTTGAACAGGCCATTGATCAACGCTCTTCAACTGGTGCCTGGAGAAATGCTCT
TTCTATTTGGGAACCTGTCTGCAATGAAATTTTCGATCGTCTGATTAACCACGCTGGGAGATTAGATAATGAAGCGTGC
GCCTGTTATTCCAAAACATACGCTCAATACTCAACCGGTTGAAGATACTTCGTTATCGACACCAGCTGCCCGATGGTGG
ATTCGTTAATTTGCGCGCTAGGAGTAATGGCTCGCGGTAATGCCATTACTTTGCCCTGATGTGTTGCGGGATGTGAAGTTT
ACTCTGAAGTGTCTCCGGGTGATAGTGTGAGAAGACTCTCGGGTATGGTCAAGTAATGAACGTGACCAGGAGCTGCT
TACTGAGGACGCACTGGATGATCTCATCCCTTCTTTTCTACTGACTGGTCAACAGACACCGGCGTTCCGGTGAAGAGTAT
CTGGTGTCTATAGAAATTTGCCGATGGGAGTCGCGTCTGTAAGCTGCTGCACCTACCAGAAAGTGATTATCGTGTCTGGTT
GGCGAGCTGGATGATGAGCAGATGGCTGCATTATCCAGATTGGGTAACGATTTATCGCCCAACAAGTGTATTGAAACGTGG
TCAGCGTTATGCAAGCGGATTGCAGAAATGAAATTTGCTGGAATATTTCTGCGCTGGCTGATGCGGAAAATATTTACGTA
AGATTATACCCGCTGATCAACACCGCCAAATTGCCATAATCAGTTGTTGCTCTTTTTTCTCACCCCGGTAACATCT
GCCCGTCAAGTGTATGCACTTCAAAAAGCCTTTACAGATAAAGAGGAATTAAGTAAAGCAGGCATTAACCTTCATGA
GCAGAAAAGCTGGGGTGATTTGAAGCTGAAGAGTTATCACTCTTTAACTTCTGTGCTTAAACCTCATCTGCAT
CAAGAAC TAGTTTTAAGTCAACGACATCAGTTTGTCTCCTGGAGCGACAGTATTGTATAAGGGCGATAAAAATGGTGTCTAAC
CTGGACAGGTCTCGTGTCCAACCTGAGTGTATAGAGAAAATGAGGGCATTCTTAAGGAACTTGAAGCCAGCACCCCTG
ATGCGACACGTTTTAGTCTACGTTTATCTGTCTTTACTTAATGCTTTTGTACAGGCCAGAAAAGCATAAAGTGGCCTGA
ATATCTCTCTGGGCCACTGTTCACCTGTATCGTGGTCTGATAATCAGACTGGGACCACGGTCCCCTGATCGTCTC
GGTCTGATTATTAGTCTGGGACCAGGTCCCCTGATCGTGGTCTGATTATTAGTCTGGGACCACGGTCCCCTGATCGT



Contents lists available at ScienceDirect

Metabolic Engineering

journal homepage: www.elsevier.com/locate/meteng

High level production of flavonoid rhamnosides by metagenome-derived Glycosyltransferase C in *Escherichia coli* utilizing dextrans of starch as a single carbon source



Constantin Ruprecht^a, Friedericke Bönisch^a, Nele Ilmberger^a, Tanja V. Heyer^a,
Erhard T.K. Haupt^b, Wolfgang R. Streit^{a,*}, Ulrich Rabausch^{a,*}

^a Department of Microbiology and Biotechnology, University of Hamburg, Ohnhorststr 18, Hamburg, Germany

^b Institute of Inorganic and Applied Chemistry, Department of Chemistry, University of Hamburg, Martin-Luther-King Platz 6, Hamburg, Germany

ARTICLE INFO

Keywords:
Glycosylation
Glycosyltransferase
Rhamnosylation
Growth-coupled biotransformation
Maltodextrin
Polyphenols
Flavonoids
Kaempferol
Quercetin
Hesperetin

ABSTRACT

Flavonoids exert a wide variety of biological functions that are highly attractive for the pharmaceutical and healthcare industries. However, their application is often limited by low water solubility and poor bioavailability, which can generally be relieved through glycosylation. Glycosyltransferase C (GtC), a metagenome-derived, bacterial glycosyltransferase, was used to produce novel and rare rhamnosides of various flavonoids, including chrysin, diosmetin, biochanin A, and hesperetin. Some of them are to our knowledge firstly described within this work. In our study we deployed a new metabolic engineering approach to increase the rhamnosylation rate in *Escherichia coli* whole cell biotransformations. The coupling of maltodextrin metabolism to glycosylation was developed in *E. coli* MG1655 with the model substrate hesperetin. The process proved to be highly dependent on the availability of maltodextrins. Maximal production was achieved by the deletion of the phosphoglucomutase (*pgm*) and UTP-glucose-1-phosphate uridylyltransferase (*galU*) genes and simultaneous overexpression of the dTDP-rhamnose synthesis genes (*rmlABCD*) as well as glucan 1,4-alpha-maltohexaoidase for increased maltodextrin degradation next to GtC in *E. coli* UHH_CR5-A. These modifications resulted in a 3.2-fold increase of hesperetin rhamnosides compared to *E. coli* MG1655 expressing GtC in 24 h batch fermentations. Furthermore, *E. coli* UHH-CR 5-A was able to produce a final product titer of 2.4 g/L of hesperetin-3'-O-rhamnoside after 48 h. To show the versatility of the engineered *E. coli* strain, biotransformations of quercetin and kaempferol were performed, leading to production of 4.3 g/L quercitrin and 1.9 g/L afzelin in a 48 h time period, respectively. So far, these are the highest published yields of flavonoid rhamnosylation using a biotransformation approach. These results clearly demonstrate the high potential of the engineered *E. coli* production host as a platform for the high level biotransformation of flavonoid rhamnosides.

1. Introduction

Glycosylation of small molecules is a common modification found within all domains of life, performed predominantly by glycosyltransferases (GTs). Glycosyltransferase family 1 GTs catalyze the transfer of sugar moieties from nucleotide diphosphate sugars to lipophilic acceptor molecules including terpenes, steroids, macrolides and polyphenols (Lairson et al., 2008). The glycosylation of small lipophilic molecules generally increases their water solubility (Lepak et al., 2015; Mi et al., 2006; Woo et al., 2012), stability (Mäkälä et al., 2016; Roscher et al., 1997; Vidal et al., 2018; Yamamoto et al., 1992) and

bioavailability (Kren, 2008; Williamson and Manach, 2005).

Technically, there are two general routes for small molecule glycosylation: First, it can be achieved chemically using protection group chemistry and Königs-Knorr addition (Koenigs and Knorr, 1901). Second, the glycosylation can be performed enzymatically either *in vitro* or *in vivo*. For the *in vitro* glycosylation engineered glycosidases are frequently employed (Bertrand et al., 2006; Slámová et al., 2018; Yang et al., 2007) together with glycoside phosphorylases (De Winter et al., 2015) using cheap substrates but often resulting in low yields (Desmet et al., 2012). Alternatively, GTs are used *in vitro* affording expensive nucleotide diphosphate (NDP) sugar donors as a co-substrate

* Corresponding authors. Department of Microbiology and Biotechnology, University of Hamburg Universität Hamburg, Ohnhorststr. 18, D-22609, Hamburg, Germany.

E-mail addresses: constantin.ruprecht@uni-hamburg.de (C. Ruprecht), friedericke.boenisch@uni-hamburg.de (F. Bönisch), wolfgang.streit@uni-hamburg.de (W.R. Streit), ulrich.rabausch@uni-hamburg.de (U. Rabausch).

<https://doi.org/10.1016/j.ymben.2019.07.002>

Received 18 February 2019; Received in revised form 14 June 2019; Accepted 7 July 2019

Available online 16 July 2019

1096-7176/ © 2019 The Authors. Published by Elsevier Inc. on behalf of International Metabolic Engineering Society. This is an open access article under the CC BY license (<http://creativecommons.org/licenses/by/4.0/>).

(Bungaruang et al., 2013; Masada et al., 2007). In contrast, *in vivo* glycosylation by GTs takes advantage of living host cells like *Escherichia coli*, continuously regenerating the NDP-sugar donors (De Bruyn et al., 2015b; Leonard et al., 2008; Lim et al., 2006; Simkhada et al., 2010; Yoon et al., 2012).

Recently, we described the first metagenome-derived glycosyltransferase GtFC of the GT Family 1 in a screening approach of a metagenome library from the river Elbe sediment in Germany (Rabausch et al., 2013). Purified GtFC *in vitro* did not utilize uridine diphosphate (UDP) sugars. But biotransformations with recombinant *E. coli* expressing GtFC resulted *inter alia* in the production of flavonoid deoxyhexosides. As in bacteria rhamnose is activated by deoxythymidine diphosphate (*dTDP*), it was assumed that GtFC utilizes *dTDP* activated sugars.

Based on the earlier findings and in the light of the indicated challenges of enzymatic glycosylation we aimed to produce higher amounts of glycosylated polyphenols (i.e. flavonoid rhamnosides) using GtFC in this study. As *in vitro* synthesis and regeneration of *dTDP*-rhamnose (*dTDP*-rha) is infeasible we chose to work in whole cell biotransformations.

In *E. coli* *dTDP*-rha is synthesized from glucose-1-phosphate (G1P) and deoxythymidine triphosphate (*dTTP*) via a four step enzymatic pathway encoded by the *rml* operon (RmlABCD) (Giraud and Naismith, 2000; Stevenson et al., 1994). Hence, the regeneration of G1P is crucial for a successful *in vivo* glycosylation process, as for every mol of glycoside produced a mol of G1P is required. Consequently, in order to increase *in vivo* glycosylation efficiency the generation of G1P has received a growing interest in the recent years, resulting in two opposite approaches, i.e. growth coupled and growth decoupled glycosylation. In growth decoupled glycosylation the genes encoding the glucose-6-phosphate isomerase (*pgi*) and NADP⁺-dependent glucose-6-phosphate dehydrogenase (*zwf*) are usually removed, thereby blocking the energy metabolism via glycolysis and the pentose phosphate pathway. In this approach glucose is channeled to G1P by overexpression of the phosphoglucomutase (*pgm*) gene and a lower level carbon source, e.g. glycerol, is fed for energy generation (Pandey et al., 2015, 2014; Simkhada et al., 2009; Thuan et al., 2017, 2013; Xia and Eiteman, 2017). However, *in vivo* production yields of glycosylated flavonoids have been rather low, below 1 g/L (Table 3). Recently, De Bruyn and colleagues developed a growth coupled glycosylation system based on coupling sucrose metabolism of *E. coli* to the glycosylation by the *Vitis vinifera* glycosyltransferase VvGT2 (De Bruyn et al., 2015a). An integrated sucrose phosphorylase creates a split metabolism constantly producing G1P for glycosylation and fructose which is used for energy generation. Using this approach production yields of glycosylated flavonoids beyond 1 g/L were achieved.

In this study, we developed a new growth coupled glycosylation approach, making use of the maltodextrin metabolism of *E. coli*. This enabled coupling of growth on dextrins of starch and rhamnosylation of flavonoids by GtFC (Fig. 1). To increase rhamnosylation, genes diverting flux from G1P, i.e. *pgm*, glucose-1-phosphatase (*aggp*), maltodextrin glucosidase (*malZ*) and UTP-glucose-1-phosphate uridylyltransferase (*galU*), were removed, and the *dTDP*-rha synthesis genes were overexpressed. Furthermore, the effect of increased dextrin degradation via the periplasmic expression of a glucan 1,4- α -maltohexaosidase (G6-amylyase) was demonstrated. The metabolic engineering efforts enabled the production of flavonoid rhamnosides in g/L scale.

2. Materials & methods

2.1. Aglycones and glycosides

Biochanin A (> 98%), chrysin (> 95%) and diosmetin (> 98%) were purchased from LKT Laboratories inc. (USA), hesperetin (> 98%) from Willows Ingredients (Ireland), kaempferol (> 98%) and naringenin (98%) from Molekula (United Kingdom) and quercetin dihydrate (> 98%) from Alfa Aesar (Germany), respectively. Analytical

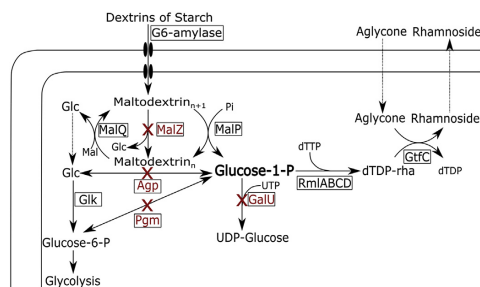


Fig. 1. Whole cell biotransformation scheme of *E. coli* K12 grown on dextrins of starch.

Long-chain dextrins are degraded by G6-amylyase to maltohexaose and shorter chain dextrins which can be taken up and metabolized by *E. coli*. Glucose-1-phosphate (G1P) is produced via the maltodextrin phosphorylase (MalP) as a precursor for *dTDP*-rhamnose (*dTDP*-rha) synthesis, whereas glucose is generated by the amylomaltase (MalQ) and the maltodextrin glucosidase (MalZ) to enter glycolysis. G1P can reenter glycolysis through the action of the glucose-1-phosphatase (Agp) or the phosphoglucomutase (Pgm) and can furthermore be converted to UDP-glucose via the action of UTP-glucose-1-phosphate uridylyltransferase (GalU). Heterologously expressed rhamnosyltransferase C (GtFC) converts flavonoid aglycones into their corresponding rhamnosides. Red crosses indicate potential genes for removal to increase hesperetin rhamnosylation in *E. coli* biotransformations. (For interpretation of the references to colour in this figure legend, the reader is referred to the Web version of this article.)

standards of quercetin-3-*O*-rhamnoside (> 98%) and kaempferol-3-*O*-rhamnoside (> 98%) were purchased from Extrasynthese (France).

2.2. Bacterial strains and cultivation

E. coli K12 MG1655 gene deletions (Table 1) were constructed using the “Quick and Easy *E. coli* Gene Deletion Kit” (Gene Bridges, Germany) according to manufacturer’s protocol. If not stated otherwise, *E. coli* strains harbouring plasmids were grown in LB medium for 18 h using the corresponding antibiotics (ampicillin 100 μ g/mL, chloramphenicol 25 μ g/mL, streptomycin 50 μ g/mL) at 37 °C.

2.2.1. Cultivation in flower plates

E. coli strains were inoculated from an overnight culture to an optical density at 600 nm (OD_{600}) of 0.1 in 1 mL M9 media (Maniatis et al., 1982), containing 1% dextrins of starch (Sigma-Aldrich) as sole carbon source (M9-Dextrin), in 48 well flowerplates (M2PLabs). The flowerplates were incubated at 1000 rpm and 28 °C. After 6 h 100 μ M IPTG and 250 μ M hesperetin was added. After 24 h of cultivation the supernatant was harvested by centrifugation (3 min, 14000 rpm) and hesperetin rhamnosylation was analyzed via HPLC.

2.2.2. Cultivation in shake flasks

E. coli K12 (MG1655), harbouring *gtfC* on pTrcHisA, was inoculated from an overnight culture to an optical density (OD_{600}) of 0.1 in 500 mL Terrific Broth medium (Roth, Germany) and cultivated at 28 °C and 150 rpm in 3 L Erlenmeyer flasks. At an OD_{600} of 1.0, *gtfC* expression was induced with 100 μ M IPTG and 500 mg of aglycone were added to the culture broth. After 48 h biotransformation the culture was harvested by centrifugation at 7,500 g and the supernatant sterile filtered. Rhamnosides were purified from the cell free (filtrated 0.2 μ m) supernatant via preparative HPLC.

2.3. Preparative HPLC purification

Hesperetin rhamnosides were purified using HPLC (Agilent 1260

Table 1
E. coli strains and plasmids used within this study.

<i>E. coli</i> derivatives	Genotype	Source
K12 (MG1655)	F, λ , <i>rph-1</i> , <i>Fnr</i> ⁺	DSMZ (#18039)
K12-WT-A	K12 (MG1655), pCCLig::G6-amylase, pTrcHisA::GtfC(opt)	This study
K12-WT-B	K12 (MG1655), pCCLig::G6-amylase, pTrcHisA::GtfC(opt), pCDF-T5::rmlOP	This study
K12-WT-C	K12 (MG1655), pTrcHisA::GtfC(opt)	This study
UHH_CR1	F, λ , <i>rph-1</i> , <i>Fnr</i> ⁺ , Δ malZ	This study
UHH_CR1-A	UHH_CR1, pCCLig::G6-amylase, pTrcHisA::GtfC(opt), pCDF-T5::rmlOP	This study
UHH_CR2	F, λ , <i>rph-1</i> , <i>Fnr</i> ⁺ , Δ agg	This study
UHH_CR2-A	UHH_CR2, pCCLig::G6-amylase, pTrcHisA::GtfC(opt), pCDF-T5::rmlOP	This study
UHH_CR3	F, λ , <i>rph-1</i> , <i>Fnr</i> ⁺ , Δ pgm	This study
UHH_CR3-A	UHH_CR3, pCCLig::G6-amylase, pTrcHisA::GtfC(opt), pCDF-T5::rmlOP	This study
UHH_CR4	F, λ , <i>rph-1</i> , <i>Fnr</i> ⁺ , Δ galU	This study
UHH_CR4-A	UHH_CR4, pCCLig::G6-amylase, pTrcHisA::GtfC(opt), pCDF-T5::rmlOP	This study
UHH_CR5	F, λ , <i>rph-1</i> , <i>Fnr</i> ⁺ , Δ pgm, Δ galU	This study
UHH_CR5-A	UHH_CR5, pCCLig::G6-amylase, pTrcHisA::GtfC(opt), pCDF-T5::rmlOP	This study
UHH_CR5-B	UHH_CR5, pTrcHisA::GtfC(opt), pCDF-T5::rmlOP	This study
UHH_CR6	F, λ , <i>rph-1</i> , <i>Fnr</i> ⁺ , Δ agg, Δ pgm	This study
UHH_CR6-A	UHH_CR6, pCCLig::G6-amylase, pTrcHisA::GtfC(opt), pCDF-T5::rmlOP	This study
UHH_CR7	F, λ , <i>rph-1</i> , <i>Fnr</i> ⁺ , Δ agg, Δ malZ	This study
UHH_CR7-A	UHH_CR7, pCCLig::G6-amylase, pTrcHisA::GtfC(opt), pCDF-T5::rmlOP	This study
UHH_CR8	F, λ , <i>rph-1</i> , <i>Fnr</i> ⁺ , Δ pgm, Δ malZ	This study
UHH_CR8-A	UHH_CR8, pCCLig::G6-amylase, pTrcHisA::GtfC(opt), pCDF-T5::rmlOP	This study
Plasmid	Properties	Source
pTrcHisA	pBR322 origin, AmpR, <i>lacI</i> , <i>trc</i> promoter	Invitrogen
pCDFDuet TM 1	SmR	Novagen
pCCLFOS	CmR	Epicentre
pTrcHisA::GtfC(opt)	Codon optimized GtfC under control of <i>trc</i>	This study
pCDF-T5::rmlOP	<i>rmlBDAC</i> under control of T5 promoter	This study
pCCLig::G6-amylase	PhuD-G6-amylase under constitutive promoter (BBa_J23108)	This study

Table 2
NMR identified glycosylation products of GtfC with different flavonoids.
Glycosylation products which were confirmed using standard substances instead of NMR are labeled with an asterisk (*), if a preferred reaction product was detected it is given in bold letters. The KnapSack database of the NAIST Comparative Genomics Laboratory from Japan was searched for known rhamnosides of the studied flavonoids.

Substrate	α -L-rhamnosides produced in this study	KnapSack listed α -L-rhamnosides
Flavone		
Chrysin	5-O-, 5,7-di-O-	-
Diosmetin	3*-O-, 5-O-	-
Isoflavone		
Biochanin A	5-O-, 5,7-di-O-	-
Flavonole		
Quercetin	3-O-*	3-O-, 7-O-
Kaempferol	3-O-*	4'-O-, 3-O-, 5-O-, 7-O-
Flavanone		
Hesperetin	3*-O-, 5-O-	7-O-
Naringenin	4'-O-, 5-O-	4'-O-, 5-O-

Infinity HPLC system) with an RP18 column (250 mm length x 21.2 mm internal diameter, 7 μ m particle size) (Agilent, USA). Sterile filtrated culture broth was loaded onto the HPLC column at a flow rate of 10 mL/min. The hesperetin rhamnosides were eluted using an acetonitrile/water step gradient (acetonitrile (A) and water (B) both containing 0.05% formic acid, 1. 0–5 min 10:90 (A:B), 2. 5.1–15 min 25:75, 3. 15.1–25 min 40:60, 4. 25.1–30 min 0:100, 5. 30.1–38 min 10:90) at 10 mL/min. Fractions were collected and analyzed using UHPLC/MS (Supplementary S2). Samples were lyophilized after solvent evaporation for NMR analysis.

2.4. Fermentation in parallel bioreactor system

A 5 ml *E. coli* preculture was inoculated in shake flasks from cryopreservation with the appropriate antibiotics and grown over night at 28 °C and 150 rpm. The biotransformation was performed in a 250 mL stirred parallel bioreactor system (DAS-Box, DASGIP, Germany) with a working volume of 100 mL at constant pH of 7.2, a stirrer controlled dissolved oxygen (DO) of 30% and a temperature of 28 °C. The growth medium consisted of Terrific Broth (Roth), containing 5% dextrins of starch, 100 μ M IPTG and 500 mg hesperetin was inoculated to an OD₆₀₀ of 1 from the preculture. The pH value was controlled using 25% ammonia and 2.5 M phosphoric acid. The supernatant was analyzed using

Table 3
Overview of flavonoid rhamnosylation in *E. coli* biotransformations. Error bars indicate confidence intervals based on four replicates using Student's *t*-distribution ($\alpha = 0.05$, $n = 4$).

Conversion product	Titer [g/L]	Carbon Source	Time [hours]	STY [mg/L/h]	Reference
Quercetin-3-O-rha	4.32 \pm 0.14	Dextrins of starch	48	90	This Study
Hesperetin-3'-O-rha	2.36 \pm 0.05	Dextrins of starch	48	49	This Study
Kaempferol-3-O-rha	1.92 \pm 0.53	Dextrins of starch	48	40	This Study
Quercetin-3-O-rha	1.18	Sucrose	30	39	De Bruyn et al. (2015b)
Fisetin-3-O-rha	0.34	Glucose	48	7	Parajuli et al. (2015)
Kaempferol-3-O-rha	0.2	Glucose	48	4	Kim et al. (2012)
Myricetin-3-O-rha	0.025	Mannitol	48	< 1	Thuan et al. (2013)
Quercetin-3-O-rha	0.024	Arabinose	48	< 1	Simkhada et al. (2010)
Taxifolin-3-O-rha	0.022	Glucose	48	< 1	Thuan et al. (2017)

HPLC over a time span of 48 h if not stated otherwise.

2.5. HPLC analysis

For quantification of the produced hesperetin-glycosides an analytical high-pressure liquid chromatography method was implemented using an Agilent ZORBAX SB-C18 column (4.6 mm internal diameter x 250 mm length, 5 μ m particle size) on a Hitachi Elite LaChrome HPLC system. Analysis was performed with acetonitrile (A) and water with 0.1% trifluoroacetic acid (B) gradient (1. 0 min 15:85 (A:B), 2. 17 min 100:0, 3. 22 min 100:0, 4. 22.1 min 5:95, 5. 30 min 5:95) at a constant flow rate of 1 mL/min. For sample preparation the cells were separated by centrifugation, and the cell-free supernatant was diluted appropriately. Hesperetin rhamnosides were quantified using linear regression of corresponding NMR confirmed standard substances (data not shown). Quercetin and Kaempferol rhamnosylation was analyzed on a Nucleoshell RP18 column (2 mm internal diameter x 100 mm length, 2.7 μ m particle size) running an acetonitrile/water gradient (acetonitrile (A) and water (B) both containing 0.1% acetic acid, 1. 0 min 10:90 (A:B) - 5 min 100:0, 2. 5–7 min 100:0, 3. 7–9 min 10:100) using an Thermo Scientific Ultimate 3000 UHPLC system at a flow rate of 0.5 mL/min. Absorption was monitored at 254 nm.

2.6. NMR spectroscopy

The spectra are completely analyzed by ^1H and ^{13}C NMR, using COSY, HSQC and HMBC-data. The spectra were recorded on a BRUKER Avance 400 I spectrometer at 400 and 100 MHz, respectively, in standard 5 mm tubes. DMSO- d_6 has been used a solvent and standard BRUKER pulse sequences have been used throughout. The mixing time for the NOESY spectra was 1.0 s, the relaxation delay 2 s.

2.7. Nucleotide sequence accession numbers

The original fosmid clones of *gtfC* was deposited in GenBank under the accession numbers JX157627 (Rabausch et al., 2013). pTrcHisA::GtfC(opt), pCDF-T5::rmlOP and pCC1Lig::G6-amylase were deposited in GenBank with the accession numbers MK802894, MK802895 and MK802896, respectively. The nucleotide sequences of *agp* (EG10033), *pgm* (EG12144), *malZ* (EG10565) and *galU* (EG11319) can be obtained from EcoCyc.

3. Results & discussion

3.1. Rhamnosylation of polyphenols by GtfC

In nature, only a few isomeric forms of flavonoid glycosides occur abundantly, mainly the 3-*O*-glycosides of flavonols, e.g. isoquercitrin, as well as the 7-*O*-glycosides of flavones, isoflavones, and flavanones. To initially determine the reaction products of glycosyltransferase C, different polyphenolic substrates including flavones (chrysin, diosmetin), isoflavones (genistein, biochanin), flavonols (quercetin, kaempferol) and flavanones (hesperetin, naringenin) were glycosylated in whole cell biotransformation approaches using *E. coli* MG1655 recombinantly expressing the glycosyltransferase gene *gtfC* (Fig. 2). The culture supernatant was purified using HPLC and NMR was performed to identify the glycosylation products (Supplementary figures – S1–S3).

GtfC was able to produce various *O*-rhamnosides of the screened flavonoids (Table 2, HPLC chromatograms in Supplementary S1). The KNApSack database of the NAIST Comparative Genomics Laboratory from Japan was searched for already known rhamnosides of the aglycones tested within this study (http://kanaya.naist.jp/knapsack_jsp/top.html, January 4th, 2019, (Afendi et al., 2012)). For chrysin, diosmetin, biochanin A and hesperetin the GtfC-produced rhamnosides are to the best of our knowledge firstly described within this study. These findings highlighted the enormous potential of GtfC for the generation

of novel flavonoid rhamnosides.

Interestingly GtfC can address the C5–OH at the A-ring of flavones, isoflavones and flavanones. The C5–OH group is hard to address due to its low reactivity resulting from intramolecular H-bonds with the C-4 carbonyl group (Liao et al., 2016). However, GtfC only forms 5-OH rhamnosides as main product for chrysin and biochanin A, where the only other OH group left is the C7–OH at the A-ring (Fig. 2A). Accordingly, the C5–OH is not the major product formed by GtfC in biotransformations of hesperetin or diosmetin, where the C3'–OH at the C-Ring is available (Fig. 3B and Supplementary S1). When the C3–OH at the A-ring of flavonols is available, GtfC produces mainly the 3-*O*-rhamnosides (Fig. 2B) and no 5-OH rhamnosylation was detected.

3.2. Hesperetin rhamnosylation in 48 well plates

The product concentration of the initial shake flask experiments to determine the glycosylation products of GtfC was unsatisfying (data not shown). Therefore, a metabolic engineering strategy, focusing on a constant supply of the co-substrate *d*TDP-rha, was developed to increase the glycosylation capability of *E. coli*. To compare the productivities of all designed *E. coli* strains biotransformation approaches were performed in flower plates in minimal media containing dextrans of starch as sole carbon source. The glycoside formation of the model substrate hesperetin was monitored using HPLC analyses and concentrations were determined using calibration curves of H5R and H3'R. *E. coli* is only able to import and utilize maltodextrin chains up to maltoheptaose, whereas longer chains are not metabolized (Ferenci, 1980). To ensure sufficient dextrin degradation a G6-amylase (EC 3.2.1.98) gene from alkalophilic *Bacillus* sp.707 was constitutively expressed and secreted into the periplasm using a codon optimized secretion signal of FhuD, showing advanced amylase activities (Samant et al., 2014). The G6-amylase degrades the longer chain dextrans reducing the size to accessible chain length, predominantly forming maltohexaose units (Kanai et al., 2004; Kimura et al., 1988). To ensure sufficient maltodextrin degradation all strains used in this study expressed a plasmid encoded G6-amylase gene if not stated otherwise. A list of production strains is given in Table 1.

The level of *d*TDP-sugars can be one rate limiting factor of glycosylation reactions as concentrations of *d*TDP-rha have been shown to be about 30-fold lower compared to UDP-glucose (UDP-glc) in *E. coli* BL21(DE3) (Lim et al., 2006). *d*TDP-rha is synthesized by *E. coli* from glucose-1-phosphate via the 4-step enzymatic pathway RmlABCD (Fig. 1). In order to increase *d*TDP-rha levels the native *rml* operon (*rmlBDAC*) of *E. coli* K12 was overexpressed in a T5-promotor controlled pCDFDuet-1 backbone (T5-*rmlOP*). Biotransformations of *E. coli* WT-A, expressing vector encoded GtfC as well as G6-amylase, produced on average 16.1 ± 0.2 mg/L of H3'R and 0.3 ± 0.1 mg/L of H5R (Fig. 3). The additional overexpression of the vector encoded *d*TDP-rha synthesis pathway led to a significant increase in hesperetin rhamnoside production to 26.3 ± 4.1 mg/L of H3'R and 0.9 ± 0.1 mg/L of H5R in *E. coli* WT-B after 48 h.

To constantly regenerate *d*TDP-rha, G1P needs to be available throughout the biotransformation which is generated via the action of maltodextrin phosphorylase (MalP) (Fig. 1) (Schwartz and Hofnung, 1967; Watson et al., 1997). Furthermore, *E. coli* metabolizes maltodextrins liberating glucose by maltodextrin glucosidase (MalZ) and 4-alpha-glucanotransferase (MalQ). G1P can reenter glycolysis through glucose-1-phosphatase (Agp) or phosphoglucomutase-1 (Pgm). G1P also is the precursor of UDP-glc formed by the UTP-glucose-1-phosphate uridylyltransferase gene *galU*.

To investigate the effect of gene deletions within the maltodextrin system of *E. coli* on the rhamnosylation capability we created single gene deletion strains of *malZ*, *agp*, *pgm* and *galU*, designated *E. coli* UHH_CR1, UHH_CR2, UHH_CR3 and UHH_CR4, respectively. Deletion of *malZ* as well as deletion of *agp* did not lead to significant improvements in productivity. Neither strain UHH_CR1-A nor UHH_CR2-A

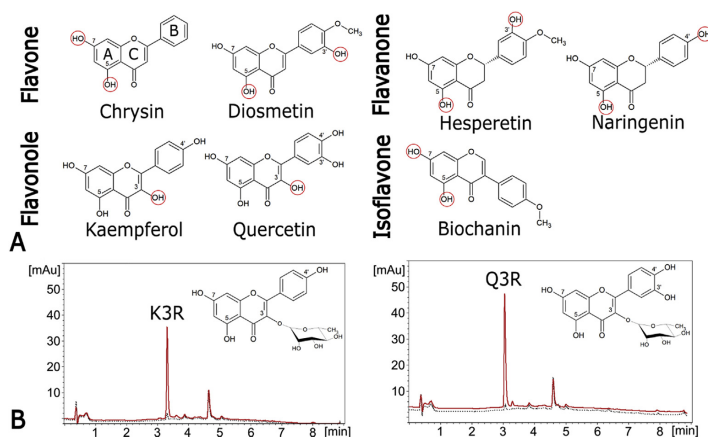


Fig. 2. Flavonoid substrates used in GtFC biotransformations. A. Substrates used in shake flask experiments to determine reaction products of GtFC. NMR confirmed hydroxyl functions addressable by GtFC are highlighted with red circles. B. UHPLC chromatograms at 254 nm after 6 h (black dashed) and 24 h (red) biotransformations of kaempferol and quercetin in solid fed-batch fermentations. Production of Kaempferol-3-O-rhamnoside (K3R at 3.15 min) and Quercetin-3-O-rhamnoside (Q3R at 3.05 min) were confirmed via UHPLC using reference substances. (For interpretation of the references to colour in this figure legend, the reader is referred to the Web version of this article.)

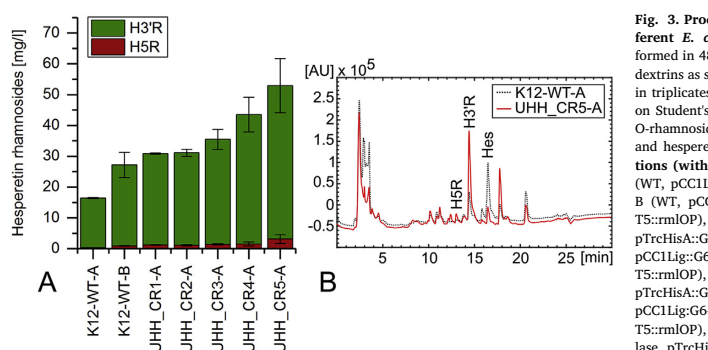


Fig. 3. Production of hesperetin rhamnosides by different *E. coli* strains. A. Biotransformations were performed in 48 well flower plates in M9 media containing 1% dextrans as sole carbon source. Experiments were performed in triplicates, error bars indicate confidence intervals based on Student's *t*-distribution ($\alpha = 0.05$, $n = 3$). Hesperetin-5-O-rhamnoside (H5R), hesperetin-3'-O-rhamnoside (H3'R) and hesperetin (Hes) peaks are indicated. **Strain designations (with genotypes) according to Table 1:** K12-WT-A (WT, pCC1Lig::G6-amylase, pTrcHisA::GtFC(opt)), K12-WT-B (WT, pCC1Lig::G6-amylase, pTrcHisA::GtFC(opt), pCDF-T5::rmlOP), UHH_CR1-A (Δ malZ, pCC1Lig::G6-amylase, pTrcHisA::GtFC(opt), pCDF-T5::rmlOP), UHH_CR2-A (Δ agp, pCC1Lig::G6-amylase, pTrcHisA::GtFC(opt), pCDF-T5::rmlOP), UHH_CR3-A (Δ pgm, pCC1Lig::G6-amylase, pTrcHisA::GtFC(opt), pCDF-T5::rmlOP), UHH_CR4-A (Δ galU, pCC1Lig::G6-amylase, pTrcHisA::GtFC(opt), pCDF-T5::rmlOP), UHH_CR5-A (Δ pgm, Δ galU, pCC1Lig::G6-amylase, pTrcHisA::GtFC(opt), pCDF-T5::rmlOP). B. HPLC chromatogram (at 254 nm) overlay of biotransformations with *E. coli* K12-WT-A and *E. coli* UHH_CR5-A, respectively.

showed any significant improvement compared to strain *E. coli* WT-B in hesperetin rhamnosylation. UHH_CR1-A yielded of 29.7 ± 0.2 mg/L of H3'R and 1.1 ± 0.2 mg/L of H5R whereas UHH_CR2-A converted 30.0 ± 1.1 mg/L of H3'R and 1.2 ± 0.1 mg/L of H5R (Fig. 3).

In contrast, *E. coli* UHH_CR3-A with perturbed *pgm* exhibited an increased production of 34.1 ± 3.2 mg/L of H3'R and 1.4 ± 0.2 mg/L of H5R. Pgm deficient *E. coli* strains grown on maltose are known to have high G1P levels that are condensed to long chain maltodextrins by reversed action of MalP (Adhya and Schwartz, 1971; Brautaset et al., 1998). This mutation is called the “Blu” phenotype as cultures can be stained blue by iodine (Roehl and Vinopal, 1979). In UHH_CR3-A the higher G1P levels could ensure an increased synthesis of *d*TDP-rha through the *rml* operon (Fig. 1).

The UTP-glucose-1-phosphate uridylyltransferase (GalU) produces UDP-glc from G1P at concentrations 30-fold higher compared to *d*TDP-rha in *E. coli* BL21(DE3) (Lim et al., 2006). Thus, GalU represents an effective sink of G1P. Consistently, the deletion of *galU* in *E. coli* UHH_CR4-A had a strong effect on production of hesperetin rhamnosides with an average conversion of 42.0 ± 5.6 mg/L of H3'R and 1.5 ± 0.6 mg/L of H5R. GalU deficient strains produce a so called deep-rough phenotype, resulting from a truncated core LPS, missing glucose residues, that effects an increased sensitivity to hydrophobic

agents due to a lower diffusion barrier (Delcour, 2009; Genevaux et al., 1999; Gustafsson et al., 1973; Schnaitman and Klana, 1993). And to our knowledge flavonoid aglycons are not actively transported into *E. coli* but permeate the diffusion barrier formed by the LPS via passive diffusion. This would imply that GalU deficient strains might also exhibit increased uptake of hesperetin, boosting the conversion through higher flux rate in the cytoplasm.

Interestingly, RmlA, catalyzing the first enzymatic step in the *d*TDP-rha biosynthesis, is also competitively inhibited by UDP-glc (Bernstein and Robbins, 1965). Thus, deletion of *galU* might have a ternary effect. The increased production may be attributed to a reduced competitive inhibition of the overexpressed RmlA, an increased uptake of the substrate hesperetin, and a higher *d*TDP-rha concentration due to eliminated formation of UDP-glc from G1P.

RmlA is not only subject of competitive inhibition by UDP-glc but also feedback inhibited by its product *d*TDP-glucose (Zuccotti et al., 2001). Competitive feedback inhibition can generally be relieved through high substrate concentrations, in this case G1P and *d*TTP. Increased G1P levels and reduced UDP-glc levels should be present in the Pgm and GalU double mutant *E. coli* UHH_CR5-A. *E. coli* UHH_CR5-A led to the highest amount of 49.7 ± 8.7 mg/L of H3'R and 3.2 ± 1.4 mg/L of H5R (Fig. 3). All other double deletion

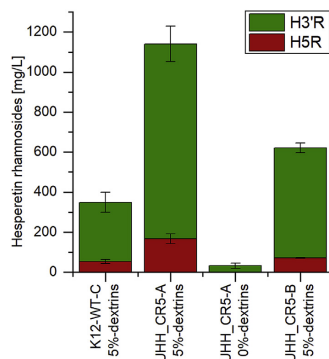


Fig. 4. Hesperetin rhamnosylation of *E. coli* in batch fermentations. Hesperetin rhamnosylation in 24 h batch fermentations in mg/L. Strain designations (with genotypes) according to Table 1: K12-WT-C (WT, pTrcHisA::GtfC(opt)), UHH_CR5-A (Δ pgm, Δ galU, pCC1Lig::G6-amylase, pTrcHisA::GtfC(opt), pCDF-T5::rmlOP), UHH_CR5-B (Δ pgm, Δ galU, pTrcHisA::GtfC(opt), pCDF-T5::rmlOP). Fermentations were performed in quadruplicates, error-bars indicate confidence intervals based on Student's *t*-distribution ($\alpha = 0.05$, $n = 4$).

combinations of the examined genes *agp*, *malZ*, *pgm*, and *galU* had no synergistic effect on hesperetin rhamnosylation or even were contra productive compared to the single deletions (Supplementary Fig. S6). In comparison to *E. coli* WT-A the productivity was increased threefold in engineered *E. coli* UHH_CR5-A (Fig. 3).

3.3. Hesperetin rhamnosylation in batch fermentations

As the aim of the study was to create performant production strains for flavonoid rhamnoside production, we further tested the established strain UHH_CR5-A in high cell density bioreactor conditions. The experiments were performed in a parallel bioreactor system, using Terrific broth (TB) media to achieve high product formation compared to minimal media (Supplementary - S7). As a benchmark a 24 h batch fermentation of *E. coli* WT-C only expressing GtfC was performed in TB-media containing an additional 5% of starch dextrans. *E. coli* WT-C was able to produce 296 ± 51 mg/L of H3'R and 54 ± 10 mg/L of H5R (Fig. 4). The best performing strain from the 48 well screening *E. coli* UHH_CR5-A produced a total amount of 1,140 mg/L with 973 ± 89 mg/L of H3'R and 167 ± 25 mg/L of H5R, respectively. These product concentrations are comparable to the state of the art glycosylation platform producing 1.12 g/L of quercetin-3-O-rhamnoside in 30 h (De Bruyn et al., 2015b).

As a control for dextrin dependency, a biotransformation was performed without supplementation of starch dextrans in TB media. Without dextrans the production of hesperetin rhamnosides by *E. coli* UHH_CR5-A diminished to 32 ± 13 mg of H3'R, whereas H5R production could not be detected after 24 h (Fig. 4A). This clearly demonstrated the coupling of glycosylation to dextrin metabolism in *E. coli* UHH_CR5-A. Without dextrin supplementation *E. coli* UHH_CR5-A could hardly produce G1P, that is essentially required for the synthesis of dTDP-rha, as in *E. coli* UHH_CR5-A the *pgm* gene is removed (Fig. 1). Pgm is responsible for the interconversion of glucose-6-phosphate (G6P) and G1P in glucose metabolism. But Pgm deficient *E. coli* strains show a strongly depressed G1P synthesis (Adhya and Schwartz, 1971; Eydallin et al., 2007).

To investigate the influence of the G6-amylase on the glycosylation yields we created the *E. coli* *pgm* and *galU* double mutant UHH_CR5-B, overexpressing GtfC and the *rml* operon, but lacking G6-amylase. In

comparison to *E. coli* UHH_CR5-A, *E. coli* UHH_CR5-B showed a reduced production of 548 ± 25 mg/L of H3'R and 72 ± 3 mg/L of H5R with a supplement of 5% (w/v) starch dextrans after 24 h (Fig. 4). Thus, the presence of G6-amylase is beneficial for the glycosylation of flavonoids but not essential.

To exclude any cell density dependencies, yields of the biotransformations were normalized against determined optical densities at 600 nm (Supplementary - S8). The different production yields observed could not be attributed to differences in cell densities as the same relation of yields was observed after normalization.

3.4. Hesperetin rhamnosylation in solid fed-batch fermentations

Dextrin supplementation in presence of G6-amylase proved to be crucial in 24 h batch fermentations. To determine the influence of a repeated feed of dextrans, an additional 50 g/L of dextrans were added after 24 h of biotransformation. These solid fed-batch fermentations were compared to 48 batch fermentations without additional dextrin feed. Using linear regression between the measured titer data points, the space time yield (STY) for the main product H3'R was determined in both setups. As the batch and solid fed-batch processes were identical up to 24 h, no significant differences were expected in production during this time span. Consistently, batch and fed-batch fermentations yielded similar concentrations of 973 ± 89 mg/L and 920 ± 55 mg/L of H3'R and 167 ± 25 mg/L and 137 ± 4 mg/L of H5R, respectively (Fig. 5). The calculated STY of the batch process was 47 ± 4 mg/L/h and the STY of the solid fed-batch was 45 ± 4 mg/L/h between start of biotransformation and 24 h of reaction. During the second 24 h of fermentation the STY of H3'R in the batch process decreased by more than 2-fold to an average of 20 ± 8 mg/L/h. *E. coli* UHH_CR5-A in batch mode produced $1,489 \pm 128$ mg/L of H3'R and 273 ± 20 mg/L H5R after 48 h. In solid fed-batch mode the production rate increased slightly after a dextrin feed to 57 ± 5 mg/L/h leading to a final production of $2,362 \pm 57$ mg/L of H3'R and 367 ± 12 mg/L of H5R after 48 h. This rhamnoside titer was to the best of our knowledge the highest production titer of a flavonoid rhamnoside published so far.

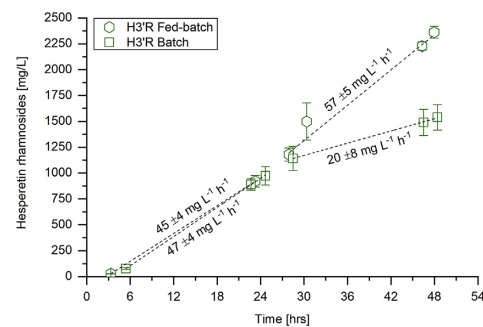


Fig. 5. Comparison of batch and solid-fed-batch fermentations of *E. coli* UHH_CR5-A.

Biotransformations of *E. coli* UHH_CR5-A expressing Glycosyltransferase C (pTrcHisA::gtfC), the dTDP-rha synthesis operon (pCDF-T5::rmlOP) and G6-amylase (pCC1Lig::G6-amylase). In fed-batch mode a feed of 5 g/L solid dextrans was supplemented after 24 h, whereas in batch mode the reaction was continued to 48 h without any supplementation. Space time yields were calculated between data points using linear regression (dashed lines) in the intervals between start and 24 h of incubation as well as after dextrin feed and 48 h of fermentation. As a side product 367 ± 12 mg/L and 273 ± 20 mg/L H5R were produced after 48 h in fed-batch and batch mode, respectively. Fermentations were performed in quadruplicates, error bars indicate confidence intervals based on Student's *t*-distribution ($\alpha = 0.05$, $n = 4$).

3.5. High-level production of quercetin and kaempferol rhamnosides

To further demonstrate that the engineered production strain *E. coli* UHH_CR5-A can produce high level rhamnosides of other flavonoids than hesperetin, biotransformations using quercetin and kaempferol as aglycones were performed. Within 48 h of fed-batch biotransformations *E. coli* UHH_CR5A was able to produce 4.32 g/L of quercetin-3-O-rhamnoside and 1.92 g/L of kaempferol-3-O-rhamnoside (Table 3). In recent glycosylation approaches the amounts of flavonoid rhamnosides produced usually were clearly below a concentration of 1 g/L (Table 3). Only De Bruyn and colleagues were able to produce 1.18 g/L of quercitrin after 30 h biotransformations in an engineered *E. coli* W strain. This strain was metabolically engineered to enable growth coupled glycosylation on sucrose (De Bruyn et al., 2015b). Compared to the sucrose phosphorylase system *E. coli* UHH-CR5-A showed a more than 2-fold increase in STY with 90 mg/L/h in the production of quercetin-3-O-rhamnoside (Table 3). The results highlight the high potential of the engineered *E. coli* UHH-CR5-A strain to produce flavonoid rhamnosides.

4. Conclusion

Directed glycosylation of flavonoids is a promising tool to alter the compound properties regarding solubility, stability, bioavailability, compatibility, and their efficacy (Kren, 2008; Williamson and Manach, 2005). In this study we coupled the rhamnosylation of flavonoids with the maltodextrin metabolism of *E. coli* and by using the metagenome-derived glycosyltransferase GtF (Rabausch et al., 2013). The combination of *pgm* and *galU* deletions together with the overexpression of a plasmid-based *rml* operon as well as a G6-amylose gene integrated into the host strain *E. coli* UHH_CR5-A enabled production of 4.3 g/L of quercetin-3-O-rhamnoside, 2.4 g/L of hesperetin-3'-O-rhamnoside, and 1.9 g/L of kaempferol-3-O-rhamnoside, which are to the best of our knowledge the highest published yields of glycosylated (i.e. rhamnosylated) flavonoids and using biotransformation.

Funding

This work was supported by the German Federal Ministry of Education and research [Grant number 031A376].

Acknowledgements

The authors want to acknowledge Dr. H. Rosenfelds technical support throughout this research project and thank him for the HPLC purification of the flavonoid rhamnosides.

Appendix A. Supplementary data

Supplementary data to this article can be found online at <https://doi.org/10.1016/j.jmben.2019.07.002>.

References

Adhya, S., Schwartz, M., 1971. Phosphoglucomutase mutants of *Escherichia coli* K-12. *J. Bacteriol.* 108, 621–626.

Afendi, F.M., Okada, T., Yamazaki, M., Hirai-Morita, A., Nakamura, Y., Nakamura, K., Ikeda, S., Takahashi, H., Altaf-Ul-Amin, Md, Darusman, L.K., Saito, K., Kanaya, S., 2012. KNApSack family databases: integrated metabolite-plant species databases for multifaceted plant research. *Plant Cell Physiol.* 53 e1–e1. <https://doi.org/10.1093/pcp/pcr165>.

Bernstein, R.L., Robbins, W., 1965. Control Aspects of Uridine S-Diphosphate Glucose and Thymidine S-Diphosphate Glucose Synthesis by Microbial Enzymes 240, vol 8.

Bertrand, A., Morel, S., Lefoulon, F., Rolland, Y., Monsan, P., Remaud-Simeon, M., 2006. Leuconostoc mesenteroides glucansucrase synthesis of flavonoid glucosides by acceptor reactions in aqueous-organic solvents. *Carbohydr. Res.* 341, 855–863. <https://doi.org/10.1016/j.carres.2006.02.008>.

Brautaset, T., Petersen, S., Valla, S., 1998. An experimental study on carbon flow in *Escherichia coli* as a function of kinetic properties and expression levels of the enzyme phosphoglucomutase. *Biotechnol. Bioeng.* 58, 299–302. [\(SICI\)1097-0290\(19980420\)58:2/3 < 299::AID-BIT27 > 3.0.CO;2-6.

Bungarung, L., Gutmann, A., Nidetzky, B., 2013. Leloir Glycosyltransferases and Natural Product Glycosylation: Biocatalytic Synthesis of the C-Glucoside Nothofagin, a Major Antioxidant of Redbush Herbal Tea. *Adv. Synth. Catal.* 355, 2757–2763. <https://doi.org/10.1002/adsc.201300251>.

De Bruyn, F., De Paep, B., Maertens, J., Beuprez, J., De Cocker, P., Mincke, S., Stevens, C., De Mey, M., 2015a. Development of an in vivo glycosylation platform by coupling production to growth: production of phenolic glucosides by a glycosyltransferase of *Vitis vinifera*. *Biotechnol. Bioeng.* 112, 1594–1603. <https://doi.org/10.1002/bit.25570>.

De Bruyn, F., Van Brempt, M., Maertens, J., Van Bellegem, W., Duchi, D., De Mey, M., 2015b. Metabolic engineering of *Escherichia coli* into a versatile glycosylation platform: production of bio-active quercetin glycosides. *Microb. Cell Factories* 14, 138. <https://doi.org/10.1186/s12934-015-0326-1>.

De Winter, K., Dewitte, G., Dirks-Hofmeister, M.E., De Laet, S., Pelantová, H., Křen, V., Desmet, T., 2015. Enzymatic glycosylation of phenolic antioxidants: phosphorylase-mediated synthesis and characterization. *J. Agric. Food Chem.* 63, 10131–10139. <https://doi.org/10.1021/acs.jafc.5b04380>.

Delcour, A.H., 2009. Outer membrane permeability and antibiotic resistance. *Biochim. Biophys. Acta* 1794, 808–816. <https://doi.org/10.1016/j.bbapap.2008.11.005>. *Outer.*

Desmet, T., Soetaert, W., Bojarová, P., Křen, V., Dijkhuizen, L., Eastwick-Field, V., Schiller, A., 2012. Enzymatic glycosylation of small molecules: challenging substrates require tailored catalysts. *Chem. Eur J.* 18, 10786–10801. <https://doi.org/10.1002/chem.201103069>.

Eydallin, G., Viala, A.M., Morán-Zorrano, M.T., Muñoz, F.J., Montero, M., Baroja-Fernández, E., Pozueta-Romero, J., 2007. Genome-wide screening of genes affecting glycogen metabolism in *Escherichia coli* K-12. *FEBS Lett.* 581, 2947–2953. <https://doi.org/10.1016/j.febslet.2007.05.044>.

Ferenci, T., 1980. The recognition of maltodextrins by *Escherichia coli*. *Eur. J. Biochem.* 108, 631–636. <https://doi.org/10.1111/j.1432-1033.1980.tb04758.x>.

Genevaux, P., Bauda, P., DuBois, M.S., Oudega, B., 1999. Identification of Tn 10 insertions in the *riaG*, *rfaP*, and *galU* genes involved in lipopolysaccharide core biosynthesis that affect *Escherichia coli* adhesion. *Arch. Microbiol.* 172, 1–8. <https://doi.org/10.1007/s002030050732>.

Giraud, M.F., Naismith, J.H., 2000. The rhamnose pathway. *Curr. Opin. Struct. Biol.* 10, 687–696. \[https://doi.org/10.1016/S0959-440X\\(00\\)0145-7\]\(https://doi.org/10.1016/S0959-440X\(00\)0145-7\).

Gustafsson, P., Nordström, K., Normark, S., 1973. Outer penetration barrier of *Escherichia coli* K-12: kinetics of the uptake of gentian violet by wild type and envelope mutants. *J. Bacteriol.* 116, 893–900.

Kanai, R., Haga, K., Akiba, T., Yamane, K., Harata, K., 2004. Biochemical and crystallographic analyses of maltohexaose-producing amylase from alkaliphilic *Bacillus* sp. 707. *Biochemistry* 43, 14047–14056. <https://doi.org/10.1021/bi048489m>.

Kim, B.G., Kim, H.J., Ahn, J.H., 2012. Production of bioactive flavonoid rhamnosides by expression of plant genes in *Escherichia coli*. *J. Agric. Food Chem.* 60, 11143–11148. <https://doi.org/10.1021/jf302123c>.

Kimura, K., Tsukamoto, A., Ishii, Y., Takano, T., Yamane, K., 1988. Cloning of a gene for maltohexaose producing amylase of an alkaliphilic *Bacillus* and hyper-production of the enzyme in *Bacillus subtilis* cells. *Appl. Microbiol. Biotechnol.* 27. <https://doi.org/10.1007/BF00251771>.

Koenigs, W., Knorr, E., 1901. Ueber einige Derivate des Traubenzuckers und der Galactose. *Berichte Dtsch. Chem. Ges.* 34, 957–981. <https://doi.org/10.1002/cber.190103401162>.

Kren, V., 2008. Glycoside vs. Aglycon: the Role of Glycosidic Residue in Biological Activity. Springer, Berlin, Heidelberg. \[https://doi.org/10.1007/978-3-540-30429-6_67\]\(https://doi.org/10.1007/978-3-540-30429-6_67\).

Lairson, L.L., Henrissat, B., Davies, G.J., Withers, S.G., 2008. Glycosyltransferases: structures, functions, and mechanisms. *Annu. Rev. Biochem.* 77, 521–555. <https://doi.org/10.1146/annurev.biochem.76.061005.092322>.

Leonard, E., Yan, Y., Fowler, Z.L., Li, Z., Lim, C.G., Lim, K.H., Koffas, M.A.G., 2008. Strain improvement of recombinant *Escherichia coli* for efficient production of plant flavonoids. *Mol. Pharm.* 5, 257–265. <https://doi.org/10.1021/mp700147z>.

Lepak, A., Gutmann, A., Kulmer, S.T., Nidetzky, B., 2015. Creating a water-soluble re-sveratrol-based antioxidant by site-selective enzymatic glycosylation. *Chembiochem* 16, 1870–1874. <https://doi.org/10.1002/cbic.201500284>.

Liao, J.-X., Fan, N.-L., Liu, H., Tu, Y.-H., Sun, J.-S., 2016. Highly efficient synthesis of flavonoid 5-O-glycosides with glycosyl ortho-alkynylbenzoates as donors. *Org. Biomol. Chem.* 14, 1221–1225. <https://doi.org/10.1039/C5OB02313K>.

Lim, E.K., Ashford, D. a., Bowles, D.J., 2006. The synthesis of small-molecule rhamnosides through the rational design of a whole-cell biocatalytic system. *Chembiochem* 7, 1181–1185. <https://doi.org/10.1002/cbic.200600193>.

Mäkilä, L., Laaksonen, O., Alanne, A.L., Kortensniemi, M., Kallio, H., Yang, B., 2016. Stability of hydroxycinnamic acid derivatives, flavonoid glycosides, and anthocyanins in black currant juice. *J. Agric. Food Chem.* 64, 4584–4598. <https://doi.org/10.1021/acs.jafc.6b01005>.

Maniatis, T., Fritsch, E.F., Sambrook, J., 1982. *Molecular Cloning: A Laboratory Manual*. Cold Spring Harbor laboratory press, New York.

Masada, S., Kawase, Y., Nagatoh, M., Oguchi, Y., Terasaka, K., Mizukami, H., 2007. An efficient chemoenzymatic production of small molecule glucosides with in situ UDP-glucose recyclin. *FEBS Letters* 581, 2562–2566. <https://doi.org/10.1016/j.febslet.2007.04.074>.

Mi, J.C., Kang, A.Y., Kyung, M.L., Oh, E., Jun, H.J., Kim, S.Y., Joong, H.A., Moon, T.W., Lee, S.J., Park, K.H., 2006. Water-soluble genistin glycoside isoflavones up-regulate antioxidant metallothionein expression and scavenge free radicals. *J. Agric. Food Chem.* 54, 3819–3826. <https://doi.org/10.1021/jf060510y>.

Pandey, R.P., Parajuli, P., Chu, L.L., Darsandhari, S., Sohng, J.K., 2015. Biosynthesis of amino deoxy-sugar-conjugated flavonoid glycosides by engineered *Escherichia coli*.](https://doi.org/10.1002/</p>
</div>
<div data-bbox=)

- Biochem. Eng. J. 101, 191–199. <https://doi.org/10.1016/j.bej.2015.05.017>.
- Pandey, R.P., Parajuli, P., Koirala, N., Lee, J.H., Park, Y. Il, Sohng, J.K., 2014. Glucosylation of isoflavonoids in engineered *Escherichia coli*. *Mol. Cells* 37, 172–177. <https://doi.org/10.14348/molcells.2014.2348>.
- Parajuli, P., Pandey, R.P., Trang, N.T.H., Chaudhary, A.K., Sohng, J.K., 2015. Synthetic sugar cassettes for the efficient production of flavonol glycosides in *Escherichia coli*. *Microb. Cell Factories* 14. <https://doi.org/10.1186/s12934-015-0261-1>.
- Rabausch, U., Juergensen, J., Ilmberger, N., Böhnke, S., Fischer, S., Schubach, B., Schulte, M., Streit, W.R., 2013. Functional screening of metagenome and genome libraries for detection of novel flavonoid-modifying enzymes. *Appl. Environ. Microbiol.* 79, 4551–4563. <https://doi.org/10.1128/AEM.01077-13>.
- Roehl, R.A., Vinopal, R.T., 1979. New maltose Blu mutations in *Escherichia coli* K-12. *J. Bacteriol.* 139, 683–685.
- Roscher, R., Schwab, W., Schreier, P., 1997. Stability of naturally occurring 2,5-dimethyl-4-hydroxy-3[2H]-furanone derivatives. *Z. Fuer Lebensm.-Unters. -Forsch. Food Res. Technol.* 204, 438–441. <https://doi.org/10.1007/s002170050109>.
- Samant, S., Gupta, G., Karthikeyan, S., Haq, S.F., Nair, A., Sambasivam, G., Sukumaran, S., 2014. Effect of codon-optimized *E. coli* signal peptides on recombinant *Bacillus stearothermophilus* maltogenic amylase periplasmic localization, yield and activity. *J. Ind. Microbiol. Biotechnol.* 41, 1435–1442. <https://doi.org/10.1007/s10295-014-1482-8>.
- Schnaitman, C. a, Klena, J.D., 1993. Genetics of lipopolysaccharide biosynthesis in enteric bacteria. *Microbiol. Rev.* 57, 655–682.
- Schwartz, M., Hofnung, M., 1967. La maltodextrine phosphorylase de *Escherichia coli*. *Eur. J. Biochem.* 2, 132–145. <https://doi.org/10.1111/j.1432-1033.1967.tb00117.x>.
- Simkhada, D., Kim, E., Lee, H.C., Sohng, J.K., 2009. Metabolic engineering of *Escherichia coli* for the biological synthesis of 7-O-xylestyryl naringenin. *Mol. Cells* 28, 397–401. <https://doi.org/10.1007/s10059-009-0135-7>.
- Simkhada, D., Lee, H.C., Sohng, J.K., 2010. Genetic engineering approach for the production of rhamnosyl and allosyl flavonoids from *Escherichia coli*. *Biotechnol. Bioeng.* 107, 154–162. <https://doi.org/10.1002/bit.22782>.
- Slámová, K., Kapešová, J., Valentová, K., 2018. "Sweet flavonoids": glycosidase-catalyzed modifications. *Int. J. Mol. Sci.* 19, 2126. <https://doi.org/10.3390/ijms19072126>.
- Stevenson, G., Neal, B., Liu, D., Hobbs, M., Packer, N.H., Batley, M., Redmond, J.W., Lindqvist, L., Reeves, P., 1994. Structure of the O antigen of *Escherichia coli* K-12 and the sequence of its rfb gene cluster. *J. Bacteriol.* 176, 4144–4156.
- Thuan, N.H., Malla, S., Trung, N.T., Dhakal, D., Pokhrel, A.R., Chu, L.L., Sohng, J.K., 2017. Microbial production of astilbin, a bioactive rhamnosylated flavanone, from taxifolin. *World J. Microbiol. Biotechnol.* 33, 1–10. <https://doi.org/10.1007/s11274-017-2208-7>.
- Thuan, N.H., Pandey, R.P., Thuy, T.T.T., Park, J.W., Sohng, J.K., 2013. Improvement of regio-specific production of myricetin-3-O- α -L-rhamnoside in engineered *Escherichia coli*. *Appl. Biochem. Biotechnol.* 171, 1956–67. <https://doi.org/10.1007/s12010-013-0459-9>.
- Vidal, A., Sanchis, V., Ramos, A.J., Marín, S., 2018. Stability of DON and DON-3-glucoside during baking as affected by the presence of food additives. *Food Addit. Contam. Part Chem. Anal. Control Expo. Risk Assess.* 35, 529–537. <https://doi.org/10.1080/19440049.2017.1401741>.
- Watson, K.A., Schinzel, R., Palm, D., Johnson, L.N., 1997. The crystal structure of *Escherichia coli* maltodextrin phosphorylase provides an explanation for the activity without control in this basic archetype of a phosphorylase. *EMBO J.* 16, 1–14. <https://doi.org/10.1093/emboj/16.1.1>.
- Williamson, G., Manach, C., 2005. Bioavailability and bioefficacy of polyphenols in humans. *Am. J. Clin. Nutr.* 81, 243S–255S. ([pii]). <https://doi.org/10.1093/ajcn/81.1.230s>.
- Woo, H.J., Kang, H.K., Nguyen, T.T.H., Kim, G.E., Kim, Y.M., Park, J.S., Kim, Duwoon, Cha, J., Moon, Y.H., Nam, S.H., Xia, Y. mei, Kimura, A., Kim, Doman, 2012. Synthesis and characterization of ampelopsin glucosides using dextranase from *Leuconostoc mesenteroides* B-1299CB4: glucosylation enhancing physicochemical properties. *Enzym. Microb. Technol.* 51, 311–318. <https://doi.org/10.1016/j.enzmictec.2012.07.014>.
- Xia, T., Eiteman, M.A., 2017. Quercetin glucoside production by engineered *Escherichia coli*. *Appl. Biochem. Biotechnol.* 182, 1358–1370. <https://doi.org/10.1007/s12010-017-2403-x>.
- Yamamoto, I., Muto, N., Murakami, K., Akiyama, J.-I., 1992. Collagen synthesis in human skin fibroblasts is stimulated by a stable form of ascorbate, 2-O- α -D-Glucopyranosyl-L-Ascorbic acid. *J. Nutr.* 122, 871–877.
- Yang, M., Davies, G.J., Davis, B.G., 2007. A glycosynthase catalyst for the synthesis of flavonoid glycosides. *Angew. Chem. Int. Ed.* 46, 3885–3888. <https://doi.org/10.1002/anie.200604177>.
- Yoon, J.-A., Kim, B.-G., Lee, W.J., Lim, Y., Chong, Y., Ahn, J.-H., 2012. Production of a novel quercetin glucoside through metabolic engineering of *Escherichia coli*. *Appl. Environ. Microbiol.* 78, 4256–4262. <https://doi.org/10.1128/AEM.00275-12>.
- Zuccotti, S., Zanardi, D., Rosano, C., Sturla, L., Tonetti, M., Bolognesi, M., 2001. Kinetic and crystallographic analyses support a sequential-ordered bi bi catalytic mechanism for *Escherichia coli* glucose-1-phosphate thymidyltransferase. *J. Mol. Biol.* 313, 831–843. <https://doi.org/10.1006/jmbi.2001.5073>.